University of Alberta

STRUCTURAL AND FUNCTIONAL STUDIES OF A CLONED Kv4 CHANNEL EXPRESSED IN THE MYOCARDIUM OF THE TUNICATE *Ciona intestinalis* AND ITS MODULATION BY AN ENDOGENOUS KChIP SUBUNIT

by

Vicenta Salvador Recatala 

A thesis submitted to the Faculty of Graduate Studies and Research in partial fulfillment of the requirements for the degree of Doctor of Philosophy

Department of Physiology

Edmonton, Alberta
Fall, 2004

Your file Votre référence
ISBN: 0-612-96014-5
Our file Notre référence
ISBN: 0-612-96014-5

Acknowledgements

I would like to thank all those whose support, encouragement, friendship and criticism helped me find the right direction and made my work in Edmonton and Bamfield a positive experience. Specifically, I would like to thank my supervisor, Dr. Andy Spencer, whose generosity, guidance and numerous insightful suggestions regarding all aspects of this thesis were invaluable for my success. I am grateful also to all my supervisory committee members: Dr. Chris Benishin (Department of Physiology) for her time and encouragement; Dr. Warren Gallin (Department of Biological Sciences) for loaning me the lab bench on which I carried all the molecular work and for his teachings in molecular biology; Dr. Peter Smith (Department of Pharmacology) for his time and for valuable suggestions on electrophysiology. I would like also to thank Dr. Susan Dunn (Department of Pharmacology) and Dr. Robert French (Dept. of Physiology and Biophysics, University of Calgary) for taking the time to read my thesis and serve as external examiners at my defense.

I am grateful to Dr. Peter Ruben (Dept. of Biology, Utah State University) for having me in his lab where I gathered all the electrophysiological data in this Thesis, and for his support and friendship. I am also thankful to all his lab members for making me feel at home in Logan and for many enthusiastic discussions, and especially thanks to Jennifer Abbruzesse for her friendship and for providing excellent technical help. This Thesis also benefited from the comments of Dr. Jim Groome (Dept. of Biological Sciences, Idaho State University) regarding voltage-protocols and data analysis.

I would like to thank Lisa Ostafinchuk and Pat Murray (Molecular Biology Research Facility, University of Alberta) for performing all sequencing electrophoresis and providing me with their expertise, and Gary Ritzel (Department of Biological Sciences) for supplying molecular biology reagents and his expertise as well.

All members of the Gallin lab, the Spencer lab and the Locke lab (in which I settled my computer, books and papers to write this Thesis) were willing to provide advice and support, I appreciate their camaraderie greatly.

During this work I have benefited from formal and informal discussions with wonderful researchers and friends: Fabián Canosa, Bryan Crawford, Inna Sokolova, Mike Harrington, Bernardo Alvarez, and Tara MacDonald. I have learned many things from them and appreciate their laughter, friendship and support.

I would like to acknowledge my parents, siblings and all my friends, who have supported me through this journey. Pilar and Juanjo Raez and Mª Carmen Muñoz for their emotional support since childhood to this day; and Linda Gourilouk, Mike Laing and Elena Nedea, for making my time in Edmonton a memorable experience.

I am grateful to the people in the tiny and artistic community of Bamfield, who opened to me their homes and their hearts during the year and a half I lived there, especially Brunhilde Niederacher, Ziggy and Greg, Andy and Barb, Terry Giddens, and John Evans. Special thanks to my good friend Guy Whyte, for his companionship during our long and cold excursions from Bamfield to San Mateo Bay to collect tunicates, and for making me laugh.

And last but not least, Lucy.

Finally, I acknowledge the C.I.H.R. and the Department of Physiology of the University of Alberta for providing financial support all through my doctoral studies.

TABLE OF CONTENTS

LIST OF TABLES

LIST OF FIGURES

LIST OF SYMBOLS, NOMENCLATURE AND ABBREVIATIONS

AP	action potential
bp	base pair(s)
°C	degrees Celsius
cDNA	complementary DNA synthesized by reverse transcription of mRNA
cRNA	capped RNA
cm	centimeter(s)
dNTP	mixture of the four deoxynucleotides 5' triphosphate (adenosine, guanine, cytosine and thymidine) in equal proportions
EGTA	ethylene glycol-bis (β-aminoethyl ether)-*N,N,N',N'*-tetraacetic acid
E_K	Equilibrium potential for K^+
G_{max}	maximal conductance
G_K	Conductance for K^+
HEPES	*N*-2-hydroxy-ethylpiperazine-*N'*-2-ethanesulfonic acid
I_{max}	maximal ionic current
I_{TO}	Transient outward current
k	slope factor of an activation or inactivation curve, measured in millivolts *per* e-fold change
K^+	potassium ion(s)
Kb	kilobase(s)
Kv	voltage gated channel selectively permeable for K^+
KChIP	K^+ channel interacting protein
KHz	Kilohertz(s)

mg	milligram(s)
min	minute(s)
mM	millimolar
mRNA	messenger RNA
ms	millisecond(s)
mV	millivolt(s)
MΩ	megaohm(s)
μL	microlitre(s)
μm	micrometre(s)
μM	micromolar
μs	microsecond(s)
nA	nanoampere(s)
ng	nanogram(s)
nL	nanolitre(s)
nt*Ciona*Kv4	N-terminal truncation mutant *Ciona*Kv4 channels
Oligo-dT	short oligonucleotide of known sequence containing a poly-T tail that hybridizes with the poly-A tail of mRNA and is used to synthesize cDNA
ORF	open reading frame
pA	picoampere(s)
PCR	polymerase chain reaction
PKA	protein kinase A
PKC	protein kinase C
RACE	rapid amplification of cDNA ends
3'-RACE	rapid amplification of the 3' end of a cDNA strand that has been synthesized from template mRNA

5'-RACE	rapid amplification of the 5' end of a cDNA strand that has been synthesized from template mRNA
RT	reverse transcription/transcriptase
s	second(s)
SEM	standard error of the mean
TEA	tetraethylamonium
τ	time constant
3'-UTR	3' untranslated region: untranslated mRNA nucleotide sequence that is downstream of a stop codon
5'-UTR	5' untranslated region: untranslated mRNA nucleotide sequence that is upstream of the start codon
$V_{0.5}$	midpoint of activation or inactivation
wt	wild type

CHAPTER 1 GENERAL INTRODUCTION

1.1 General aspects of voltage-gated potassium (Kv) channels

Introduction

Potassium (K^+) currents have a role in maintaining the resting potential and re-polarizing the membrane potential after a depolarization, such as an action potential (Hille, 1992). Potassium (K^+) currents can be broadly categorized by their inactivation kinetics. "Delayed rectifier" currents inactivate very slowly, if at all (Hodgkin and Huxley, 1952), while "A-type" currents inactivate relatively rapidly, in the order of milliseconds at a held activating voltage (Connor and Stevens, 1971; Neher, 1971). Kv channels are the molecular effectors of these currents, as demonstrated by expression of the *Shaker* locus in *Xenopus* oocytes (Christie et al., 1989; Timpe et al., 1988) and in a mammalian cell line (Leonard et al., 1989). The first gene encoding a Kv channel, *Drosophila Shaker*, was cloned by Kamb et al. (1987) by chromosome walking of the *Shaker* locus. Subsequently, three other channel genes that belong to the same family (*Shab*, *Shaw* and *Shal)* were cloned by screening a *Drosophila* cDNA library at low stringency with *Shaker* probes (Butler et al., 1989). In *Drosophila*, each of these gene subfamilies is represented by a single gene. However, alternative splicing is a

mechanism used by arthropods to increase the diversity of Kv channels (Schwarz et al., 1988; Baro et al., 2001).

Diversification of the Kv channel family appears to have occurred early in evolution, before the triploblast lineage split from the diploblasts, as evidenced by a study by Jegla et al. (1995). These authors used a PCR-based method that used degenerate primers designed to amplify the region that is most conserved between the four *Shaker* related subfamilies (*Shaker* or Kv1, *Shab* or Kv2, *Shaw* or Kv3 and *Shal* or Kv4) and found that a hydrozoan jellyfish has Kv channels that can be ascribed to one of the four major Kv channel subfamilies, which suggests that these channels had already diversified in the common ancestor to diploblasts and triploblasts. Based on their nucleic acid and protein parsimony analyses, Strong et al. (1993) suggested that duplication of an ancestral Kv gene gave rise to two clades, the *Shaker/Shal* clade and the *Shaw/Shab* clade, and a successive duplication of each clade generated the Kv complement found in *Drosophila.*

Structural aspects of Kv channels

A functional Kv channel is formed by four α subunits, which co-assemble (Jan and Jan, 1990; MacKinnon, 1991) to define a central pore, the conduction pathway (Doyle et al., 1998). Kvα subunits encoded by different genes within the same Kvα channel subfamily (Kv1, Kv2, Kv3 or Kv4) can co-assemble to form functional heteromultimeric channels (Christie et al., 1990; Isacoff et al., 1990; Ruppersberg et al., 1990). However, Kvα subunits from different subfamilies do not co-assemble

(Covarrubias et al., 1991). Members of the Kv5 to Kv9 subfamilies cannot form functional tetramers by themselves but they heteromultimerize with Kv2α subunits to form functional channels whose properties differ from homotetramers formed exclusively by Kv2α subunits (Kramer et al., 1998; Salinas et al., 1997a, 1997b). Kv channel pore-forming (Kvα) subunits contain six hydrophobic membrane-spanning segments (S1-S6) of about 20 amino acids each in an α-helix conformation that are connected by intracellular or extracellular loops. Both termini (NH_2 and $COOH^-$) of the α subunits are intracellular (Papazian et al., 1987; Tempel et al., 1987). Every third residue of the S4 segment is positively charged, which identifies this segment as the voltage sensor (Papazian et al., 1991). The T1 domain (also known as the NAB domain), an N-terminal cytoplasmic domain consisting of ~100 amino acids, is a recognition domain that prevents association of α subunits from different Kv subfamilies (Li et al., 1992). In addition, the T1 domain appears to play an important role in conduction (Kreusch et al., 1998) and mutations in T1 altered the midpoint voltage of activation and closing kinetics in an *Aplysia Shaker* channel (Cushman et al., 2000). Selectivity for K^+ ions in Kv channels is provided by the K^+ selectivity filter signature sequence (TVGYG), which is in the pore domain (P-domain), within the loop between S5 and S6 (Yellen et al., 1991; Yool and Schwartz, 1991). Figure 1-1 shows a diagram of the secondary structure of a Kvα subunit, indicating the positions of the pore region, the S4 domain and the T1 domain.

The last two trans-membrane segments (S5 and S6) and the pore region of the six trans-membrane segment-containing Kv channels (6TM channels), whose structure

has been just described, are true homologues to the two trans-membrane domains and pore loop of the channel subunits that form inward rectifier channels, which are the structurally simplest voltage-gated channels. Thus, each subunit of these channels has only two trans-membrane domains (2TM channels) flanking a pore loop (Ho et al., 1993). However, it is not clear whether 2TM channels preceded the appearance of 6TM channels, because a protist, *Paramecium tetraurelia,* has six genes for 6TM potassium channels (Jegla and Salkoff, 1996) and several prokaryotes also have both 2TM and 6TM channels (*e.g.* Jiang et al., 2004).

Functional aspects of Kv channels

Kv channels are activated by a change in electric field across the plasma membrane, a process that is coupled to the displacement of electrical charges in Kvα subunits (Schoppa et al., 1992). This movement of gating charges is brought about by conformational changes of the channel molecule (Cha and Bezanilla, 1997), but there is no consensus yet regarding the precise structural modifications of the channel protein that occur in response to this voltage change across the membrane. Using fluorescence resonance energy transfer (FRET), Glauner et al. (1999) and Cha et al. (1999) were able to measure relative distances between S4 segments in a *Shaker* channel in resting and activated channels. Their data suggested that the S4 segment rotates 180^{o} during activation. However, the crystallized structure of a bacterial Kv channel (KvAP)

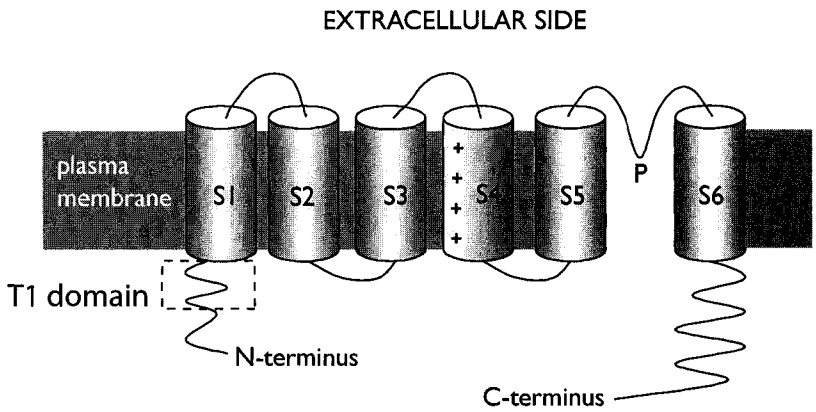

Figure 1-1. Proposed transmembrane topology of a Kvα subunit in two dimensions. Each transmembrane segment (S1-S6) is an α helix. Positive symbols in S4 denote positively charged amino acids that determine the function of this segment as a voltage-sensing domain. The first 20-30 amino acids of the N-terminus is a structural element for fast inactivation in some voltage-gated potassium channels. The T1 domain has a role in subunit-subunit recognition during assembly in the plasma membrane, and forms part of the ionic conduction pathway, as explained in section 1.1.

revealed that in these channels, the S4 segment lies intracellularly and forms part of a structure that was termed the "voltage-paddle" (Jiang et al., 2003). Each voltage-paddle is formed by an S4 segment attached to the rest of the channel subunit by an S3 loop and the S4-S5 linker (Jiang et al., 2003). Recently, these authors have elucidated the crystal structure of the KvAP channel in the open conformation (Jiang et al., 2004), in which the voltage-paddles appear at the outer perimeter of the channel, close to the extra-cellular solution, with the S4 segment exposed to the plasma membrane. These results led Jiang et al. (2003, 2004) to propose that upon a change in the membrane potential, these voltage-paddles, located at the periphery of the channel, move from their resting location on the cytoplasmic side towards the extracellular side by crossing the plasma membrane. However, as Lainé et al. (2004) have noted in a recent review, most other functional data obtained with very different methods converge on a parsimonious model of the structure of *Shaker* in which S4 is a trans-membrane segment that is surrounded by other trans-membrane segments. Furthermore, it has been argued that although protein crystallography is usually a reliable method to assess the native conformation of proteins, the antibody used to immobilize KvAP was large and rigid, which may have induced an artificial conformation (Lainé et al., 2004).

The mechanisms that lead to occlusion of the pore and inactivation of Kv channels are best studied for *Shaker* channels and are termed N-type inactivation and C-type inactivation (Choi et al., 1991). N-type inactivation is a rapid process by which the first ~20 amino acids of the N-terminus act as an inactivation particle that occludes the inner mouth of the pore, in the open state (Hoshi et al., 1990). The specific region of

the inner mouth that interacts with the inactivation particle is the cytoplasmic S4-S5 linker (Isacoff et al., 1991). This inactivation mechanism is best explained with the "ball and chain" model, in which the "ball" refers to the first ~20 amino acids of the N-terminus, or the inactivation particle, and the "chain" represents a stretch of amino acids after the ball domain (Hoshi et al., 1990). C-type inactivation of *Shaker* is a slower process than N-type inactivation, and depends on residues of the pore region (between S5 and S6) and external residues of the S6 domain (Hoshi et al., 1991; López-Barneo et al., 1993). C-type inactivation of *Shaker* occurs from the open state (Baukrowitz and Yellen, 1995) and is brought about by conformational changes that close the outer pore of the channel (Ogielska et al., 1995).

Modulation of Kv channels by β subunits, post-translational processing and phosphorylation

Kvα subunits often associate with small cytoplasmic subunits, termed Kvβ subunits that modulate their activity. Kvβ subunits were initially co-purified from brain tissue with dendrotoxin, a toxin used to purify Kvα subunits (Rehm and Lazdunski, 1988; Parcej and Dolly, 1989) and are cytoplasmic proteins of ~300 amino acids, lacking transmembrane segments, that bind to the T1 domain of Kvα subunits (Gulbis et al., 2000; Sewing et al., 1996; Yu et al., 1996). The Kvβ1 and Kvβ2 isoforms associate with Kvα subunits of the Kv1 subfamily (Kvβ1: Sewing et al., 1996; Kvβ2: Shi et al., 1996), and Kvβ3 associate with Kvα subunits of the Kv2 subfamily (Fink et al., 1996). Kvβ2 subunits bind to Kvα subunits while the latter are embedded in the

membrane of the endoplasmic reticulum (ER) and may act as chaperones (Shi et al., 1996), even aiding in the anchoring of Kvα/β subunit complexes to the cytoskeleton (Nakahira et a., 1996). Kvβ subunits also modulate the electrophysiological properties of Kv channels. For example, the N-terminal domain of Kvβ3 subunits behaves as an inactivation ball, conferring rapid inactivation properties to Kv1.5 channels that normally produce non-inactivating currents (Leicher et al., 1998). Kvβ2 subunits also modulate the biophysical parameters of the same channels (Kv1.5), by altering the voltage-dependence of activation and inactivation, and moderately accelerating their inactivation kinetics (Uebele et al., 1996).

Kv channels also have sites for glycosylation. For example, *Shaker* channels are glycosylated at two amino acid residues of the extracellular loop that connects transmembrane segments S1 and S2. Blocking glycosylation of the channel did not change folding or assembly of the four subunits, nor any biophysical properties (Santacruz-Toloza et al., 1994). Nevertheless, glycosylation stabilizes the conformation of the channel protein (Khanna et al., 2001), perhaps by allowing its interaction with the chaperone protein calnexin (Spiro, 2000).

The function of Kv channels can also be regulated by protein phosphorylation. For instance, Kv4.3 channels, which typically conduct transient A-type currents, produced non-inactivating currents when their N-terminus was phosphorylated by protein kinase C (PKC) (Covarrubias et al., 1994). In another example, phosphorylation of Kv1.1 channels by PKC decreased the conductance of these channels, leading to a significant reduction in the amplitude of their currents (Peretz et al., 1996).

1.2 Kv4 channels

Introduction

Kv4 channels mediate A-type currents in neurons (Sheng et al., 1992; Tsaur et al., 1992). These currents shape the post-synaptic response to excitatory inputs (Sheng et al., 1992), regulate firing frequency (Tierney and Harris-Warrick, 1992) and modulate excitability in response to signaling by second messengers (Hoffman and Johnston, 1998). Dendritic Kv4 channels appear to have a role in reducing the amplitude of action potentials that originate in the neuronal soma and back-propagate to the dendrites (Hoffman et al., 1997). Kv4 channels are targeted to the soma and dendrites but not to the axon (Sheng et al., 1992). This targeting is mediated, at least in part, by a highly conserved domain that contains two leucines, the di-leucine motif, which is located in the C-terminus of Kv4 channels (Rivera et al., 2003). Kv4 channels whose di-leucine motif had been deleted showed a different distribution pattern from the wild type, as they inserted in the axon and in the proximal region of the dendrites.

Kv4 channels mediate an A-type current in cardiac muscle, often referred to as the I_{TO} current (Dixon et al., 1996). In ventricular myocytes, Kv4.2 channels are more abundant in the T-tubules (Takeuchi et al., 2000), although the mechanism responsible for the spatial distribution of Kv4 channels in myocytes is not known. The main function of Kv4 channels in cardiac muscle is to shape the re-polarization phase of the action potential. Thus, the I_{TO} current produces most of the re-polarization phase of the cardiac action potential of small mammals (e.g. mouse) and the initial, rapid phase of

the complex re-polarization of the cardiac action potential of larger mammals (e.g. human) (Sanguinetti, 2002). Kv4 channels carry the A-type currents in smooth muscle (Amberg et al., 2002b) although the role of these currents in the physiology of smooth muscle contraction is not well understood. The A-type current of colonic myocytes has a midpoint of inactivation of –65 mV, and the membrane potential between slow waves in this tissue is about –60 mV, which suggest that these channels have a role in re-polarizing the membrane between slow waves (Amberg et al., 2002a). Furthermore, the steady-state inactivation curve for these smooth muscle Kv4 channels is very steep, which supports their role in the maintenance of the membrane potential, because this type of inactivation curve implies that small changes in membrane voltage result in large changes in the proportion of the Kv4 channels that are available for activation (Amberg et al., 2002a).

Relationship between structure and function in Kv4 channels

The Kv4 gene subfamily in mammals comprises three genes, which are: Kv4.1 (Pak et al., 1991), Kv4.2 (Roberds and Tamkun, 1991), and Kv4.3 (Serôdio et al., 1996). A comparison between the predicted amino acid sequences of the three mammalian Kv4 channel isoforms revealed that the sequences of the six trans-membrane segments (S1-S6) and the N-terminal domain are highly conserved. In contrast, the C-terminal domain of these channels is highly variable (Pak et al., 1991). The diversity of mammalian Kv4 channels is further increased by alternative splicing. For example, alternative splicing of the Kv4.3 gene isoform generates at least three

different Kv4.3 channels (Kong et al., 1998; Takimoto et al., 1997). In addition, it has been shown that heteromeric channels formed by Kv4.2 and Kv4.3 subunits are functional and occur *in vivo* (Guo et al., 2002). Interestingly, these authors demonstrated that myocytes expressing a dominant negative Kv4.2 channel but functional Kv4.3 channels do not produce A-type currents, suggesting that the I_{TO} current is produced by heteromeric Kv4.2/Kv4.3 channels.

Activation of Kv4 channels is relatively rapid and voltage-dependent, as for all Kv channels (previous section). Currents produced by Kv4 channels are transient, A-type currents that inactivate significantly within ~ 100 ms, although the mechanism(s) responsible for rapid inactivation kinetics is not fully understood. The decay of Kv4.1 channel currents can be fitted by the sum of three exponentials, where the first (fast) exponential process contributes relatively little to inactivation (less than 20 %), whereas the second (intermediate) and third (slow) components of inactivation each contribute approximately 40% to the total decay (Jerng and Covarrubias, 1997). However, inactivation of Kv4.2 channels can be satisfactorily fitted with a bi-exponential function, where the first component contributes most to current decay (~73%) and a second component contributes a further ~23% to inactivation. Fitting the decay phase of currents produced by Kv4.2 channels to a three exponent function revealed the presence of a third component of inactivation, but its contribution to current decay is minimal, approximately 4% (Bähring et al., 2001a).

In contrast with Kv1 (*Shaker*) channels, where deletion of the N-terminus (first 20 amino acids) completely abolished fast inactivation (Hoshi et al., 1990), deletion of

the N-terminus (first 30 or 40 amino acids) of Kv4 channels slows inactivation, but does not prevent a relatively fast current decay, and therefore does not eliminate the transient nature of Kv4 currents. Moreover, deleting the N-terminus has different effects on the inactivation of currents produced by the three Kv4 isoforms. For instance, while this deletion abolishes the fast component of inactivation of Kv4.1 channels (Pak et al., 1991; Jerng and Covarrubias, 1997), it only slows the same component of Kv4.2 channels, without eliminating it (Bähring et al., 2001a). A C-terminal region (between amino acids 420-550) that is positively charged appears to have a role in fast inactivation of Kv4.1 channels, since deletion of this region abolished the fast component of inactivation. Jerng and Covarrubias (1997) proposed that the C-terminus of Kv4 channels has a role in stabilizing the N-terminus of these channels near the cytoplasmic side of the pore. This suggestion was based on the fact that the N-terminus of Kv4 channels is hydrophobic, unlike the N-terminus of *Shaker*, which is positively charged, a property that facilitates its attraction to the inner mouth of the pore.

It is not known whether Kv4 channels exhibit C-type inactivation. C-type inactivation of *Shaker* is prevented by tetraethylamonium (Choi et al., 1991), and is slowed by a high external potassium concentration (Baukrowitz and Yellen, 1995), whereas these two factors do not appear to affect inactivation of Kv4.1 (Jerng and Covarrubias, 1997) or Kv4.2 channels (Bähring et al., 2001c). Occlusion of the inner mouth of the channel, in the open state, by the inactivation particle causes inactivation of *Shaker* (Hoshi et al., 1990), and therefore it is said that *Shaker* inactivates from the open state. However, it appears that inactivation of Kv4 channels from the open state is

transient, and most of the inactivation of these channels occurs from the closed state (Bähring et al., 2001a; Gebauer et al., 2004).

Another characteristic of Kv4 channels is their relatively rapid recovery from inactivation. Heterologously expressed Kv4 channels recover from inactivation with time constants of a few hundreds of milliseconds (*e.g.* Serôdio et al., 1994), whereas Kv channels from other subfamilies that also produce A-type currents recover from inactivation with slower time constants (~ 0.5-5 s for Kv1.4: Roeper et al., 1997).

Modulation of Kv4 channels

Like other Kv channels, Kv4 channels can be, in theory, directly phosphorylated since they contain sites for phosphorylation by protein kinase A (PKA), protein kinase C (PKC) and mitogen-activated protein kinase ERK (Adams et al., 2000; Anderson et al., 2000; Baldwin et al., 1991). However, the effect of protein kinases on the activity of Kv4 channels is dependent on the expression system. For example, phosphorylation of Kv4.2 channels in their native environment by PKA and PKC shifted their midpoint of activation in the depolarizing direction, and thus, more depolarization was required to activate the same number of phosphorylated than unphosphorylated channels (Hoffman and Johnston, 1998). However, PKC phosphorylation of Kv4.2 channels that were heterologously expressed in *Xenopus* ooctyes reduced current amplitude, an effect mediated by a decrease in single channel conductance (Nakamura et al., 1997).

Data from Yuan et al. (2002) provide clues as to the causes of this discrepancy. These authors demonstrated that PKC and PKA may not directly phosphorylate the channel protein in its native environment, even though these channels have phosphorylation sites for PKA and PKC. Instead, they may phosphorylate other substrates that converge onto mitogen-activated protein kinases (MAPKs) and it is this kinase that phosphorylates the channel.

Kv4 channels do not appear to be directly modulated by palmitoylation or glycosylation, as noted in Birnbaum et al. (2004). Although removal of sialic acid with neuraminidase has been shown to decrease the cardiac I_{TO} current (Ufret-Vincenty et al., 2001). This must be an indirect effect, as a Prosite scan (http://ca.expasy.org/prosite) revealed that Kv4 channels do not have glycosylation sites in their regions that are exposed to the extracellular medium.

Modulation by K^+ channel interacting proteins (KChIPs)

Kv4 channels have different properties when expressed heterologously than when recorded *in situ*, and these native properties were restored by co-expressing these channels with total mRNA, which was a good first indication that these channels are modulated by other proteins (Serôdio et al., 1994). A hallmark property of Kv4 channels that was restored upon co-expression with total mRNA was a fast recovery from inactivation (Serôdio et al., 1994). Further investigations revealed the identities of these accessory modulatory proteins of mammalian Kv4 channels (see Chapter 3, Introduction), an aspect that is extensively covered in a recent review on Kv4 channels

(Birnbaum et al., 2004). Of all the proteins that associate with Kv4 channels and modulate their expression levels and/or biophysical parameters, the KChIPs are the best studied. KChIPs are EF-hand containing proteins that belong to the recoverin/neuronal calcium sensor super-family of Ca^{2+} binding proteins (Burgoyne and Weiss, 2001). Mammalian tissues express four KChIP isoforms (KChIP1-3: An et al., 2000; KChIP4: Morohashi et al., 2002). KChIP isoforms 1 to 3 increase the amplitude of the Kv4 currents (An et al., 2000). This effect is mediated through binding to the N-terminus of Kv4 channels, since the N-termini of Kv4 channels contain a large proportion of hydrophobic residues that. Thus, by hiding these hydrophobic residues KChIPs facilitate the trafficking of the vesicles from the ER to the Golgi apparatus, and to the plasma membrane, since the channels embedded in the membrane of these vesicles have their N-terminus in contact with the aqueous cytoplasm (Shibata et al., 2003). This proposed mechanism of augmentation of A-type current is supported by the finding that increases in the amplitude of the Kv4 currents by KChIPs are not the result of an increase in single channel conductance (Beck et al., 2002). The physical association between Kv4 and KChIP occurs in the endoplasmic reticulum and depends, in some cases, on palmitoylation of KChIPs, since mutation of the palmitoylation sites of KChIP2 correlated with a decrease in the expression of Kv4 channels in the plasma membrane (Takimoto et al., 2002). Unlike the KChIP isoforms 1-3, KChIP4 does not increase the amplitude of the Kv4 currents and does not appear to have a function as a chaperone (Holmqvist et al., 2002; Shibata et al., 2003).

The N-termini of Kv4 channels have at least two domains that bind to KChIPs; one comprises amino acids 7-11 and another comprises amino acids 71-90. Most residues of the first region are hydrophobic and are thought to bind to a similarly hydrophobic region of KChIP, whereas the residues of the second domain are mostly hydrophilic and are thought to form a dock for KChIP; in addition, this second domain is sufficient for binding to KChIP (Scannevin et al., 2004).

Besides increasing Kv4 current density by facilitating the transport of the Kv4-containing vesicles to the plasma membrane (Shibata et al., 2003), KChIPs modulate many different biophysical parameters of all three Kv4 channel isoforms. For example, KChIPs 1 to 3 shift the midpoint of activation of Kv4.2 currents in a hyperpolarizing direction (An et al., 2000; Van Hoorick et al., 2003), which implies that the extent of depolarization required to activate a certain number of Kv4.2 channels is less when these channels are associated with KChIPs than when they are not. In contrast, KChIP4 shifts the activation midpoint of Kv4 channels in a depolarizing direction (Holmqvist et al., 2002). KChIP1 accelerates activation of Kv4.1 (Beck et al., 2002) and Kv4.2 channels (Nakamura et al., 2001) but not of Kv4.3 channels (Beck et al., 2002). In contrast, KChIP4 slows activation of Kv4 channels (Holmqvist et al., 2002). KChIP1 enhances inactivation of Kv4.1 and Kv4.3 channels by accelerating the process of inactivation from the closed state (Beck et al., 2002). The KChIP2 and KChIP3 isoforms moderately slow inactivation of Kv4 channels (An et al., 2000), while the KChIP4a isoform is more effective in slowing inactivation of all Kv4 channels so that current passing through these channels resemble delayed rectifier currents (Holmqvist et

al., 2002). Because KChIP binds to the N-terminus of Kv4 channels (An et al., 2000; Bähring et al., 2001b; Scannevin et al., 2004), and this domain is involved in inactivation of these channels, it seems likely that the slowing effect of most KChIPs on inactivation kinetics is exerted by physically hindering the mobility of the N-terminus.

KChIP subunits bind to Kv4 channels in the hearts of small and large mammals and thus modulate the parameters of the I_{TO} current (Guo et al., 2002). In the heart of large mammals (*e.g.* human, dog), there is a gradient of density of I_{TO} current across the ventricular wall, with the current density being greater in the epicardium than in the endocardium (Liu et al., 1993). This gradient is not correlated with differential spatial expression of Kv4 channel mRNA across the ventricular wall, but to increased levels of KChIP mRNA in the epicardium relative to the endocardium (Rosati et al., 2001).

1.3 Rationale and thesis organization

In this Introduction, I have described the biophysical properties and modulation of the three mammalian Kv4 channel isoforms. In some cases, the differences in the biophysical properties of these isoforms can be attributed to differential modulation in different cells where they are expressed, for example by different accessory subunits and phosphorylation events in their native environment. However, different Kv4 channel isoforms heterologously expressed in the same system produce currents with distinct biophysical parameters. The three genes that form the mammalian Kv4 gene subfamily likely arose from a single original gene of an ancestral chordate; since many

vertebrate multi-gene families are represented by single gene families in the genome of *Ciona intestinalis*, http://genome.jgi-f.org/ciona4/ciona4.home.html (Dehal et al., 2002), a species that belongs to the most primitively branching clade of the chordates, the Urochordata, or tunicates (Adoutte et al., 2000).

Several BLAST searches for Kv4 genes in the genome of *Ciona intestinalis*, using the deduced amino acid sequences of several Kv4 channels from GenBank, resulted in one robust hit, in scaffold[1] 168 (release version 1.0 of this genome), which indicated that this genome contains, not surprisingly, only one gene for Kv4 channels. The characterization of biophysical parameters of this Kv4 channel could help identifying the biophysical characteristics that might represent evolutionary innovations, if they are exclusive to some or all of the three mammalian isoforms. It seems likely that modifications to the biophysical parameters of the Kv4 channels that were acquired during the evolution of the vertebrates contributed to the development of new excitability features of nerve and muscle tissue. Recently, a Kv4 channel from the tunicate *Halocynthia roretzi* was characterized (Nakajo et al., 2003), but data were insufficient to compare the biophysical properties of this tunicate Kv4 channel with the well-characterized biophysical properties of jellyfish (Jegla and Salkoff, 1997), arthropod (Baro et al., 1996) and mammalian Kv4 channels.

Because Kv4 channels play a crucial role in determining the properties of excitable tissues, it seemed plausible that the myocardium of *Ciona intestinalis* (Fig. 1-

[1] To sequence the genome of *Ciona intestinalis*, the genomic DNA from the sperm of a specimen was sheared into fragments of about 3 kb in size, which were cloned into plasmids and then sequenced. The sequences that overlapped were assembled into scaffolds (Dehal et al., 2000).

2), which has long been regarded as a primitive model of the vertebrate heart (Morad and Cleeman, 1980), would express this Kv4 channel gene. A major reason for this supposition is that re-polarization of the action potential of vertebrate cardiac myocytes is complex and mediated by Kv4-dependent A-type currents. The tunicate heart also generates action potentials with several re-polarization phases (Kriebel, 1967).

An interesting feature of Kv4 channels is their modulation by several accessory subunits. In particular, modulation of Kv4 channels by KChIPs is well described. BLAST searches in the genome of *Ciona intestinalis* identified only one gene for KChIP subunits. Because modulation by KChIPs appears to be a general feature of Kv4 channels, it is likely an ancient mechanism for increasing the diversity of biophysical phenotypes of Kv4 channels. However, no KChIPs have been isolated from invertebrates, making the cloning and co-expression of a KChIP with a Kv4 channel from a representative of an early chordate a valuable contribution.

Chapter 2 describes the genomic structure, the sequence and the characterization of the biophysical properties of a wild type Kv4 channel that is expressed in the myocardium of the basal chordate *Ciona intestinalis* (*Ciona*Kv4). Chapter 3 provides a description of the genomic structure, nucleotide and amino acid sequence of a KChIP-like subunit that is also expressed in the myocardium of *Ciona intestinalis* (*Ciona*KChIP), and a description of the effects of *Ciona*KChIP on the biophysical activity of *Ciona*Kv4.

Since the N-termini of mammalian Kv4 channels have a dual role as an inactivation particle (as explained in section in section 1.1) and as a binding site for

KChIPs (as explained in section 1.2), I created an N-truncation mutant of *Ciona*Kv4 that lacked the first 2-32 amino acids (nt*Ciona*Kv4), since a similar deletion has been used to study the role of the N-terminus in mammalian Kv4 channels (*e.g.* Pak et al., 1991). The biophysical properties of *Ciona*Kv4 and nt*Ciona*Kv4 are compared in Chapter 2. To evaluate the role of the N-terminus of *Ciona*Kv4 in binding to and modulation by *Ciona*KChIP, nt*Ciona*Kv4 was co-expressed with *Ciona*KChIP. The results of these experiments are included in Chapter 3, and compared with the results of co-expressing wild-type *Ciona*Kv4 channels with *Ciona*KChIP subunits.

The data provided by this thesis is central for discussing the possible conserved and adaptive features of Kv4 channels in Chapter 4. In this Chapter, I also discuss the possible evolution of Kv4 channels and KChIP subunits within the vertebrate lineage. Finally, I discuss the possible implications of the data presented in this thesis for the function of the tunicate heart.

A

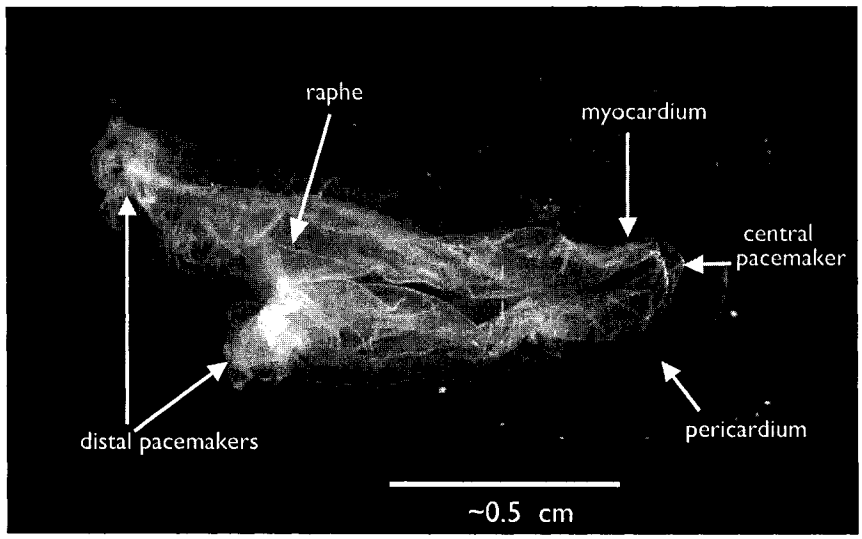

B

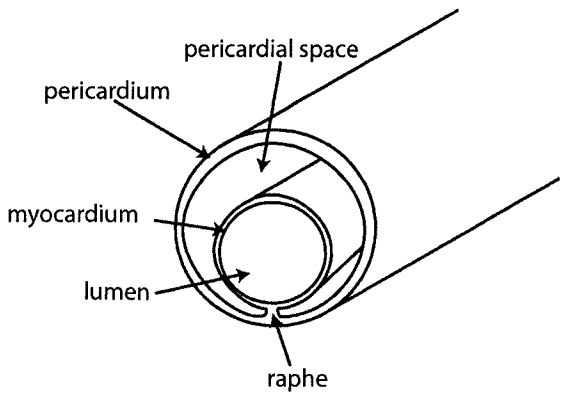

Figure 1-2. Structure of the V-shaped heart of *Ciona intestinalis*. *A*, Photograph of the whole heart structure, indicating the major features. *B*, diagram of a transverse section of one of the arms of this heart. The myocardium is a tubular structure whose walls are a monolayer of musculoendothelial cells. The pericardium is a tubular structure external to the myocardium, and attached to the latter along its length by connective tissue, the raphe (Oliphant and Cloney, 1972). Contractions are initiated at each end of the heart, by the distal pacemakers; occassionally, contractions are initiated from the middle part of the heart, which suggests that another pacemaker is located in this region (Kriebel, 1968).

1.4 Literature cited

Adams JP, Anderson AE, Varga AW, Dineley KT, Cook R, Pfaffinger PJ, Sweatt JD (2000) The A-type potassium channel Kv4.2 is a substrate for the mitogen-activated protein kinase ERK. J Neurochem 75:2277-2287

Adoutte A, Balavoine G, Lartillot N, Lespinet O, Prud'homme, B, de Rosa R (2000) The new animal phylogeny: Reliability and implications. Proc Natl Acad Sci USA 97:4453-4456

Amberg GC, Baker SA, Koh SD, Hatton WJ, Murray KJ, Horowitz B, Sanders KM (2002a) Characterization of the A-type potassium current in murine gastric antrum. J Physiol 544:417-428

Amberg GC, Koh SD, Hatton WJ, Murray K, Monaghan K, Horowitz B, Sanders KM (2002b) Contribution of Kv4 channels toward the A-type potassium current in murine colonic myocytes. J Physiol 544:403-415

An WF, Bowlby MR, Betty M, Cao J, Ling HP, Mendoza G, Hinson JW, Mattsson KI, Strassle BW, Trimmer JS, Rhodes KJ (2000) Modulation of A-type potassium channels by a family of calcium sensors. Nature 403:553-556

Anderson AE, Adams JP, Qian Y, Cook RG, Pfaffinger PJ, Sweatt JD (2000) Kv4.2 phosphorylation by cyclic AMP-dependent protein kinase. J Biol Chem 275:5337-5346

Bähring R, Boland LM, Varghese A, Gebauer M, Pongs O (2001a) Kinetic analysis of open- and closed-state inactivation transitions in human Kv4.2 A-type potassium channels. J Physiol 535:65-81

Bähring R, Dannenberg J, Peters HC, Leicher T, Pongs O, Isbrandt D (2001b) Conserved Kv4 N-terminal domain critical for effects of Kv channel-interacting protein 2.2 on channel expression and gating. J Biol Chem 276:23888-23894

Bähring R, Milligan CJ, Vardanyan V, Engeland B, Young BA, Dannenberg J, Waldschutz R, Edwards JP, Wray D, Pongs O (2001c) Coupling of voltage-dependent potassium channel inactivation and oxidoreductase active site of Kvβ subunits. J Biol Chem 276:22923-22929

Baldwin TJ, Tsaur ML, Lopez GA, Jan YN, Jan LY (1991) Characterization of a mammalian cDNA for an inactivating voltage-sensitive K^+ channel. Neuron 7:471-483

Baro DJ, Coniglio LM, Cole CL, Rodriguez HE, Lubell JK, Kim MT, Harris-Warrick RM (1996) Lobster *shal*: comparison with *Drosophila shal* and native potassium currents in identified neurons. J Neurosci 16:1689-1701

Baro DJ, Quiñones L, Lanning CC, Harris-Warrick RM, Ruiz M (2001) Alternate splicing of the *shal* gene and the origin of I_A diversity among neurons in a dynamic motor network. Neuroscience 106:419-432

Baukrowitz T, Yellen G (1995) Modulation of K^+ current by frequency and external $[K^+]$: a tale of two inactivation mechanisms. Neuron 15:951-960

Beck EJ, Bowlby M, An WF, Rhodes KJ, Covarrubias M (2002) Remodelling inactivation gating of Kv4 channels by KChIP1, a small-molecular-weight calcium-binding protein. J Physiol 538:691-706

Birnbaum SG, Varga AW, Yuan L-L, Anderson AE, Sweatt JD, Schrader LA (2004) Structure and function of Kv4-family transient potassium channels. Physiol Rev 84:803-833

Burgoyne RD, Weiss JL (2001) The neuronal calcium sensor family of Ca^{2+}-binding proteins. Biochem J 353:1-12

Butler A, Wei A, Baker K, Salkoff L (1989) A family of putative potassium channel genes in *Drosophila*. Science 243:943-947

Cha A, Bezanilla F (1997) Characterizing voltage-dependent conformational changes in the *Shaker* K^+ channel with fluorescence. Neuron 19:1127-1140

Cha A, Snyder GE, Selvin PR, Bezanilla F (1999) Atomic scale movement of the voltage-sensing region in a potassium channel measured via spectroscopy. Nature 402:809-813

Choi KL, Aldrich RW, Yellen G (1991) Tetraethylammonium blockade distinguishes two inactivation mechanisms in voltage-activated K^+ channels. Proc Nat Acad Sci USA 88:5092-5095

Christie MJ, Adelman JP, Douglass J, North RA (1989) Expression of a cloned rat brain potassium channel in *Xenopus* oocytes. Science 244:221-224

Christie MJ, North RA, Osborne PB, Douglass J, Adelman J (1990) Heteropolymeric potassium channels expressed in *Xenopus* oocytes from cloned subunits. Neuron 4:405-411

Connor JA, Stevens CF (1971) Voltage clamp studies of a transient outward membrane current in gastropod neural somata. J Physiol 213:21-30

Covarrubias M, Wei AA, Salkoff L (1991) *Shaker*, *Shal*, *Shab*, and *Shaw* express independent K^+ current systems. Neuron 7:763-773

Covarrubias M, Wei A, Salkoff L, Vyas TB (1994) Elimination of rapid potassium channel inactivation by phosphorylation of the inactivation gate. Neuron 13:1403-1412

Cushman SJ, Nanao MH, Jahng AW, DeRubeis D, Choe S, Pfaffinger PJ (2000) Voltage dependent activation of potassium channels is coupled to T1 domain structure. Nat Struct Biol 7:403-407

Dixon JE, Shi W, Wang H-S, McDonald C, Yu H, Wymore RS, Cohen IS, McKinnon D (1996) Role of the Kv4.3 K^+ channel in ventricular muscle. A molecular correlate for the transient outward current. Circ Res 79:659-668

Dehal P, Satou Y, Campbell RK, Chapman J, Degnan B, De Tomaso A, Davidson B, Di Gregorio A, Gelpke M, Goodstein DM, Harfuji N, Hastings KEM, Ho I, Hotta K, Huang W, Kawashima T, Lemaire P, Martinez D, Meinertzhagen IA, Necula S, Nonaka M, Putnam N, Rash S, Saiga H, Satake M, Terry A, Yamada L, Wang H-G, Awazu S, Azumi K, Boore J, Branno M, Chin-bow S, DeSantis R, Doyle S, Francino P, Keys DN, Haga S, Hayashi H, Hino K, Imai KS, Inaba K, Kano S, Kobayashi K, Kobayashi M, Lee B-I, Makabe KW, Manohar C, Matassi G, Median M, Mochizuki Y, Mount S, Morishita T, Miura S, Nakayama A, Nishizaka S, Nomoto H, Ohta F, Oishi K, Rigoutsos I, Sano M, Sasaki A, Sasakura Y, Shoguchi E, Sin-I T, Sapagnuolo A, Stainier D, Suzuki MM, Tassy O, Takatori N, Tokuoka M, Yagi K, Yoshizaki F, Wada S, Zhang C, Hyatt PD, Larimer F, Detter C, Doggett N, Glavina T, Hawkins T, Richardson P, Lucas S, Kohara Y, Levine M, Satoh N, Rokhsar DS (2002) The draft genome of *Ciona intestinalis*: Insights into chordate and vertebrate origins. Science 298:2157-2167

Doyle DA, Cabral JM, Pfuetzner RA, Kuo A, Gulbis JM, Cohen SL, Chait BT, MacKinnon, R (1998) The structure of the potassium channel: Molecular basis of K^+ conduction and selectivity. Science 280:69-77

Fink M, Duprat F, Lesage F, Heurteaux C, Romey G, Barhanin J, Lazdunski M (1996) A new K^+ channel beta subunit to specifically enhance Kv2.2 (CDRK) expression. J Biol Chem 271:26341-26348

Gebauer M, Isbrandt D, Sauter K, Callsen B, Nolting A, Pongs O, Bähring R (2004) N-type inactivation features of Kv4.2 channel gating. Biophys J 86:210-223

Glauner KS, Mannuzzu LM, Gandhi CS, Isacoff EY (1999) Spectroscopic mapping of voltage sensor movement in the *Shaker* potassium channel. Nature 402:813-817

Gulbis JM, Zhou M, Mann S, MacKinnon R (2000) Structure of the cytoplasmic β subunit-T1 assembly of voltage-dependent K^+ channels. Science 289:123-127

Guo W, Li H, Aimond F, Johns DC, Rhodes KJ, Trimmer JS, Nerbonne JM (2002) Role of heteromultimers n the generation of myocardial transient outward K^+ currents. Circ Res 90:586-593

Hille B (1992) Ionic channels of excitable membranes (2nd ed.). Sunderland, MA: Sinauer

Ho K, Nichols CG, Lederer WJ, Lytton J, Vassilev PM, Kanazirska MV, Hebert SC (1993) Cloning and expression of an inwardly rectifying ATP-regulated potassium channel. Nature 362:31-38

Hodgkin AL, Huxley AF (1952) Currents carried by sodium and potassium ions through the membrane of the giant axon of *Loligo*. J Physiol 116:449-472

Hoffman DA, Johnston D (1998) Downregulation of transient K^+ channels in dendrites of hippocampal CA1 pyramidal neurons by activation of PKA and PKC. J Neurosci 18:3521-3528

Hoffman DA, Magee JC, Colbert CM, Johnston D (1997) K^+ channel regulation of signal propagation in dendrites of hippocampal pyramidal neurons. Nature 387:869-875

Holmqvist MH, Cao J, Hernandez-Pineda R, Jacobson MD, Carroll KI, Sung MA, Betty M, Ge P, Gilbride KJ, Brown ME, Jurman ME, Lawson D, Silos-Santiago I, Xie Y, Covarrubias M, Rhodes KJ, Distefano PS, An WF (2002) Elimination of fast inactivation in Kv4 A-type potassium channels by an auxiliary subunit domain. Proc Natl Acad Sci USA 99:1035-1040.

Hoshi T, Zagotta WN, Aldrich RW (1990) Biophysical and molecular mechanisms of *Shaker* potassium channel inactivation. Science 250:533-538

Hoshi T, Zagotta WN, Aldrich RW (1991) Two types of inactivation in *Shaker* K^+ channels: effects of alterations in the carboxy-terminal region. Neuron 7:547-556

Isacoff EY, Jan YN, Jan LY (1990) Evidence for the formation of heteromultimeric potassium channels in *Xenopus* oocytes. Nature 345:530-534

Isacoff EY, Jan YN, Jan LY (1991) Putative receptor for the cytoplasmic inactivation gate in the Shaker K^+ channel. Nature 353:86-90

Jan LY, Jan YN (1990) How might the diversity of potassium channels be generated? Trends Neurosci 13:415-419

Jegla T, Grigoriev N, Gallin WJ, Salkoff L, Spencer AN (1995) Multiple *Shaker* potassium channels in a primitive metazoan. J Neurosci 15:7989-7999

Jegla T, Salkoff L (1996) A multigene family of novel K^+ channels from *Paramecium tetraurelia*. Receptors Channels 3:51-60

Jegla T, Salkoff L (1997) A novel subunit for Shal potassium channels radically alters activation and inactivation. J Neurosci 17:32-44

Jerng HH, Covarrubias M (1997) K^+ channel inactivation mediated by the concerted action of the cytoplasmic N- and C-terminal domains. Biophys J 72:163-174

Jiang Y, Ruta V, Chen J, Lee A, MacKinnon R (2003) The principle of gating charge movement in a voltage-dependent K^+ channel. Nature 423:42-48

Jiang QX, Wang DN, MacKinnon R (2004) Electron microscopic analysis of KvAP voltage-dependent K^+ channels in an open conformation. Nature 430:806-810

Kamb A, Iverson LE, Tanouye MA (1987) Molecular characterization of *Shaker*, a *Drosophila* gene that encodes a potassium channel. Cell 50:405-413

Khanna R, Myers MP, Lainé M, Papazian DM (2001) Glycosylation increases potassium channel stability and surface expression in mammalian cells. J Biol Chem 276:34028-34034

Kong W, Po S, Yamagishi T, Ashen MD, Stetten G, Tomaselli GF (1998) Isolation and characterization of the human gene encoding Ito: further diversity by alternative mRNA splicing. Am J Physiol 275:H1963-H1970

Kramer JW, Post MA, Brown AM, Kirsch GE (1998) Modulation of potassium channel gating by coexpression of Kv2.1 with regulatory Kv5.1 or Kv6.1 α-subunits. Am J Physiol 274:C1501-C1510

Kriebel ME (1967) Conduction velocity and intracellular action potentials of the tunicate heart. J Gen Physiol 50:2097-2107

Kriebel ME (1968) Studies on cardiovascular physiology of tunicates. Biol Bull 134:434-455

Kreusch A, Pfaffinger PJ, Stevens CF, Choe S (1998) Crystal structure of the tetramerization domain of the *Shaker* potassium channel. Nature 392:945-948

Lainé M, Papazian DM, Roux B (2004) Critical assessment of a proposed model of Shaker. FEBS Lett 564:257-263

Leicher T, Bähring R, Isbrandt D, Pongs O (1998) Coexpression of the KCNA3B gene product with Kv1.5 leads to a novel A-type potassium channel. J Biol Chem 273:35095-35101

Leonard RJ, Karschin A, Jayashree-Aiyar S, Davidson N, Tanouye MA, Thomas L, Thomas G, Lester HA (1989) Expression of *Drosophila* Shaker potassium channels in mammalian cells infected with recombinant vaccinia virus. Proc Nat Acad Sci USA 86:7629-7633

Li M, Jan YN, Jan LY (1992) Specification of subunit assembly by the hydrophilic amino-terminal domain of the *Shaker* potassium channel. Science 257:1225-1230

Liu DW, Gintant GA, Antzelevitch C (1993) Ionic bases for electrophysiological distinctions among epicardial, midmyocardial, and endocardial myocytes from the free wall of the canine left ventricle. Circ Res 72:671-687

López-Barneo J, Hoshi T, Heinemann SH, Aldrich RW (1993) Effects of external cations and mutations in the pore region on C-type inactivation of *Shaker* potassium channels. Receptors Channels 1:61-71

MacKinnon R (1991) Determination of the subunit stoichiometry of a voltage-activated potassium channel. Nature 350:232-235

Morad M, Cleemann L (1980) Tunicate heart a possible model for the vertebrate heart. Fed Proc 39:3188-3194

Morohashi Y, Hatano N, Ohya S, Takikawa R, Watabiki T, Takasugi N, Imaizumi Y, Tomita T, Iwatsubo T (2002) Molecular cloning and characterization of CALP/KChIP4, a novel EF-hand protein interacting with presenilin 2 and voltage-gated potassium channel subunit Kv4. J Biol Chem 277:14965-14975

Nakahira K, Shi G, Rhodes KJ, Trimmer JS (1996) Selective interaction of voltage-gated K^+ channel β-subunits with α-subunits. J Biol Chem 271:7084-7089

Nakajo K, Katsuyama Y, Ono F, Ohtsuka Y, Okamura Y (2003) Primary structure, functional characterization and developmental expression of the ascidian Kv4-class potassium channel. Neurosci Res 45:59-70

Nakamura TY, Coetzee WA, Vega-Saenz de Miera E, Artman M, Rudy B (1997) Modulation of Kv4 channels, key components of rat ventricular transient outward K^+ current, by PKC. Am J Physiol 273:H1775-H1786

Nakamura TY, Nandi S, Pountney DJ, Artman M, Rudy B, Coetzee WA (2001) Different effects of the Ca^{2+} -binding protein, KChIP1, on two Kv4 subfamily members, Kv4.1 and Kv4.2. FEBS Lett 499:205-209

Neher E (1971) Two fast transient current components during voltage clamp on snail neurons. J Gen Physiol 58:36-53

Ogielska EM, Zagotta WN, Hoshi T, Heinemann SH, Haab J, Aldrich RW (1995) Cooperative subunit interactions in C-type inactivation of K channels. Biophys J:69:2449-2457

Oliphant LW, Cloney RA (1972) The ascidian myocardium: sarcoplasmic reticulum and excitation-contraction coupling. Z. Zellforch 129:395-412

Pak MD, Baker K, Covarrubias M, Butler A, Ratcliffe A, Salkoff L (1991) mShal, a subfamily of K^+ channel cloned from mammalian brain. Proc Nat Acad Sci USA 88:4386-4390

Papazian DM, Schwarz TL, Tempel BL, Jan YN, Jan LY (1987) Cloning of genomic and complementary DNA from *Shaker,* a putative potassium channel gene from *Drosophila.* Science 237:749-753

Papazian DM, Timpe LC, Jan YN, Jan LY (1991) Alteration of voltage-dependence of *Shaker* potassium channel by mutations in the S4 sequence. Nature 349:305-310

Parcej DN, Dolly JO (1989) Dendrotoxin acceptor from bovine synaptic plasma membranes. Binding properties, purification and subunit composition of a putative constituent of certain voltage-activated K^+ channels. Biochem J 257:899-903

Peretz T, Levin G, Moran O, Thornhill WB, Chikvashvili D, Lotan I (1996) Modulation by protein kinase C activation of rat brain delayed-rectifier K^+ channel expressed in *Xenopus* oocytes. FEBS Lett 381:71-76

Rehm H, Lazdunski M (1988) Purification and subunit structure of a putative K^+-channel protein identified by its binding properties for dendrotoxin I. Proc Natl Acad Sci USA 85:4919-4923

Rivera JF, Ahmad S, Quick MW, Liman ER, Arnold DB (2003) An evolutionarily conserved di-leucine motif in Shal K^+ channels mediates dendritic targeting. Nat Neurosci 6:243-250

Roberds SL, Tamkun MM (1991) Cloning and tissue-specific expression of five voltage-gated potassium channel cDNAs expressed in rat heart. Proc Nat Acad Sci USA 88:1798-1802

Roeper J, Lorra C, Pongs O (1997) Frequency-dependent inactivation of mammalian A-type K^+ channel Kv1.4 regulated by Ca^{2+}/calmodulin-dependent protein kinase. J Neurosci 17:3379-3391

Rosati B, Pan Z, Lypen S, Wang H-S, Cohen I, Dixon JE, McKinnon D (2001) Regulation of *KChIP2* potassium channel β subunit gene expression underlies the gradient of transient outward current in canine and human ventricle. J Physiol 533:119-125

Ruppersberg JP, Schroter KH, Sakmann B, Stocker M, Sewing S, Pongs O (1990) Heteromultimeric channels formed by rat brain potassium-channel proteins. Nature 345:535-537

Salinas M, Duprat F, Heurteaux C, Hugnot J-P, Lazdunski M (1997a) New modulatory α subunits for mammalian *Shab* K^+ channels. J Biol Chem 272:24371-24379

Salinas M, de Weille J, Guillemare E, Lazdunski M, Hugnot J-P (1997b) Modes of regulation of *Shab* K^+ channel activity by the Kv8.1 subunit. J Biol Chem 272:8774-8780

Sanguinetti MC (2002) Reduced outward K^+ current and cardiac hypertrophy: causal relationship or epiphenomenon? Circ Res 90:497-499

Santacruz-Toloza L, Huang Y, John SA, Papazian DM (1994) Glycosylation of *Shaker* potassium channel protein in insect cell culture and in *Xenopus* oocytes. Biochemistry 33:5607-5613

Scannevin RH, Wang K, Jow F, Megules J, Kopsco DC, Edris W, Carroll KC, Lü Q, Xu W, Xu Z, Katz AH, Olland S, Lin L, Taylor M, Stahl M, Malakian K, Somers W, Mosyak L, Bowlby MR, Chanda P, Rhodes KJ (2004) Two N-terminal domains of Kv4 K^+ channels regulate binding to and modulation by KChIP1. Neuron 41:587-598

Schoppa NE, McCormack K, Tanouye MA, Sigworth FJ (1992) The size of gating charge in wild-type and mutant Shaker potassium channels. Science 255:1712-1715

Schwarz TL, Tempel BL, Papazian DM, Jan YN, Jan LY (1988) Multiple potassium-channel components are produced by alternative splicing at the *Shaker* locus in *Drosophila*. Nature 331:137-142

Serôdio P, Kentros C, Rudy B (1994) Identification of molecular components of A-type channels activating at subthreshold potentials. J Neurophysiol 72:1516-1529

Serôdio P, Vega-Saenz de Miera E, Rudy B (1996) Cloning of a novel component of A-type K^+ channels operating at subthreshold potentials with unique expression in heart and brain. J Neurophysiol 75:2174-2179

Sewing S, Roeper J, Pongs O (1996) Kvβ1 subunit binding specific for *Shaker*-related potassium channel α subunits. Neuron 16:455-463

Sheng M, Tsaur L, Jan YN, Jan LY (1992) Subcellular segregation of two A-type K^+ channel proteins in rat central neurons. Neuron 9:271-284

Shi G, Nakahira K, Hammond S, Rhodes KJ, Schechter LE, Trimmer JS (1996) β subunits promote K^+ channel surface expression through effects early in biosynthesis. Neuron 16:843-852

Shibata R, Misonou H, Campomanes CR, Anderson AE, Schrader LA, Doliveira LC, Carroll KI, Sweatt JD, Rhodes KJ, Trimmer JS (2003) A fundamental role for KChIPs in determining the molecular properties and trafficking of Kv4.2 potassium channels. J Biol Chem 278:36445-36454

Spiro RG (2000) Glucose residues as key determinants in the biosynthesis and quality control of glycoproteins with *N*-linked oligosaccharides. J Biol Chem 275:35657-35660

Strong M, Chandy KG, Gutman GA (1993) Molecular evolution of voltage-sensitive ion channel genes: On the origins of electrical excitability. Mol Biol Evol 10:221-242

Takeuchi S, Takagishi Y, Yasui K, Murata Y, Toyama J, Kodama I (2000) Voltage-gated K^+ channel, Kv4.2, localizes predominantly to the transverse-axial tubular system of the rat myocyte. J Mol Cell Cardiol 32:1361-1369

Takimoto K, Li D, Hershman KM, Li P, Jackson ED, Levitan ES (1997) Decreased expression of Kv4.2 and novel Kv4.3 K^+ channel subunit mRNAs in ventricles of renovascular hypertensive rats. Circ Res 81:533-539

Takimoto K, Yang EK, Conforti L (2002) Palmitoylation of KChIP splicing variants is required for efficient cell surface expression of Kv4.3 channels. J Biol Chem 277:26904-26911

Tempel BL, Papazian DM, Schwarz TL, Jan YN, Jan LY (1987) Sequence of a probable potassium channel component encoded at *Shaker* locus of *Drosophila*. Science 237:770-775

Tierney AJ, Harris-Warrick RM (1992) Physiological role of the transient potassium current in the pyloric circuit of the lobster stomatogastric ganglion. J Neurophysiol 67:599-609

Timpe LC, Schwarz TL, Tempel BL, Papazian DM, Jan YN, Jan LY (1988) Expression of functional potassium channels from *Shaker* cDNA in *Xenopus* oocytes. Nature 331:143-145

Tsaur ML, Sheng M, Lowenstein DH, Jan YN, Jan LY (1992) Differential expression of K^+ channel mRNAs in the rat brain and down-regulation in the hippocampus following seizures. Neuron 8:1055-1067

Uebele VN, England SK, Chaudhary A, Tamkun MM, Snyders DJ (1996) Functional differences in Kv1.5 currents expressed in mammalian cell lines are due to the presence of endogenous Kvβ2.1 subunits. J Biol Chem 271:2406-2412

Ufret-Vincenty CA, Baro DJ, Santana LF (2001) Differential contribution of sialic acid to the function of repolarizing K^+ currents in ventricular myocytes. Am J Physiol 281:C464-C474

Van Hoorick D, Raes A, Keysers W, Mayeur E, Snyders DJ (2003) Differential modulation of Kv4 kinetics by KCHIP1 splice variants. Mol Cell Neurosci 24:357-366

Yellen G, Jurman ME, Abramson T, MacKinnon R (1991) Mutations affecting internal TEA blockade identify the probable pore-forming region of a K^+ channel. Science 251:939-942

Yool AJ, Schwarz TL (1991) Alteration of ionic selectivity of a K^+ channel by mutation of the H5 region. Nature 349:700-704

Yu W, Xu J, Li M (1996) NAB domain is essential for the subunit assembly of both α-α and α-β complexes of *Shaker*-like potassium channels. Neuron 16:441-453

Yuan LL, Adams JP, Swank M, Sweatt JD, Johnston D (2002) Protein kinase modulation of dendritic K^+ channels in hippocampus involves a mitogen-activated protein kinase pathway. J Neurosci 22:4860-4868

CHAPTER 2 THE STRUCTURE AND FUNCTION OF A Kv4-LIKE POTASSIUM CHANNEL EXPRESSED IN THE MYOCARDIUM OF THE TUNICATE, *Ciona intestinalis*

2.1 Introduction

Drosophila Shal related voltage-gated ion channels are encoded in mammals by the Kv4 gene subfamily (Kv4.1: Pak et al., 1991; Kv4.2: Roberds and Tamkun, 1991; and Kv4.3: Serôdio et al., 1994). Kv4 channels mediate the transient outward current in cardiac myocytes (I_{TO}; Dixon et al., 1996), smooth muscle (Amberg et al., 2002), and neurons (I_{SA}; Serôdio et al., 1994). Interestingly, the expression of Kv4 channel subtypes in the brain is non-uniform, with some areas expressing mostly Kv4.2 channels (*e.g.* caudata putamen), and others expressing Kv4.3 channels predominantly (*e.g.* superior colliculus) (Serôdio et al., 1996). The heart also appears to exhibit a non-overlapping distribution of these two Kv4 channels; in the rat, Kv4.2 channels are highly expressed in the ventricle but not in the atrium, and expression of Kv4.3 channels is higher in the atrium than in the ventricle (Dixon and McKinnon, 1994; Roberds and Tamkun, 1991; Serôdio et al., 1996). Kv4.1 channels are a less common

subtype in brain and heart (Baldwin et al., 1991; Roberds and Tamkun, 1991; Serôdio et al., 1994). To relate the relevant functional parameters of Kv4 channels to the function of the excitable tissues of mammals it should be helpful to compare the structure and function of these mammalian Kv4 isoforms with Kv4 channels from more basal taxa. A few Kv4 (*Shal*) channels have been cloned from invertebrates, including a jellyfish *Shal* (Jegla and Salkoff, 1997), a fly *Shal* (Butler et al., 1989), a spiny lobster *Shal* (Baro et al., 1996) and a tunicate *Shal* (Nakajo et al., 2003). It is presumed that two large-scale genomic duplications occurred during vertebrate evolution, after divergence from the tunicate lineage (Sidow, 1996), which suggests that the gene complement of extant tunicates approximates that of the ancestral chordate. To understand the origin of the vertebrate Kv4 channel isoforms, we investigated, in detail, the biophysical properties of a Kv4 channel of *Ciona intestinalis*, a member of the Urochordata (Tunicates), which are the first branching clade within the chordates.

Because Kv4 channels are essential for producing the characteristic excitability patterns of mammalian cardiac myocytes we chose to isolate Kv4 channel orthologues(s) from the heart of *Ciona intestinalis*. The heart of *Ciona intestinalis* generates relatively complex action potentials (APs) that display three phases of repolarization, with an early partial repolarization immediately after the upstroke (Kriebel, 1967; Anderson, 1968). This first repolarization is reminiscent of phase I (or "notch") of the vertebrate cardiac AP, which is mediated by the *Ito* current carried by Kv4 channels (Dixon et al., 1996). The tunicate heart is formed by a single layer of musculoendothelial cells arranged helically about the long axis (Schulze, 1964). This

tubular structure is surrounded by a mono-layered pericardium to which it attaches, along its length, by connective tissue (Goddard, 1972; Kalk, 1970). Each myocyte has an electrically silent extra-luminal side that faces the pericardial fluid, and an electrically excitable surface that faces the lumen of the heart. Propagation along the luminal face is functionally coupled to contraction (Kriebel, 1973; Weiss and Morad, 1974). Two pacemakers located at each end of the heart generate APs whose repolarization phase lasts ~2 s at 10°C, and propagate at a velocity of ~0.6 to1.2 cm s^{-1} (Kriebel, 1967).

We used the genomic database for *Ciona intestinalis* (http://genome.jgi-psf.org/ciona4/ciona4.home.html) and the Rapid Amplification of cDNA Ends (RACE) technique to detect and amplify Kv4-type channels from heart cDNA. Our data demonstrate that the tunicate heart expresses a Kv4-type channel (*Ciona*Kv4). Currents mediated by *Ciona*Kv4 channels inactivated rapidly when heterologously expressed in *Xenopus* oocytes. Fast inactivation of Kv4 channels differs from fast inactivation of *Shaker*, which occurs by occlusion of the internal side of the pore, in the open state, by the first ~20 amino acids of the N-terminus (Hoshi et al., 1990). In Kv4 channels, fast inactivation is a multi-exponential process that still occurs in Kv4 channels lacking the first ~30 amino acids (Pak et al., 1991). Interestingly, the N-termini of Kv4.1 Kv4.2 and Kv4.3 channels appear to have different roles in fast inactivation and other parameters, and these roles differ between the three subtypes. Whereas deletion of amino acids 2-32 of Kv4.1 channels eliminated the early fast component of inactivation and slowed activation kinetics (Pak et al., 1991; Jerng and Covarrubias, 1997), deletion

of the first ~40 amino acids of Kv4.2 slowed, but did not eliminate the early component of inactivation, and did not alter activation kinetics (Bähring et al., 2001). To evaluate the role of the putative N-terminal inactivation ball of the tunicate Kv4 channel, an N-deletion mutant of *Ciona*Kv4 lacking amino acids 2-32 was constructed (nt*Ciona*Kv4) and its biophysical properties were evaluated and compared with those of wild type channels.

2.2 Materials and Methods

Tissue extraction.

Specimens of *Ciona intestinalis* were purchased from the Marine Biology Laboratory (MBL, Massachusetts, US) and kept in a seawater aquarium at 12°C until used. The heart, enclosed in the pericardium, was excised in DEPC-treated artificial seawater whose composition was (mM): NaCl (425), KCl (9), $CaCl_2$ (9.3), $MgS0_4$ (25.5), $MgCl_2$ (23), HEPES (10). This heart complex was pinned onto a base of Sylgard (Dow Corning) in a Petri dish and the pericardium and raphe (connective tissue that joins the pericardium to the myocardium) were cut away. The isolated myocardium was rinsed in filtered DEPC-treated artificial seawater several times in order to remove any remaining blood cells and cellular debris and then frozen at -80°C.

RT-PCR for Kv4 homologues

Total RNA was extracted from heart tissue (4 to 6 hearts per experiment) using the "Totally RNA" kit (Ambion). Single-stranded cDNA was synthesized with AMV-RT (Invitrogen) at 42° C for 60 min.

Fragments of cDNA were obtained using a polymerase chain reaction (PCR) using primers 1719 and 1723 (Table 2-1) that were designed to bind to regions of a Kv4 transcript encoded by different exons. Each 50 µl PCR reaction contained: 1 x Opti-Prime Buffer (Stratagene) (10 mM Tris•HCl, 1.5 mM $MgCl_2$, 25 mM KCl at pH 8.3), 0.5 unit of Taq polymerase 0.25 mM of each dNTP, 1 µM forward and reverse primer, and 1 µL cDNA. PCR temperatures were: 30 s at 94° C, then 30 x (30 s at 94° C, 1 min. at 55° C and 1 min. at 72° C) followed by 5 min. at 72° C.

Rapid Amplification of cDNA 3' End (3'-RACE)

The GeneRacer Kit (Invitrogen) was used to perform a 3'-RACE assay. Briefly, total RNA was extracted from *Ciona intestinalis* heart tissue and cDNA was synthesized using an oligo-dT primer with unique sequence at the 3' end provided with the kit. Each 50 µl 3'-RACE assay contained: 1 x Opti-Prime Buffer (Stratagene) (10 mM Tris•HCl, 1.5 mM $MgCl_2$, 25 mM KCl at pH 8.3), 0.5 unit of Taq polymerase, 0.25 mM of each dNTP, 1 µM forward primer and reverse primer and 2 µL cDNA. The sense primer (1665, Table 1) bound to an internal sequence of the Kv channel; the anti-sense primer, supplied with the kit, bound to the specific sequence of the oligo-dT primer. The temperature conditions were: 30 s at 94° C, followed by 5x (30 s at 94° C,

30 s at 65° C, 3 min. at 72° C), 25 x (30 s at 94° C, 30 s at 60° C, 3 min. at 72° C) followed by 5 min. at 72° C. The RACE products were sequenced with the forward primers used in this assay. Next, new forward primers were designed to bind downstream within these sequences in nested 3'-RACE assays. Successive nested RACE assays were done until the first 3'-RACE assay product was fully sequenced.

Alignment and phylogenetic tree

Amino acid sequences of a set of eighteen representative Kv4 channels from vertebrates and invertebrates were aligned with T-Coffee software (Notredame et al., 2000). Regions that contained extensive gaps were edited out, leaving a data matrix that includes the T1 domain and the membrane-spanning core (trans-membrane domains S1 to S6), giving a total of 405 characters. MrBayes (Huelsenbeck and Ronquist, 2001) was used to determine the phylogenetic relationships of the channel sequences. The default parameters for protein sequences were used. A total of 200,000 cycles were run; the topology and branch length of every 100^{th} tree was saved. The Bayesian maximum likelihood tree was obtained by taking a consensus of the collected trees after a 101 tree burn-in. The nodes on the tree are labeled with the posterior probability for each node; nodes with a probability of one were left unlabelled. The tree was visualized using Treeview (Page, 1996).

Cloning of full-length cDNA of *Ciona*Kv4

The full-length open reading frame for *Ciona*Kv4 was amplified with sense primers containing the start codon and a Kozak consensus site (a sequence that enhances transcription) for the 5' end, and anti-sense primers designed to bind downstream of the translational termination codon (1729 and 1795, Table 1). Primers also contained restriction sites to allow directional insertion of the PCR products into pXT7 (Dominguez et al., 1995). Each 50 μL PCR reaction contained: 1 x Opti-Prime Buffer (Stratagene) (10 mM Tris•HCl, 1.5 mM $MgCl_2$, 25 mM KCl at pH 8.3), 0.5 unit of Taq polymerase, 1 unit of Pfu, 0.2 mM of each dNTP, 1 μM forward primer (1719) and reverse primer (1795, Table 1) and 2 μL cDNA, The temperatures were: 30 s at 94° C, 25 x (30 s at 94° C, 30 s at 60° C, 3 min. at 72° C) followed by 5 min. at 72° C. The resulting PCR products were then digested with appropriate restriction enzymes, ligated with appropriately digested pXT7 plasmid and transformed into *E. coli*. Clones were sequenced to verify that no mutation had been introduced by PCR. This construct was linearized with SalI and cRNA was synthesized using the T7 mMessage mMachine kit (Ambion).

Construction of an N-truncation mutant (nt*Ciona*Kv4) of *Ciona*Kv4

To generate a mutant channel lacking amino acids 2-32 of the N-terminus domain, a diluted aliquot of the *Ciona*Kv4 clone was amplified by PCR. The composition of the PCR reactions and the temperature conditions were as described in the previous section. The forward primer (1809, Table 1) was designed to bind to the

*Ciona*Kv4 clone starting from nucleotide 97. A start codon, Kozak consensus sequence and an XhoI site were added to this primer. The reverse primer (1795, Table 1) was the same as used for the full-length clone. These PCR products were inserted into pXT7 and transformed into *E. coli*. Clones were sequenced to verify the deletion and to check that the undeleted sequence had no mutations introduced by PCR.

Oocyte preparation

Oocytes from *Xenopus laevis* were surgically removed and dissociated using 2 mg/ml collagenase 1A (Sigma) in a solution containing (mM): NaCl (96), KCl (4), $MgCl_2$ (20) and HEPES (5), pH 7.4. Oocytes were incubated at 18 C in culture medium containing (mM): NaCl (96), KCl (2), $MgCl_2$ (1), $CaCl_2$ (1.8), HEPES (5), Na-pyruvate (2.5), pH 7.4 with 100 mg/l gentamycin and 3% horse serum (Gibco BRL). 24 or 48 hours following oocyte isolation, ~16 ng of *Ciona*Kv4 or ~8 ng of nt*Ciona*Kv4 cRNA were injected into each *Xenopus* oocyte. Immediately prior to each experiment the vitelline membrane was manually removed after treatment in a hyperosmotic solution containing (mM): NaCl (96), KCl (2), $MgCl_2$ (20), HEPES (5) and mannitol (400), at pH 7.4.

Voltage-clamp recordings

All recordings were made from cell-attached macro-patches (Hamill et al., 1981). The pipettes contained ND96 solution, with the following composition (mM): NaCl (96), KCl (2), $MgCl_2$ (1), $CaCl_2$ (1.8) and HEPES (5), at pH 7.4. During the

recordings, oocytes were bathed in a grounded, isopotential solution thereby ensuring that the potential applied by the recording pipette would be the true membrane potential for the macro-patch. This bath solution contained (mM): NaCl (9.6), KCl (88), EGTA (11), HEPES (5), pH 7.4. Patch pipettes were pulled from aluminosilicate glass, and were coated with dental wax, and fire-polished before each experiment. Only pipettes that had resistances between 0.7 and 1.4 MΩ were used. Membrane seals were obtained by applying negative pressure. Voltage-clamp and data acquisition were carried out with an EPC-9 patch-clamp amplifier (HEKA, Lambrecht, Germany) controlled with PULSE software (HEKA) running on a Power MacIntosh G4 computer. Data were acquired at sampling intervals of 50 μs and low-pass filtered at 5 kHz during acquisition. Bath temperature was maintained at 12 ± 0.2° C with a Peltier device controlled by an HCC-100A temperature controller (Dagan, Minneapolis, MN, USA). The holding potential was set at –100 mV and leak subtraction was performed with a P/4 protocol. PulseFit (HEKA), Igor Pro (Wavemetrics, Lake Oswego, OR, USA) and Instat (GraphPad Software, San Diego, CA, USA) software were used for analyses and graphing. Conductances were calculated using the equation $g_K = I_{peak} / (V-E_K)$, where g_K is the potassium conductance, I_{peak} is the peak amplitude of the K^+ current to a test pulse, V is the voltage at which the current was measured, and E_K is the measured potassium equilibrium potential. Conductance-voltage relationships and steady-state inactivation curves were fitted in Igor Pro by a sigmoid (Boltzmann) distribution of the form:

$f(V) = G_{max}/\{1 + \exp[(V_{0.5} - V) / k]\}^n$, where G_{max} is the maximal conductance, V is the voltage of the depolarizing pulse (for activation) or the prepulse voltage (for inactivation), and k is the slope factor. For a first order Boltzmann (n = 1), used to fit conductance-voltage relationships and steady-state inactivation curves, $V_{0.5}$ is the voltage at which activation or inactivation is half maximal. For a fourth order Boltzmann (n=4), used to fit conductance-voltage relationships only, $V_{0.5}$ gives an estimate for the midpoint voltage of activation for each subunit. Time constants of activation were obtained from a fit of the rising phase of the currents to the Hodgkin-Huxley model of the form: $I(t) = I_{max} \{1- \exp[-t/\tau]\}^n$ where I_{max} is the maximum current obtained in the absence of inactivation, τ is the activation time constant and n = 4. An exponential function was used to fit the relationship between time constant of activation and voltage, in order to estimate the voltage necessary to increase the current amplitude by a factor of e. To study the decay of the current as a function of time, decaying phases of the outward currents evoked by test pulses between +30 mV and +80 mV were fitted to the equation: $I(t) = I_0 + I_1 \exp(-t/\tau_1) + I_2 \exp(-t/\tau_2)$, where τ_1 and τ_2 represent the fast and the slow time constants of inactivation, respectively, I_1 and I_2 represent the relative contribution of each component to inactivation, and I_0 is the offset. The voltage dependence of steady-state inactivation was determined by measuring the peak current evoked with a depolarizing pulse to +50 mV as a function of the voltage of a preceding 10 s prepulse test (between –130 and –30 mV). To

investigate the kinetics of channel closing, tail currents were evoked at several membrane potentials, from –160 to –40 mV, applied after a brief (10-15 ms) depolarizing pulse to +50 mV. Tail currents obtained with pulses from –160 to –100 mV were used for analyses.

Statistical analyses

Statistical comparisons were carried out using the Student t test, or the alternative Welch t test when there were significant differences between the standard deviations of the two groups. Data are represented as the mean ± SEM, and n is the number of macro-patches. One macro-patch *per* oocyte was used in the analyses, in order to account for experimental variability.

2.3 Results

Cloning of a Kv4 channel from the heart of *Ciona intestinalis*

A search of the *C. intestinalis* genomic database (release version 1.0) at http://genome.jgi-psf.org/ciona4/ciona4.home.html for Kv4 channel genes using the sequences of several vertebrate homologues suggested that there is only one Kv4 channel gene, which was located in scaffold 168. An alignment of this *Ciona* channel with mammalian Kv4 channels suggested the positions of the exon/intron boundaries for the first 1400 bp (Fig. 2-1A). To detect expression of this Kv4-like channel, the sequences of the predicted first and second exons were used to design primers (1719

and 1723, Table 2-1) to amplify part of the transcript from heart cDNA. Figure 2-1B shows the products of this PCR run on an agarose gel. Their sequence was identical to the predicted section of scaffold 168. Prior to cloning the open reading frame (ORF) it was necessary to amplify the 3' end of the Kv4 transcript using a 3'-RACE assay (Fig. 2-2) because the alignment between the 3'-end of vertebrate Kv4 channels and scaffold 168 (Fig. 2-1A) did not reveal the location of the stop codon. Since the first methionine codon in the predicted ORF agreed with the start codon of all other Kv4 channels, a 5'-RACE assay was unnecessary and the predicted exon regions within the first 1400 bp were used to design primers to amplify the 5' end. The DNA fragments amplified by PCR (5'-end) or RACE (3'-end) were sequenced on both strands and assembled. Primers containing the start and stop codon were designed and used to amplify the ORF of *Ciona*Kv4 (1729 and 1795, Table 2-1), which was inserted and maintained in pXT7.

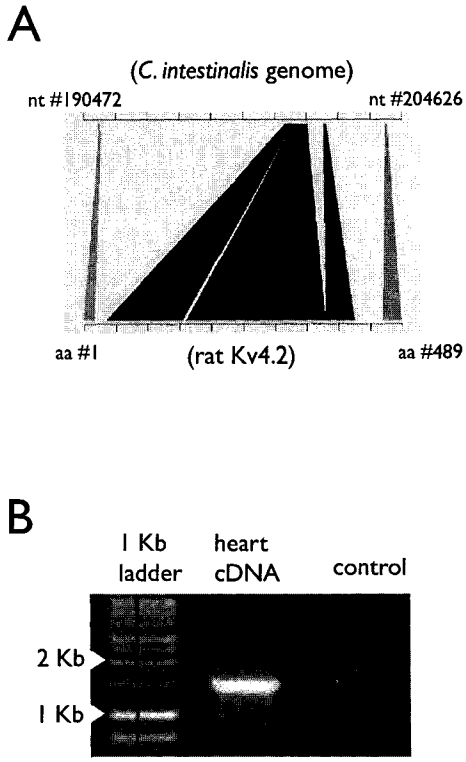

Figure 2-1. The heart of the tunicate *Ciona intestinalis* expresses a Kv4-like channel. *A*, Alignment of the deduced amino acid sequence of rat Kv4.2 (accession number Q9Z0V2) and scaffold 168 of the *Ciona intestinalis* genome database (release version 1.0). *B*, RT-PCR products amplified from a transcript for a Kv4-like channel using cDNA from the heart of *C. intestinalis*, and forward and reverse primers designed to bind to the sequences predicted as the first and second exons in *A*. Expected size of this fragment was ~1100 bp. No cDNA was added to the control reaction.

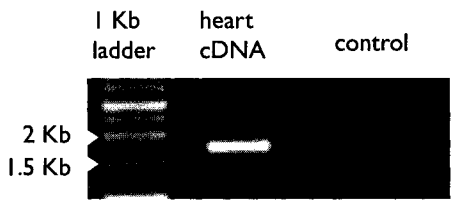

Figure 2-2. Amplification of the 3' end of a Kv4 transcript from the heart of *Ciona intestinalis*. Products of a 3'-RACE assay corresponding to the 3' end of the transcript of a Kv4-like channel, using cDNA from the heart of *C. intestinalis*. The size of this 3' transcript was ~1500 bp. No cDNA was added to the control reaction.

Table 2-1. Sequences of the primers used to amplify part or the full transcript for *Ciona*Kv4 from cDNA of the heart of *C. intestinalis*. F is the forward primer and R the reverse primer in a pair.

Primer #	Primer sequence
1665 (F)	5'-GACGGATCTACAGCCAAAATCAAAGACA-3'
1719 (F)	5'-ATGGCAACAGCAGTAGCAGCTTGG-3'
1723 (R)	5'-GCTGCCGGTATGCTCGTGAATGTAGT-3'
1729 (F)	5'-GGCTCGAGGCCGCCACCATGGCAACAGCAGTAGC-3'
1795 (R)	5'-GGCCTAGGCAAAGTCCCGCCGCTACAGTGAG-3'
1809 (F)	5'-GGCTCGAGGCCGCCACCATGAACCGACGTAAAACAAAAGAC-3'

Genomic structure and amino acid sequence analyses of *Ciona*Kv4

The nucleotide sequence of *Ciona*Kv4 (ORF and 3'-untranslated region) is deposited in GenBank (accession number AY514487[2]). An alignment between the sequences of the transcript of *Ciona*Kv4 and its gene in the genomic database (scaffold 168) showed ~96% identity between their nucleotide sequences. This alignment was used to deduce the exon/intron boundaries of the gene for *Ciona*Kv4 (Fig. 2-3).

*Ciona*Kv4 is encoded in ~17.8 Kb, of which 2.4 Kb encode the ORF. The first exon encodes the first amino acids of the N-terminus. The second exon, 1070 bp in length, codes for most of the channel protein, including the T1 domain, transmembrane domains S1-S5, and the first part of the pore domain. The second intron interrupts the sequence of the K^+ selectivity filter motif (GYG), since the last bp of the second exon and the first two bp of the third exon encode the first G of this motif. The second part of the pore region and the S6 transmembrane domain are encoded by exon 3. The last exon, which codes for most of the C-terminus of *Ciona*Kv4, contains the stop codon (TAG) and most of the 3'-UTR sequence.

Figure 2-4 shows an alignment between the predicted amino acid sequences of *Ciona*Kv4 and selected mammalian and invertebrate Kv4 channels. The six trans-membrane domains (S1-S6), the pore region, and the first ~23 amino acids of the N-terminus of all Kv4 channels show high sequence similarity. The C-terminal motif PTPP located ~30 amino acids upstream the C-termini of mammalian Kv4 channels

[2] The published GenBank script for *Ciona*Kv4 is shown in Appendix A.

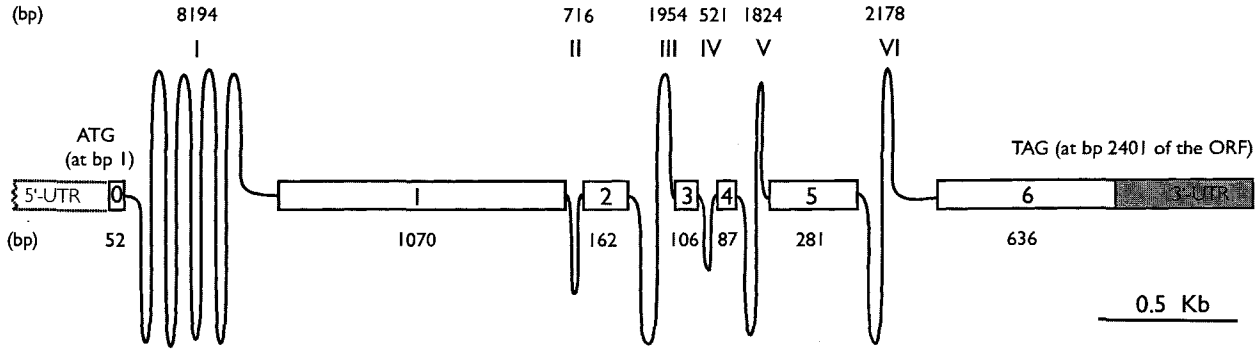

Figure 2-3. Exon/intron structure of the *Ciona*Kv4 gene. Diagram showing the organization of the *Ciona*Kv4 gene based on an alignment between the transcript sequence for *Ciona*Kv4 and scaffold 168 of the genomic database for *C. intestinalis* (Release Version 1.0). Exons are shown as boxes and numbered in Arabic numerals (from 0 to 6). Introns are shown as solid lines and numbered in Roman numerals (from I to VI). Approximate intron sizes (in bp) are indicated above the introns. Exon sizes (in bp) are indicated below the boxes. Sizes are drawn approximately to scale. The 3'-UTR region is represented by a box shaded in grey. The box representing the 5'-UTR region is delimited with a discontinuous line to indicate that the sequence of this region was not determined in this study.

(Petrecca et al., 2000), was not found in *Ciona*Kv4, although *Ciona*Kv4 shares the first residue of this motif (P) and the preceding residue (I) with all mammalian Kv4 channels (residues 651-652 in *Ciona*Kv4, Fig. 2-4). The conserved di-leucine motif, which consists of sixteen amino acids that spans positions 474-489 and is involved in the targeting of membrane proteins (Rivera et al., 2003) was also found in *Ciona*Kv4 (Fig. 2-4).

The C-terminal domain of *Ciona*Kv4 and the N-terminus contained, respectively, two and one putative sites for phosphorylation by cAMP-dependent protein kinase A (PKA). Additionally, the N-terminus of *Ciona*Kv4 contained four sites for phosphorylation by protein kinase C (PKC); another four putative sites for PKC phosphorylation were found in the C-terminus; and another such site was found in the intracellular loop between membrane-spanning domains S4 and S5 (Fig. 2-4).

In the phylogenetic tree shown in Figure 2-5, rooting with the cnidarian Kv4 sequences resolves the arthropod and chordate Kv4 channels into sister groups. *Ciona*Kv4 and TuKv4, a Kv4 channel cloned from the tunicate *Halocynthia roretzi* (Nakajo et al., 2003), form a single clade, as would be expected. This tunicate clade in turn is the sister group to the clade containing the Kv4.1, Kv4.2 and Kv4.3 paralogs from vertebrates, indicating that the duplication and divergence that gave rise to the three vertebrate Kv4 channels occurred after the divergence of the vertebrate lineage from the tunicate lineage.

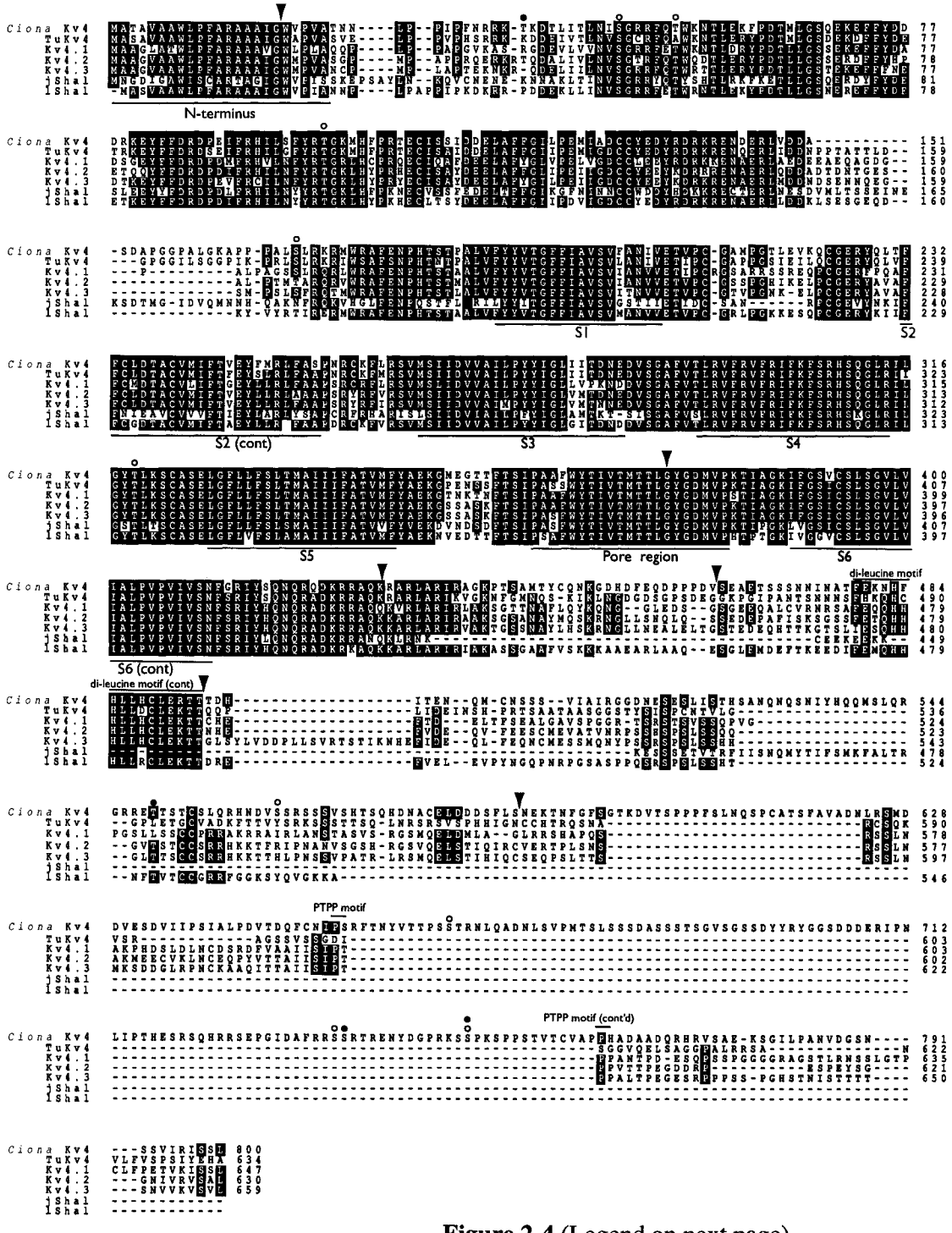

Figure 2-4 (Legend on next page)

Figure 2-4. Alignment and sequence comparison of Kv4 channels from diverse metazoans. Alignment of the deduced amino acid sequence of the three mammalian Kv4 isoforms (Kv4.1, Kv4.2 and Kv4.3), their tunicate homologues (*Ciona*Kv4 and TuKv4), lobster *Shal* (lShal) and jellyfish *Shal* (jShal). T-Coffee software (Notredame et al., 2000) was used to align these sequences, with the following accession numbers: *Ciona*Kv4, AAS00646; TuKv4 (from *Halocynthia roretzi*), BAC53863; Kv4.1, 27436981; Kv4.2, 9790093; Kv4.3, 6653655; lShal, AAA81592; jShal, AAB39750. Residues that are identical for at least four of the seven channels are shown in reverse lettering (white on black). Membrane spanning domains S1-S6, the pore region and the N-terminus are underlined. Arrowheads indicate exon/intron boundaries for *Ciona*Kv4 only. Putative phosphorylation sites for cAMP-dependent protein kinase (PKA) and protein kinase C (PKC) are indicated with filled circles and open circles, respectively.

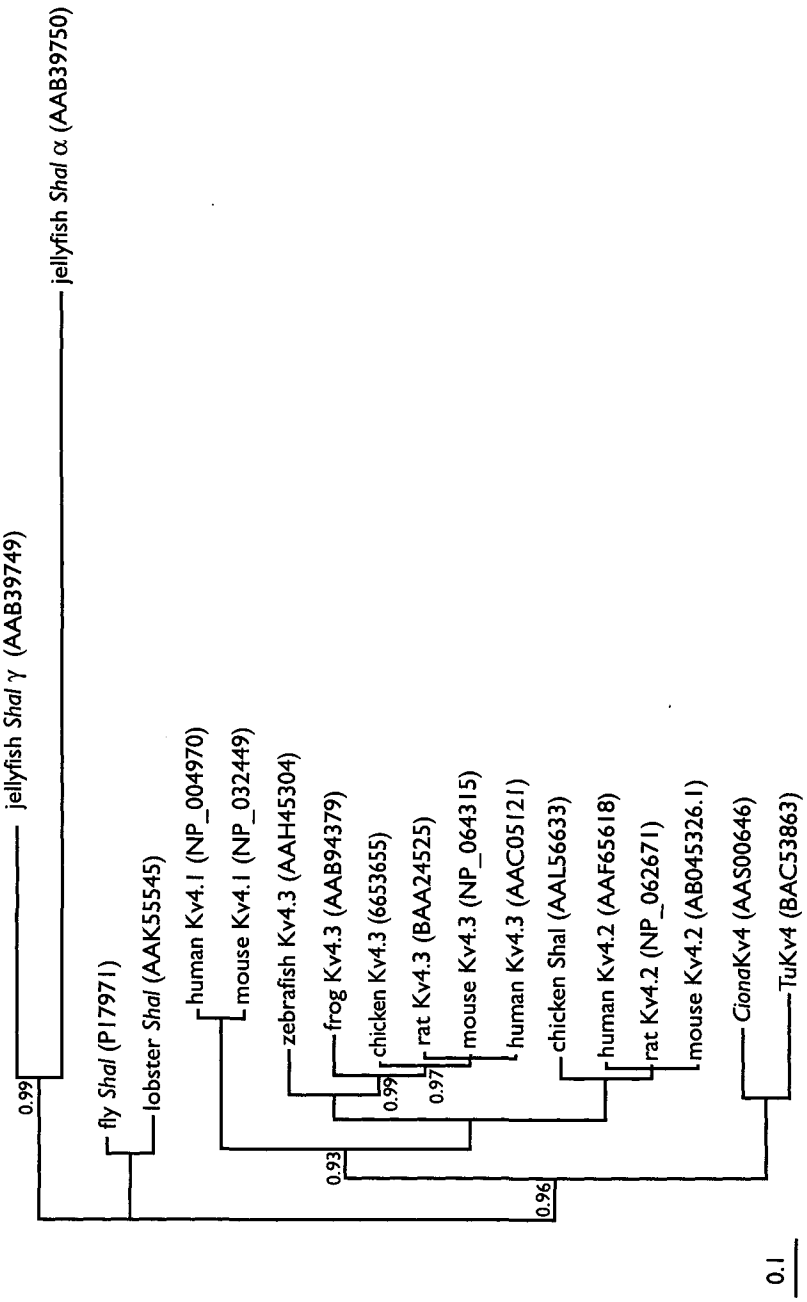

Figure 2-5 (Legend on next page)

Figure 2-5. Phylogenetic relationships of Kv4 channels from different species. Two cnidarian Kv4 channels were used as an out-group to polarize the relationships of the other channels. The two arthropod channels group together as a sister group to the chordate channels. The two tunicate channels, from *Halocynthia roretzi* and *Ciona intestinalis*, group together and are basal to the clade containing all three paralogs of the vertebrates. All of the vertebrate channels group within one of three paralog clades, indicating that the three vertebrate Kv4 paralogs were present in the common ancestor of all vertebrates, but not in the common ancestor of vertebrates and tunicates. The scale bar represents a divergence equivalent to an average of a 10% change in amino acids. Numbers above or below the lines indicate Bayesian posterior probability calculated by the MrBayes program; unlabelled nodes have a posterior probability of 1. Accession numbers of the protein sequences are indicated in parentheses.

Activation parameters of the currents produced by *Ciona*Kv4 and an N-deletion mutant (nt*Ciona*Kv4)

*Ciona*Kv4 and an N-terminus deletion mutant (nt*Ciona*Kv4) that lacked amino acids 2-32 were heterologously expressed in *Xenopus* oocytes. Macroscopic currents were recorded using the macro-patch technique 2 to 5 days after mRNA injection. Biophysical parameters of the expressed channels are summarized in Table 2-2.

To activate macroscopic currents, test pulses of 500 ms ranging from –100 to +80 mV were delivered in 10 mV increments from a holding potential of –100 mV. Currents from oocytes expressing *Ciona*Kv4 channels yielded A-type currents that showed relatively fast activation and inactivation (Fig 2-6A). Currents produced by oocytes expressing the N-deletion mutant (nt*Ciona*Kv4) inactivated significantly more slowly than currents produced by oocytes expressing wild type channels (Fig. 2-6B). Peak amplitudes of nt*Ciona*Kv4 currents were ~ 50 % greater than those produced by wild type channels (Fig. 2-7A). For instance, average peak currents produced by *Ciona*Kv4 and nt*Ciona*Kv4 during a pulse to +50 mV were 207 ± 27 pA and 307 ± 33 pA respectively ($n = 16$, $p < 0.05$, Welch t test). The sigmoid rising phase of the macroscopic currents were fitted with a Hodgkin-Huxley related equation. The time constants of activation (τ_{act}) during a test pulse to +50 mV were 3.4 ± 0.2 ms ($n = 11$) for *Ciona*Kv4 and 3.2 ± 0.3 ms ($n = 12$) for nt*Ciona*Kv4 (Fig. 2-7B).

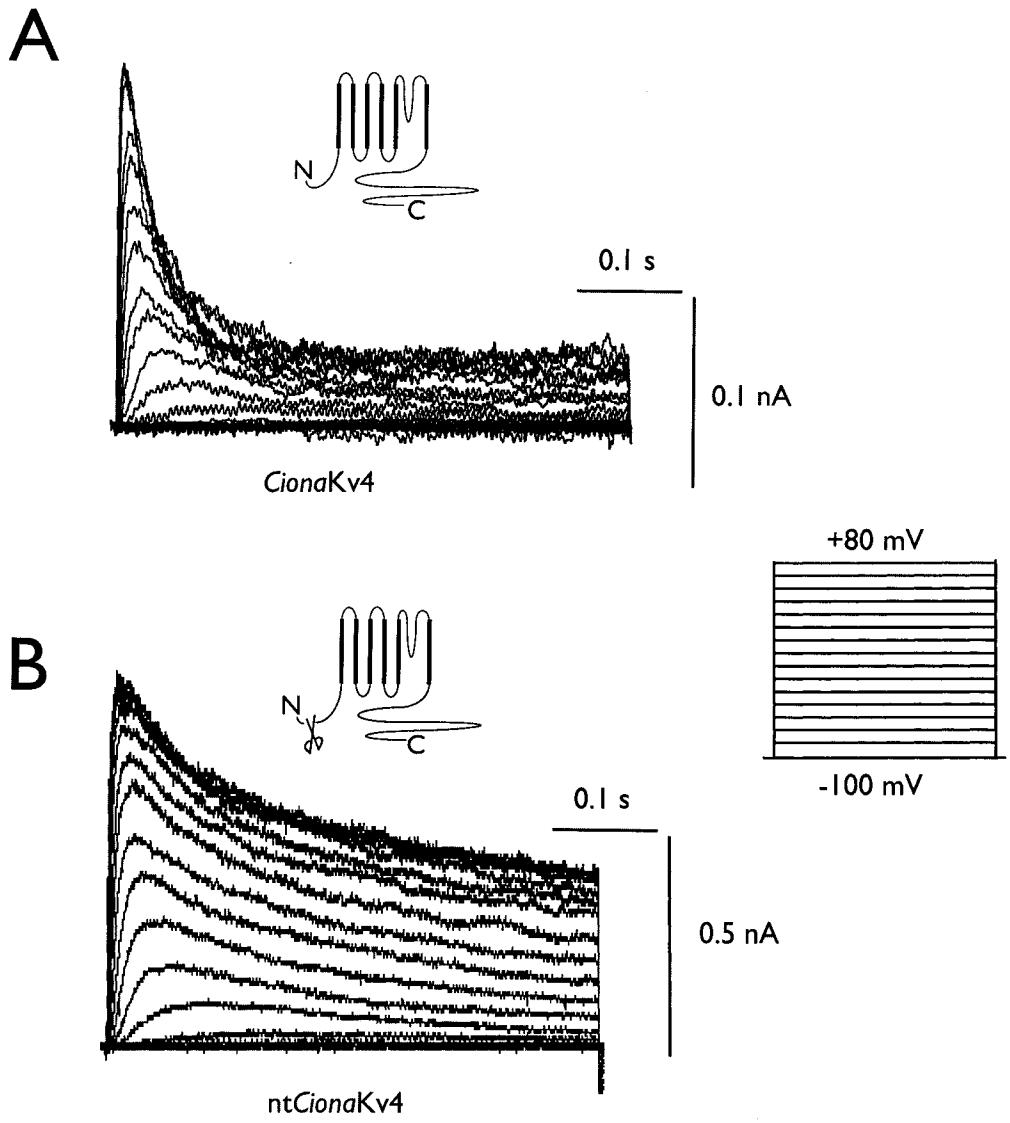

Figure 2-6. Currents produced by *Ciona*Kv4 and an N-terminal deletion mutant (nt*Ciona*Kv4). *A*, Representative family of outward currents recorded from *Xenopus* oocytes expressing *Ciona*Kv4 channels. *B*, Representative family of outward currents recorded from *Xenopus* oocytes expressing nt*Ciona*Kv4 channels. Recordings were made using the macro-patch technique. Currents were evoked by depolarizing the macro-patches for 0.5 s. from a holding potential of –100 mV from –100mV to +80mV in 10 mV steps. The baseline 5 ms immediately before and immediately after the depolarization pulses was saved, and tail currents are therefore not shown.

The kinetics of activation was unaltered by N-terminal deletion ($p > 0.05$ Student t test). Solid lines in Figure 2-7B represent single exponential fits to the relationships between τ_{act} and voltage. The voltage-dependence of activation kinetics was similar for *Ciona*Kv4 and nt*Ciona*Kv4 channels, increasing by a factor of e for every 26 or 29 mV of voltage change, respectively. Conductance-voltage relationships for wild type and mutant channels are shown in Figure 2-7C. The subunit $V_{0.5}$ (p. 44) from the fourth order Boltzmann fits to relationships between normalized peak conductance and test voltage gives an estimate of the voltage at which channels begin to activate. These voltages were –27 ± 2 mV (n = 16) for *Ciona*Kv4 and –36 ± 1 mV (n = 16) for nt*Ciona*Kv4 ($p < 0.0001$, Student t test). Conductance at these voltages represented approx. 7% of the maximal conductance. The slope of activation for each subunit were 31 ± 2 mV/e-fold (n = 16) for *Ciona*Kv4, and 28 ± 1 mV/e-fold (n = 16) for nt*Ciona*Kv4 ($p = 0.05$, Welch t test).

For easy comparison with other studies, I also performed first order Boltzmann fits to these relationships (normalized peak conductance *versus* voltage). These had significantly different midpoints of activation ($V_{0.5}$) of 20 ± 2 mV (n = 16) for *Ciona*Kv4 and 8 ± 2 mV (n = 16) for nt*Ciona*Kv4 channels ($p < 0.0001$, Student t test). The slopes for these curves were 22 ± 1 mV/e-fold and 20 ± 1 mV/e-fold, respectively ($p > 0.05$, Welch t test). Solid curves in Figure 2-7C correspond to first order Boltzmann fits.

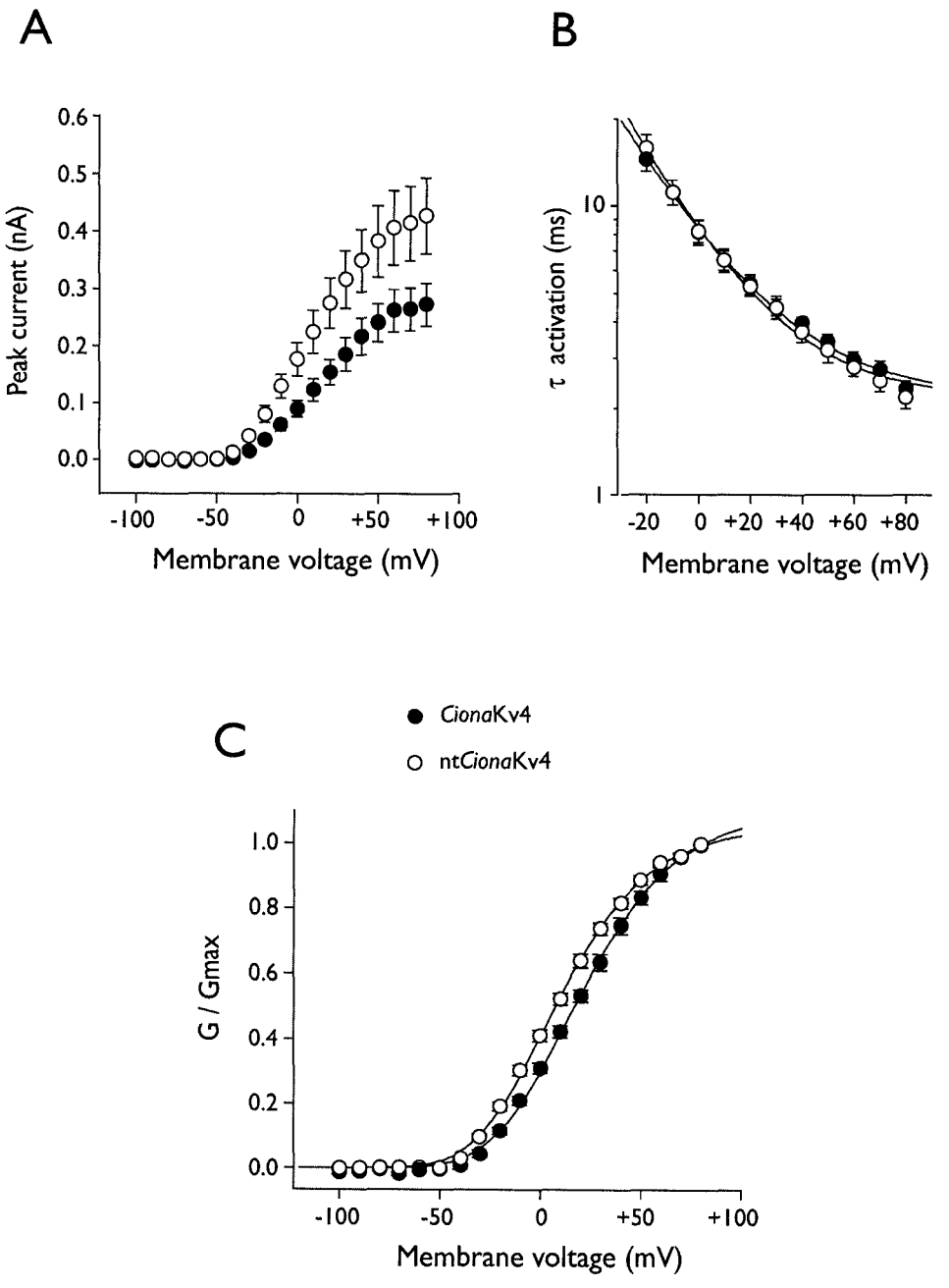

Figure 2-7 (Legend on next page)

Figure 2-7. Activation properties of currents mediated by *Ciona*Kv4 and an N-terminal deletion mutant (nt*Ciona*Kv4). *A,* Averaged peak current-voltage relationships for *Ciona*Kv4 and nt*Ciona*Kv4. *B,* Relationships between time constant of macroscopic activation (τ activation) and voltage for *Ciona*Kv4 (filled circles) and nt*Ciona*Kv4 (open circles). Time constant of activation values were derived from Hodgkin-Huxley fits to the rising phase of macroscopic outward currents during test pulses between -20 mV and +80 mV from a holding potential of –100 mV. Solid curves represent single exponential fits to these relationships. *C,* Normalized peak conductance-voltage relationships for *Ciona*Kv4 (filled circles) and nt*Ciona*Kv4 (open circles). Solid curves represent first order Boltzmann fits of the averaged data. Data represent mean ± SEM (n = 16 in all cases)

Inactivation parameters of *Ciona*Kv4 and an N-deletion mutant (nt*Ciona*Kv4) currents

The decay phase of the outward currents obtained with test pulses between +20 mV and +80 mV was well fitted by a double exponential function with fast (τ_1) and slow (τ_2) time constants of inactivation. Macroscopic currents produced by *Ciona*Kv4 and nt*Ciona*Kv4 channels in response to a depolarizing pulse to +50 mV from a holding potential of –100 mV are superimposed in Figure 2-8A to highlight the differences in their inactivation kinetics. Double exponential fits are shown as solid lines. The time constants and relative contribution of fast and slow inactivation components differed significantly between the two channels. For instance, during a pulse to +50 mV from a holding potential of –100 mV, the fast component of inactivation was significantly more rapid in wild type (~26 ms) than in mutated channels (~56 ms) ($p < 0.001$, Welch t test). Moreover, fast inactivation contributed more to current decay in the wild type channel than in the N-deletion mutant (~82% *vs* ~49% respectively). The slow inactivation time constant in wild type channels was around 147 ms and accounted for ~18% of the current decay, whereas in nt*Ciona*Kv4 the time constant of the slow inactivation component was ~380 ms and contributed to ~51% of the total decay. The differences between *Ciona*Kv4 and nt*Ciona*Kv4 regarding the slow component of inactivation were also statistically significant ($p < 0.01$, Welch t test). Figure 2-8B compares τ_1 and τ_2 values for *Ciona*Kv4 and nt*Ciona*Kv4 currents evoked by depolarizing pulses between +20 and +80 mV, showing that truncation of the N-

terminus of *Ciona*Kv4 significantly increased time constants for the fast and slow components of inactivation at each voltage. Fast and slow time constants of inactivation were voltage independent (for voltages between +20 mV and +80 mV) for both channels. To analyze steady-state inactivation, oocyte macro-patches were held for 10 s at voltages ranging from –150 to +30 mV and then depolarized to a test pulse of +50 mV for 500 ms. Figure 2-9A shows the mean normalized peak currents plotted as a function of prepulse potentials. These relationships were well fitted by a first order Boltzmann distribution, with midpoints of inactivation ($V_{0.5}$) of –72 ± 2 mV (n = 7) for *Ciona*Kv4 and -73 ± 2 mV (n = 7) for nt*Ciona*Kv4. The difference between the midpoints of inactivation was not statistically significant ($p > 0.05$, Student t test), suggesting that the N-terminus of *Ciona*Kv4 does not contribute to steady-state inactivation properties. Similarly the slopes of these curves were not significantly different ($p > 0.05$, Student t test): 3.6 ± 0.2 mV/e-fold (n = 7) for *Ciona*Kv4 and 3.7 ± 0.2 mV/e-fold (n = 7) for nt*Ciona*Kv4.

A double-pulse protocol was used to assess the rate of recovery from inactivation at –100 mV. Briefly, a first test pulse to +50 mV lasting for 1 s. was separated by a recovery pulse to -100 mV of increasing duration (50-2000 ms) from a second pulse to +50 mV. The currents evoked by the second pulse of a double-pulse protocol were normalized to the currents produced by the first pulse and plotted against the duration of the interpulse interval. The kinetics of recovery from inactivation were plotted as the amplitude of the current evoked by the second pulse relative to the current

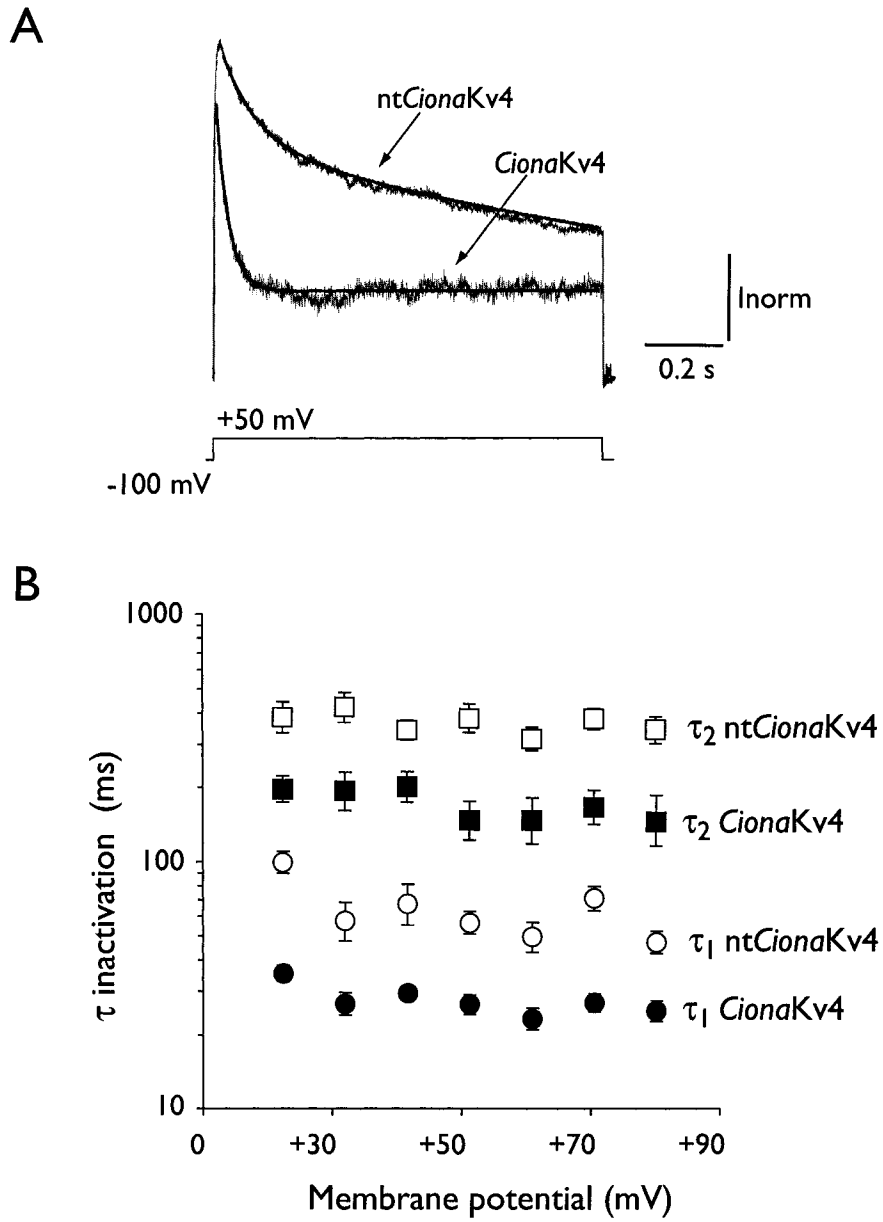

Figure 2-8. Inactivation kinetics of currents mediated by *Ciona*Kv4 and an N-terminal deletion mutant (nt*Ciona*Kv4). *A*, Comparison of macroscopic currents produced by *Ciona*Kv4 and nt*Ciona*Kv4 channels in response to a pulse to +50 mV from a holding potential of -100 mV. Currents are normalized to peak for comparsion. B, Relationships between time constants of inactivation (τ inactivation) and voltage. Fast (τ_1) and slow (τ_2) inactivation time constants were obtained from double exponential fits to currents during test pulses between +20 mV and +80 mV from a holding potential of -100 mV. Data represent mean ± SEM.

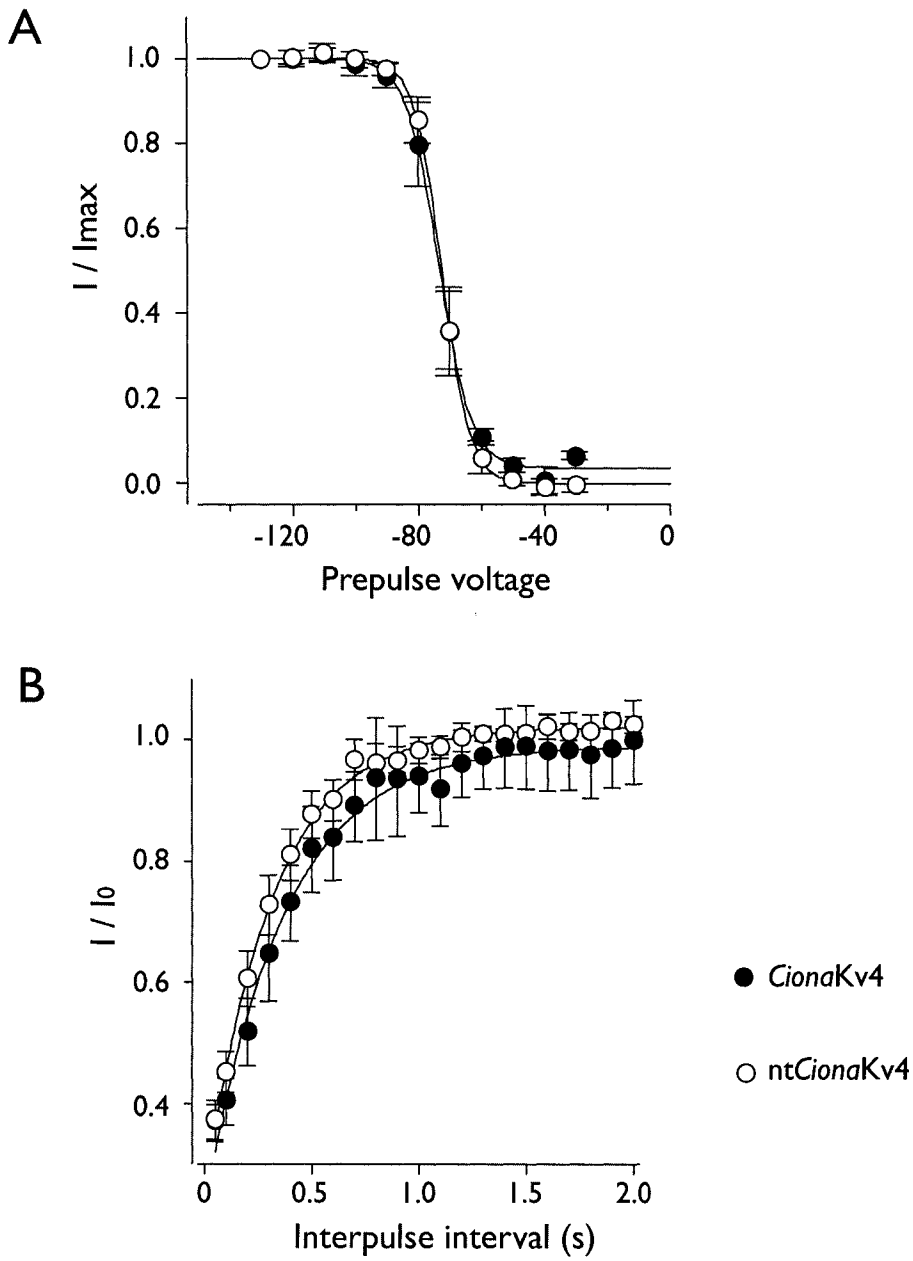

Figure 2-9. Inactivation properties of currents mediated by *Ciona*Kv4 and an N-terminal deletion mutant (nt*Ciona*Kv4). A, Voltage-dependence of steady-state inactivation for *Ciona*Kv4 (filled circles) or nt*Ciona*Kv4 (open circles), plotted as the relationship between normalized peak current during a pulse to +50 mV and the voltages of the conditioning prepulses (from -130 mV to -30 mV). Solid curves represent Boltzmann fits of the averaged data. B, Inactivation recovery kinetics at -100 mV for *Ciona*Kv4 (filled circles) or nt*Ciona*Kv4 (open circles). Solid curves represent fits of the averaged data to a single exponential function. Data represent mean ± SEM.

evoked by the first pulse as a function of the duration of the recovery interval. This relationship was well fitted by a single exponential function with recovery time constants from inactivation (τ_{rec}) of 387 ± 47 ms (n = 7) for *Ciona*Kv4 and 331 ± 50 ms (n = 8) for nt*Ciona*Kv4 ($p > 0.05$, Student t test, Fig. 2-9B).

Deactivation parameters of *Ciona*Kv4 and an N-deletion mutant (nt*Ciona*Kv4) currents

To investigate the kinetics of channel closing of both *Ciona*Kv4 and nt*Ciona*Kv4, tail currents were evoked at membrane potentials ranging from –160 to –40 mV, after a brief (10-15 ms) depolarizing pulse to +50 mV (Fig. 2-10A,B). The decay of tail currents during pulses ranging from –160 to –100 mV were well fitted by single exponential functions from which deactivation time constants were obtained (τ_{deact}). For example, during a pulse to –130 mV, currents produced by *Ciona*Kv4 and nt*Ciona*Kv4 deactivated with time constants of 4.8 ± 0.3 ms (n = 10) and 7.2 ± 0.8 ms (n=12) respectively, which were significantly different ($p < 0.05$, Welch t test, Fig. 2-10C). These data suggest that the N-terminus of *Ciona*Kv4 has a role in accelerating deactivation in *Ciona*Kv4.

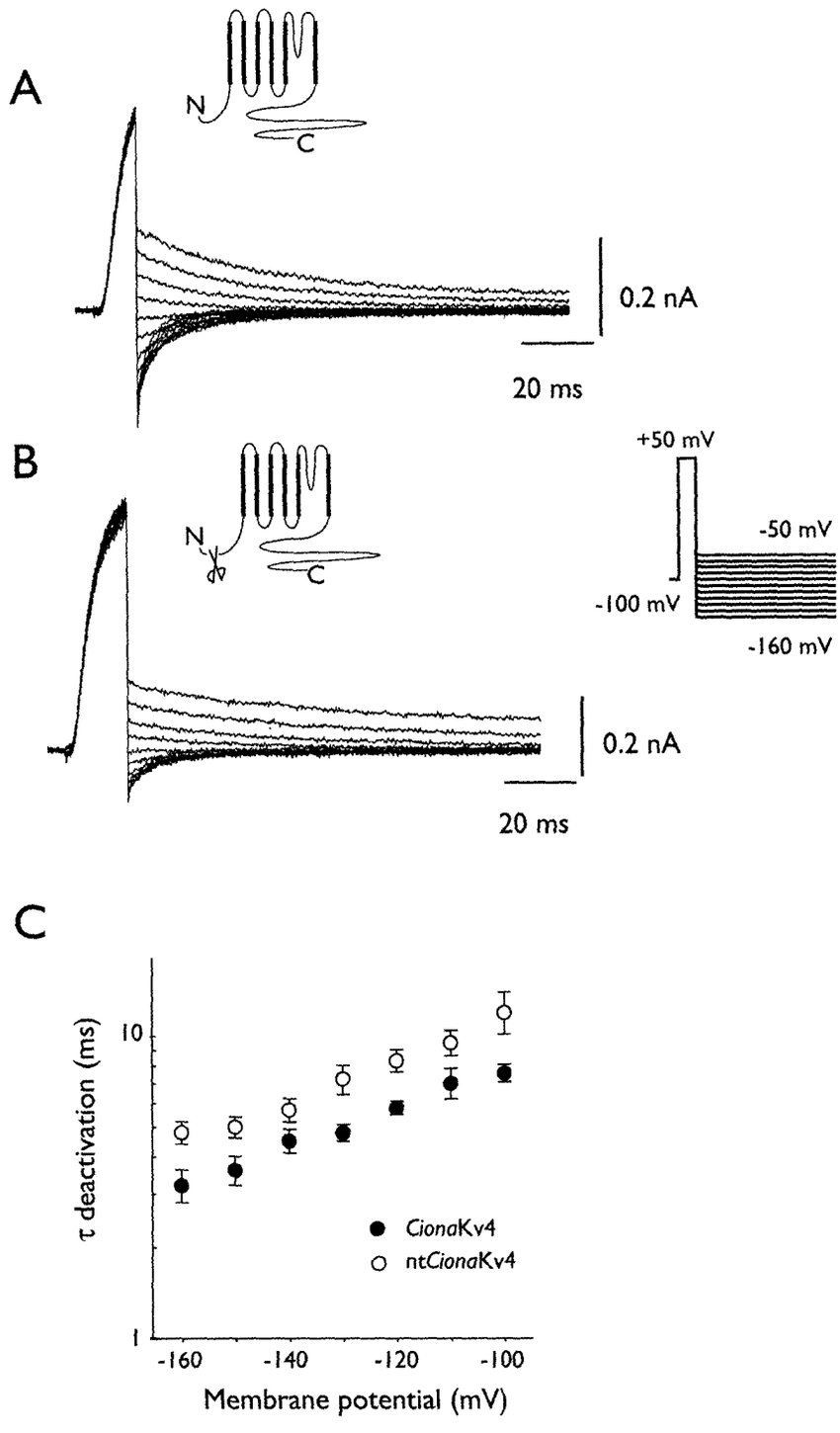

Figure 2-10 (Legend on next page)

Figure 2-10. Comparison between open-state deactivation properties of *Ciona*Kv4 and an N-terminal deletion mutant (nt*Ciona*Kv4). *A*, Representative set of tail currents from *Ciona*Kv4. *B*, Representative set of tail currents from nt*Ciona*Kv4. Tail currents were evoked by repolarizing pulses to potentials between –160 mV and –40 mV following a pulse to +50 mV. The length of the depolarizing pulse (between 10 and 15 ms) was adjusted each time to activate a maximum number of channels just prior to reaching peak amplitude. *C*, Relationships between time constant of deactivation (τ deactivation) and voltage for *Ciona*Kv4 (filled circles) and nt*Ciona*Kv4 (open circles). Time constants of deactivation were obtained from single exponential fits to the inward tail currents during test potentials between –160 and –100 mV. Data represent mean ± SEM.

Table 2-2. Biophysical parameters of currents produced by *Ciona*Kv4 and an N-terminus deletion mutant (nt*Ciona*Kv4) expressed in *Xenopus* oocytes. Number of replicates is indicated in parentheses.

	Channel	
Biophysical parameter	*Ciona*Kv4	nt*Ciona*Kv4
I_{peak} in pA at +50 mV	207 ± 27 (16)	307 ± 33 (16)[b]
τ_{act} in ms at +50 mV	3.4 ± 0.2 (11)	3.2 ± 0.3 (12)
Inactivation in ms at +50 mV		
τ_1	26 ± 2	56 ± 6[a]
A_1	82%	49%
τ_2	147± 26	381 ± 50[a]
A_2	18%	51%
τ_{rec} in ms at -100 mV	387 ± 47 (7)	331 ± 50 (8)
τ_{deact} in ms at -130 mV	4.8 ± 0.3 (10)	7.2 ± 0.8 (12)[b]
*Steady-state activation**		
$V_{0.5}$ (mV)	+20 ± 2 (16)	+8 ± 2 (16)[a]
k (mV / e-fold)	22 ± 1 (16)	20 ± 1 (16)
Steady-state inactivation		
$V_{0.5}$ (mV)	-72 ± 2 (7)	-73 ± 2 (7)
k (mV / e-fold)	3.6 ± 0.2 (7)	3.7 ± 0.2 (7)

[a] significantly different from *Ciona*Kv4 with $p < 0.01$

[b] significantly different from *Ciona*Kv4 with $0.01 < p < 0.05$

* calculated from first order Boltzmann fits

2.4 Discussion

In this study, we used a molecular approach to detect and characterize a Kv4-type channel expressed in the heart of the tunicate *Ciona intestinalis*. Using PCR and the 3'-RACE assay, we obtained the sequence of the ORF and the 3'-UTR of the transcript for *Ciona*Kv4. We determined the structure of the *Ciona*Kv4 gene by aligning the sequence of its transcript with the genomic database for this species. We cloned *Ciona*Kv4 and an N-deletion mutant (nt*Ciona*Kv4) that lacked amino acids 2-32 and analyzed the functional properties of their expressed channels in *Xenopus* oocytes.

Comparing the genomic structure of *Ciona*Kv4 with mammalian Kv4 channels

The genomic structure of *Ciona*Kv4 (Fig. 2-3) was similar to the genomic structures of the three mammalian Kv4 channel genes, which have been previously characterized (Isbrandt et al., 2000). Interestingly, the *Ciona*Kv4 gene contains an additional intron that partitions the codons for the first seventeen amino acids onto an additional exon. For comparison, exons 2-7 of *Ciona*Kv4 were numbered 1-6 because the relative sizes of exons 2-7 correspond to exons 1-6 of mammalian Kv4 channels. The exon that encodes the first seventeen amino acids of *Ciona*Kv4 is referred to as "exon 0" and is located ~8 Kb upstream of exon 1 (Fig. 2-3). As in mammalian Kv4 channel genes, exon 1 of *Ciona*Kv4 encodes the transmembrane domains S1-S5 and the first part of the pore domain of *Ciona*Kv4, exon 2 encodes the second part of the pore and transmembrane domain S6, and exons 3-6 encode the C-terminus. The intron

between exons 1 and 2 in *Ciona*Kv4 interrupts the coding sequence of the K^+ selectivity sequence GYG at exactly the same position as the equivalent intron of mammalian Kv4 genes. The sixth exon of *Ciona*Kv4 is larger in this gene than in its mammalian counterparts, encoding a comparatively longer C-terminus.

Comparing *Ciona*Kv4 currents with other Kv4 currents

*Ciona*Kv4 produced A-type currents that activated and inactivated with relatively rapid kinetics. The decay phase of these currents was best fitted with a double exponential function (Fig. 2-7A). The relative contribution of the fast inactivation component (~82%) was comparable to that of lobster *Shal* (Baro et al., 1996), Kv4.2 (Bähring et al., 2001) and Kv4.3 (Wang et al., 2002), but was significantly greater than the <20% for Kv4.1 channels (Jerng and Covarrubias, 1997). The midpoint of activation of *Ciona*Kv4, ~ +20 mV (Fig. 2-7C), is considerably depolarized with respect to other Kv4 channels (Table 2-3). The midpoint of activation of the Kv4 channel cloned from another tunicate (*Halocynthia*) was significantly left-shifted with respect to *Ciona*Kv4, as measured from Figure 2 of Nakajo et al. (2003) (Table 2-3). Perhaps the basis for this relatively depolarized midpoint of activation lies in differences in domains other than the positively charged S4 membrane-spanning segment, such as S1-S3 (Papazian et al., 1995) or T1 (Minor et al., 2000), because the S4 domain of *Ciona*Kv4, a major domain involved in activation gating (Papazian et al., 1991), is identical to that of other Kv4 channels (Fig. 2-4). Alternatively, perhaps the unique phosphorylation sites of *Ciona*Kv4 (e.g. PKA site at position 37, Fig. 2-4) are

responsible for the rightward shift of its activation midpoint, because phosphorylation of Kv4 channels is known to alter their gating properties (*e.g.* Martel et al., 1998).

Although most Kv4 channels share two arginine residues located after the S6 domain (R429 and R432 in *Ciona*Kv4, Fig. 2-4) that are crucial in determining the midpoint of inactivation in vertebrate Kv4 channels (Hatano et al., 2004), their midpoints of inactivation are different. The midpoint of inactivation of *Ciona*Kv4 (~ -72 mV), which differed slightly from that of the *Halocynthia* Kv4 channel (~ -80 mV, Nakajo et al., 2003), was similar to that of two arthropod *Shal* channels and Kv4.1 channels, and more hyperpolarized than the inactivation midpoint of Kv4.2 and Kv4.3 channels (Table 2-3). Interestingly, the jellyfish *Shal*, whose midpoint of inactivation is around –106 mV (Jegla and Salkoff, 1997) contains only one of these two arginines (Fig. 2-4).

Activation time constants of *Ciona*Kv4 currents were ~ 3.4 ms at +50 mV with the temperature held at 12° C. Lower values, between ~0.7-1.7 ms at room temperature, have been reported for mammalian Kv4 channels (Bähring et al., 2001; Franqueza et al., 1999). However, the fast inactivation time constant of *Ciona*Kv4 at 12° C was about 26 ms, similar to lobster *Shal* (~31 ms at 16° C, Baro et al., 1996) and mammalian *Shal* (~23 ms at 22-23° C; Pak et al., 1991), which suggests that inactivation kinetics of Kv4 channels are less constrained by temperature than activation kinetics.

Table 2-3. Comparison between the midpoints of steady-state activation and inactivation of invertebrate, tunicate and mammalian Kv4 channels.

Kv4 subtype	Activation $V_{0.5}$ (mV)	Inactivation $V_{0.5}$ (mV)	Source
Jellyfish *Shal*	-39	-106	Jegla and Salkoff (1997)
Lobster *Shal*	-40	-71	Baro et al. (1996)
Fly *Shal*	-36	-66	Baro et al. (1996)
TuKv4	~ -20	-80	Nakajo et al. (2003)
*Ciona*Kv4	+20	-72	This paper
Mouse Kv4.1	-8	-69	Pak et al. (1991)
Rat Kv4.2	-1	-55	Blair et al. (1991)
Human Kv4.3	-13	-50	Dilks et al. (1999)

*Ciona*Kv4 channels required ~ 1s to fully recover from inactivation at –100 mV, with a recovery time constant of ~387 ms (Fig. 2-9B). Similar values have been reported for jellyfish and fly *Shal* (Jegla and Salkoff, 1997) and Kv4.2 (Serôdio et al., 1994) for the same membrane potential. Kv4.1 channels recover fully from inactivation within 300-400 ms at –100mV (Serôdio et al., 1994), while Kv4.3 channels recover from inactivation relatively rapidly, with recovery time constants of less than 200 ms, also at –100 mV (Dixon et al., 1996). In conclusion, invertebrate Kv4 channels, including *Ciona*Kv4, exhibit lower rates of recovery from inactivation than the mammalian Kv4.1 and Kv4.3 channel subtypes, suggesting that relatively slow kinetics of recovery is a primitive feature of Kv4 channels.

Role of the N-terminus of *Ciona*Kv4

The first N-terminal amino acids of *Ciona*Kv4 are likely involved in regulating membrane expression, since deletion of these residues resulted in increased current amplitude relative to wild type channels when expressed in *Xenopus* oocytes (Fig. 2-7A). This result mimicked the effect of deleting a similar fragment from mammalian Kv4 channels (Bähring et al., 2001; Shibata et al., 2003). It has been shown that the hydrophobicity of most of the first ~30 amino acids of Kv4 channels impedes the trafficking of these channels to the membrane (Shibata et al., 2003).

Deletion of amino acids 2-32 of *Ciona*Kv4 slowed the fast component of inactivation by ~2-fold (Fig 2-8A,B), slowed deactivation kinetics (Fig. 2-10) and did not affect activation kinetics (Fig. 2-7). This suggests that the role of the N-terminus of

*Ciona*Kv4 in inactivation is comparable to the role of the N-terminus of Kv4.2 channels because deleting the first 40 amino acids of Kv4.2 channels had similar effects (Bähring et al., 2001). In addition, the N-terminus of *Ciona*Kv4 also contributes to the voltage-dependence of activation, since deletion of this domain resulted in a significant shift of the activation midpoint by about 12 mV in the hyperpolarizing direction relative to wild type channels (Fig. 2-7C).

In summary, the N-terminus of *Ciona*Kv4 contributes to several biophysical parameters in a similar fashion as the N-terminus of Kv4.2 channels (Bähring et al., 2001) but differs from the role of the N-terminus of Kv4.1 channels, since in the latter, deletion of this domain results in currents that activate with slower kinetics with respect with wild type channels and in a complete removal of the earlier fast component of inactivation (Pak et al., 1991; Jerng and Covarrubias, 1997).

Implications for the evolution of Kv4 channels

*Ciona*Kv4 is the only gene for Kv4 channels in the genome of *C. intestinalis.* Together with the basal position of the tunicate Kv4 clade relative to the three vertebrate Kv4 channel subtypes (Fig. 2-5), this establishes that the common ancestor of the chordates had a single Kv4 type channel and that early in the evolution of the vertebrates there was a duplication that led to two clades (the Kv4.1 clade and the Kv4.2/Kv4.3 clade) followed by a second duplication that gave rise to the final vertebrate complement of these channels. Comparing the biophysical properties of the mammalian Kv4 channels with those of their tunicate sister group and other cloned

invertebrate Kv4 channels is a first step to identifying common, conserved features of Kv4 channels, as well as properties that have evolved uniquely in the mammalian isoforms. Common biophysical features of *Ciona*Kv4 and two arthropod *Shal* channels are: (1) A predominant contribution of the fast component of inactivation over the slower component to overall macroscopic inactivation; this is also a characteristic of Kv4.2 and Kv4.3, but not of Kv4.1 channels, where the slower component predominates over the faster component; (2) a midpoint of inactivation around –70 mV, which is also characteristic of Kv4.1 but not of Kv4.2 or Kv4.3 channels, which have more depolarized values of midpoint of inactivation, and (3) a rate of recovery from inactivation that is relatively slow, with a time constant ~ 390 ms, similar to Kv4.2 but not to Kv4.1 nor Kv4.3 channels, which have faster recovery kinetics. This suggests that the mechanism of inactivation of Kv4.1 channels, the more depolarized inactivation midpoint of Kv4.2 and Kv4.3 channels, and the relatively fast recovery kinetics of Kv4.1 and Kv4.3 channels could represent more recent evolutionary innovations.

Possible role of *Ciona*Kv4 in the tunicate heart

In the mammalian heart, Kv4.2 or Kv4.3 channels are the molecular effectors of the I_{TO} current that contributes to re-polarization phase I of the AP (Dixon et al., 1996). Since APs produced by the tunicate heart show an initial repolarization phase immediately after the upstroke (Kriebel, 1967) that is reminiscent of phase I of the mammalian cardiac AP, it is tempting to speculate that *Ciona*Kv4 is the molecular effector of the "notch" of the tunicate cardiac AP.

The peristaltic beat of the tunicate heart is initiated by pacemakers at each end of the heart tube (Anderson, 1968), although the identity of the ion channels responsible for this pacemaking activity is not known. Analyses of the possible regional distribution of *Ciona*Kv4 in the tunicate heart could help to clarify whether this channel is involved in pacemaking activity of this tissue.

Summary and Conclusions

We have cloned a Kv4-like channel expressed in the heart of the tunicate *Ciona intestinalis*, *Ciona*Kv4. The structure of the *Ciona*Kv4 gene was almost identical to the structure of mammalian Kv4 channel genes. The clade formed by the two tunicate Kv4 channels branched basal to the three vertebrate Kv4 channels in a phylogenetic tree. Because *Ciona*Kv4 occupies a critical position between invertebrate Kv4 channels and the three vertebrate Kv4 channel isoforms, we compared the biophysical parameters of *Ciona*Kv4 with those of these other Kv4 channels in order to identify conserved and non-conserved properties. However, for a better comparative analysis it would be desirable to examine a larger population of invertebrate cloned Kv4 channels. Like arthropod *Shal* channels, *Ciona*Kv4 had a fast component of inactivation that contributed to most of the overall inactivation, a relatively hyperpolarized midpoint of inactivation (~ –72 mV), and a time constant of recovery from inactivation that is relatively slow (~ 400 ms). The mammalian Kv4 isoforms each have at least one functional characteristic that is not shared by *Ciona*Kv4 or arthropod *Shal* channels. For instance, in Kv4.1 channels a slow mechanism of inactivation predominates over a

fast mechanism, and these channels recover ~2-fold faster from inactivation than other Kv4 channels; Kv4.2 and Kv4.3 channels have a relatively depolarized midpoint of inactivation (~ -50 mV).

The diversification of the Kv4 channel gene in the vertebrate lineage resulted in three Kv4 channel subtypes with modified biophysical properties relative to *Shal* channels from more basal taxa. It seems likely that these modifications contributed to the development of new functions of nerve and muscle tissues in vertebrates.

2.5 Literature cited

Amberg GC, Koh SD, Hatton WJ, Murray KJ, Monaghan K, Horowitz B, Sanders KM (2002) Contribution of Kv4 channels toward the A-type potassium current in murine colonic myocytes. J Physiol 544(2):403-415

Anderson M (1968) Electrophysiological studies on initiation and reversal of the heart beat in *Ciona intestinalis*. J Exp Biol 49:363-385

Bähring R, Boland LM, Varghese A, Gebauer M, Pongs O (2001) Kinetic analysis of open- and closed-state inactivation transitions in human Kv4.2 A-type potassium channels. J Physiol 535.1:65-81

Baldwin TJ, Tsaur ML, Lopez GA, Jan YN, Jan LY (1991) Characterization of a mammalian cDNA for an inactivating voltage-sensitive K^+ channel. Neuron 7: 471-483

Baro DJ, Coniglio LM, Cole CL, Rodriguez HE, Lubell JK, Kim MT, Harris-Warrick RM (1996) Lobster *shal*: comparison with *Drosophila shal* and native potassium currents in identified neurons. J Neurosci 16:1689-1701

Blair TA, Roberds SL, Tamkun MM, Hartshorne RP (1991) Functional characterization of RK5, a voltage-gated K^+ channel cloned from the rat cardiovascular system. FEBS Lett 295:211-213

Butler A, Wei AG, Baker K, Salkoff L (1989) A family of putative potassium channel genes in *Drosophila*. Science 243:943-947

Dilks D, Ling H-P, Cockett M, Sokol P, Numann R (1999) Cloning and expression of the human Kv4.3 potassium channel. J Neurophysiol 81:1974-1977

Dixon JE, McKinnon D (1994) Quantitative analysis of potassium channel mRNA expression in atrial and ventricular muscle of rats. Circ Res 75: 252-260

Dixon JE, Shi W, Wang H-S, McDonald C, Yu H, Wymore RS, Cohen IS, McKinnon D (1996) The role of the Kv4.3 K^+ channel in ventricular muscle: a molecular correlate for the transient outward current. Circ Res 79:659-668

Dominguez I, Itoh K, Sokol SY (1995) Role of glycogen synthase kinase 3β as a negative regulator of dorsoventral axis formation in *Xenopus* embryos. Proc Natl Acad Sci USA 92:8498-8502

Franqueza L, Valenzuela C, Eck J, Tamkun MM, Tamargo J, Snyders DJ (1999) Functional expression of an inactivating potassium channel (Kv4.3) in a mammalian cell line. Cardiovasc Res 41: 212-219

Goddard CK (1972) Structure of the heart of the ascidian *Pyura praeputialis* (Heller). Aust J Biol Sci 25:645-647

Hamill OP, Marty A, Neher E, Sakmann B, Sigworth FJ (1981) Iimproved patch-clamp techniques for high-resolution current recordings from cells and cell-free membrane patches. Pflügers Arch 391:85-100

Hatano N, Ohya S, Muraki K, Clark RB, Giles WR, Imaizumi Y (2004) Two arginines in the cytoplasmic C-terminal domain are essential for voltage-dependent regulation of A-type K^+ current in the Kv4 channel subfamily. J Biol Chem 279:5450-5459

Hoshi T, Zagotta WN, Aldrich RW (1990) Biophysical and molecular mechanisms of *Shaker* potassium channel inactivation. Science 250:533-538

Huelsenbeck JP, Ronquist F (2001) MRBAYES: Bayesian inference of phylogenetic trees. J Bioinf 17:754-5

Isbrandt D, Leicher T, Waldschütz R, Zhu X, Luhmann U, Michel U, Sauter K, Pongs O (2000) Gene structures and expression profiles of three human KCND (Kv4) potassium channels mediating A-type currents I_{TO} and I_{SA}. Genomics 64:144-154

Jegla T, Salkoff L (1997) A novel subunit for Shal potassium channels radically alters activation and inactivation. J Neurosci 17:32-44

Jerng HH, Covarrubias M (1997) K^+ channel inactivation mediated by the concerted action of the cytoplasmic N- and C-terminal domains. Biophys J 72:163-174

Kalk M (1970) The organization of a tunicate heart. Tissue Cell 2:99-118

Kriebel ME (1967) Conduction velocity and intracellular action potentials of the tunicate heart. J Gen Physiol 50:2097-2107

Kriebel ME (1973) Action potential occurs only on the lumen surface of tunicate myocardial cells. Comp Biochem Physiol 46:463-468

Martel J, Dupuis G, Dechênes P, Payet MD (1998) The sensitivity of the human Kv1.3 (hKv1.3) lymphocyte K^+ channel to regulation by PKA and PKC is partially lost in HEK 293 host cells. J Membr Biol 161:183-196

Minor DL, Lin Y-F, Mobley BC, Avelar A, Jan YN, Jan LY, Berger JM (2000) The polar T1 interface is linked to conformational changes that open the voltage-gated potassium channel. Cell 102:657-670

Nakajo K, Katsuyama Y, Ono F, Ohtsuka Y, Okamura Y (2003) Primary structure, functional characterization and developmental expression of the ascidian Kv4-class potassium channel. Neurosci Res 45:59-70

Notredame C, Higgins D, Heringa J (2000) T-Coffee: a novel method for multiple sequence alignments. J Mol Biol 302:205-217

Page RD (1996) TreeView: an application to display phylogenetic trees on personal computers. J Compt Appl Biosci 12:357-358

Pak MD, Baker K, Covarrubias M, Butler A, Ratcliffe A, Salkoff L (1991) mShal, a subfamily of A-type K^+ channel cloned from mammalian brain. Proc Natl Acad Sci USA 88:4386-4390

Papazian DM, Shao XM, Seo S-A, Mock AF, Huang Y, Wainstock DH (1995) Electrostatic interactions of S4 voltage sensor in *Shaker* K^+ channel. Neuron 14:1293-1301

Papazian, DM, Timpe LC, Jan YN, Jan LY (1991) Alteration of voltage-dependence of *Shaker* potassium channel by mutations in the S4 sequence. Nature 349:305-310

Petrecca K, Miller DM, Shrier A (2000) Localization and enhanced current density of the Kv4.2 potassium channel by interaction with the actin-binding protein filamin. J Neurosci 20:8736-8744

Rivera JF, Ahmad S, Quick MW, Liman ER, Arnold DB (2003) An evolutionarily conserved di-leucine motif in Shal K^+ channels mediates dendritic targeting. Nat Neurosci 6:243-250

Roberds SL, Tamkun MM (1991) Cloning and tissue-specific expression of five voltage-gated potassium channel cDNAs expressed in rat heart. Proc Nat Acad Sci USA 88:1798-1802

Schulze W (1964) On the ultrastructure of the heart tubes of *Ciona intestinalis L.* Experientia 20:265-266

Serôdio P, Kentros C, Rudy B (1994) Identification of molecular components of A-type channels activating at subthreshold potentials. J Neurophysiol 72:1516-1529

Serôdio P, Vega-Saenz de Miera E, Rudy B (1996) Cloning of a novel component of A-type K^+ channels operating at subthreshold potentials with unique expression in heart and brain. J Neurophysiol 75: 2174-2179

Shibata R, Misonou H, Campomanes CR, Anderson AE, Schrader LA, Doliveira LC, Carroll KI, Sweatt JD, Rhodes KJ, Trimmer JS (2003) A fundamental role for KChIPs in determining the molecular properties and trafficking of Kv4.2 potassium channels. J Biol Chem 278:36445-36454

Sidow A (1996) Gen(om)e duplications in the evolution of early vertebrates. Curr Opin Genet Dev 6: 715-722

Wang S, Patel SP, Qu Y, Hua P, Strauss HC, Morales MJ (2002) Kinetic properties of Kv4.3 and their modulation by KChIP2b. Biochem Biophys Res Commun 295: 223-229

Weiss J, Morad M (1974) Single cell layered heart: electromechanical properties of the heart of Boltenia ovifera. Science 186:750-752

CHAPTER 3 CHARACTERIZATION OF A KChIP-LIKE SUBUNIT EXPRESSED IN THE MYOCARDIUM OF THE TUNICATE *Ciona intestinalis*. A FUNCTIONAL STUDY ON A PRIMITIVE Kv4/KChIP COMPLEX[3]

3.1 Introduction

Kv4 channels form supra-molecular complexes with several accessory subunits, including Kvβ subunits (Nakahira et al., 1996; Yang et al., 2001), K^+ channel interacting proteins (KChIPs, An et al., 2000), CD26-related dipeptidyl amino peptidase-like protein (DPPX, Nadal et al., 2003), frequenin (Nakamura et al., 2001), Minimal K subunits (MinK, Deschênes and Tomaselli, 2002), MinK-related peptide 1 (MiRP1, Deschênes and Tomaselli, 2002), neuronal calcium sensor-1 (Guo et al., 2002) and filamin (Petrecca et al., 2000). Kv4 channels expressed in stomatogastric neurons

[3] Data presented in Chapter 2, which describes the biophysical properties of *Ciona*Kv4 and an N-terminal deletion mutant (nt*Ciona*Kv4) are presented again in this chapter as control data in order to evaluate the effects of the accessory subunit *Ciona*KChIP on both these channels (wild-type and N-deletion mutant).

of an invertebrate, the spiny lobster (*Palinurus interruptus*), are modulated by frequenin subunits that are also expressed in these neurons (Zhang et al., 2003). It seems likely that lobster *Shal* is additionally modulated by endogenous KChIP subunits, because co-expression with human KChIP1 increased current amplitude, slowed inactivation kinetics, accelerated recovery from inactivation and shifted the midpoints of activation and inactivation of this Kv4 channel (Zhang et al., 2003). KChIPs, a family of Ca^{2+} binding proteins (Burgoyne and Weiss, 2001), are integral components of Kv4 channel supra-molecular complexes (An et al., 2000). KChIP isoforms 1 to 3, but not KChIP4, increase the density of Kv4 currents (An et al., 2000; Shibata et al., 2003), and all four KChIP isoforms modify the kinetics and gating properties of Kv4 channels (An et al., 2000; Holmqvist et al., 2004). The modulation of expression levels and biophysical activity of Kv4 channels by KChIPs (An et al., 2000) has important implications in the excitability properties of the tissues where they are expressed. For example, epicardial and endocardial myocytes express the same amount of Kv4 mRNA, the channel that conducts the I_{TO} current (Dixon et al., 1996), the amplitude of which determines the shape and duration of the cardiac action potential (Mitchell et al., 1984). However, epicardial cells produce larger I_{TO} currents than endocardial cells (Litovsky and Antzelevitch, 1988). Since KChIPs increase the density of Kv4 currents (An et al., 2000), Rosati et al. (2003) hypothesized that the greater amplitude of the I_{TO} current in the epicardium may be correlated with greater levels of KChIP2 mRNA in this region and found this to be the case. Therefore, to gain further clues on how these accessory

subunits have contributed to the evolution of electrical excitability, it is important to study the modulation of potassium channels by endogenous accessory subunits from selected taxa that represent critical branching points in evolution. We proposed that a Kv4 channel previously cloned from the myocardium of the basal chordate *Ciona intestinalis* (*Ciona*Kv4, Salvador-Recatalà et al., submitted) might be modulated by tunicate KChIP(s). After confirming that a KChIP subunit (*Ciona*KChIP) is expressed in the myocardium of *Ciona intestinalis*, we cloned it and co-expressed it with *Ciona*Kv4 channels in *Xenopus* oocytes in order to study whether *Ciona*KChIP would modulate its expression and/or biophysical parameters.

Since the N-terminus of Kv4 channels appears to be required for modulation by KChIPs (Bähring et al., 2001), we investigated the contribution of the N-terminus of *Ciona*Kv4 to modulation by *Ciona*KChIP, by analyzing currents produced by an N-terminal deleted mutant channel lacking amino acids 2-32 (nt*Ciona*Kv4) in the presence and absence of *Ciona*KChIP.

3.2 Materials and Methods

Tissue and RNA extraction

Specimens of *Ciona intestinalis* were purchased from the Marine Biology Laboratory (MBL, Massachusetts, US) and kept in a seawater aquarium at 12°C until used. Dissection of the myocardium was performed as described previously (Salvador-Recatalà et al., submitted) and used immediately or frozen at -80°C until used. Total

RNA was extracted from heart tissue (4 to 6 hearts per experiment) using the "Totally RNA" kit (Ambion).

Rapid Amplification of cDNA 3' End (3'-RACE) for KChIP

The GeneRacer Kit (Invitrogen) was used to perform a 3'-RACE assay. Briefly, cDNA was synthesized from RNA previously extracted from heart tissue using an oligo-dT primer with a unique sequence at the 3' end provided with the kit. Each 50 µl 3'-RACE assay contained: 1 x Opti-Prime Buffer (Stratagene) (10 mM Tris•HCl, 1.5 mM $MgCl_2$, 25 mM KCl at pH 8.3), 0.5 unit of Taq polymerase, 0.25 mM of each dNTP, 1 µM each of forward primer and reverse primer and 2 µL of cDNA. A sense primer (5'-CAGTTGTTGGGATCGCATGT-3') that hybridized to an internal region, and an anti-sense primer supplied by the kit that hybridized to the specific sequence of the oligo-dT primer. The temperature conditions were: 30 s at 94° C, followed by 5x (30 s at 94° C, 30 s at 65° C, 1 min. at 72° C), 25 x (30 s at 94° C, 30 s at 60° C, 1 min. at 72° C) followed by 5 min. at 72° C. The first ~300 bp of these RACE products were sequenced with the forward primer used in this assay. This sequence was used to design a new forward primer to hybridize downstream of the initial site in a nested 3'-RACE assay. Successive nested RACE assays were performed in the same fashion until the first 3'-RACE assay product was fully sequenced.

PCR for the 5' end of the KChIP transcript

The 5' end of the KChIP transcript was amplified by PCR, with a forward primer designed to bind from the start of the coding region (5'-ATGTCTCTCTCGCTATCTTAACCATGGTGAC-3'), as annotated in the genomic database of *Ciona intestinalis*, and a reverse primer (5'-GACGCTGTACAGAAACTTCAAAAACGAG-3') designed so that the fragment amplified would overlap with the fragment amplified previously by 3'-RACE.

Cloning of full-length ORF of *Ciona*KChIP

The full-length transcript of *Ciona*KChIP was amplified with a sense primer containing an XhoI site, a Kozak consensus sequence, the start codon and 26 futher bases encoding the 5' end of the KChIP ORF (5'-GGCTCGAGGCCGCCACCATGTCTCTCGCTATCTTAACCATGGTGAC-3') and an anti-sense primer containing a SpeI site, designed to hybridize downstream of the translational termination codon (5'-GGACTAGTAACGCCAGAAACGCCGCCTTGATGGAGCTATAACGC-3'). These restriction sites were added to allow directional insertion of the PCR products into pXT7 (Dominguez et al., 1995). Each 50 μL PCR reaction contained: 1 x Opti-Prime Buffer (Stratagene) (10 mM Tris•HCl, 1.5 mM $MgCl_2$, 25 mM KCl at pH 8.3), 0.5 unit of Taq polymerase, 1 unit of Pfu, 0.2 mM of each dNTP, 1 μM each of forward and reverse primer, and 2 μL of cDNA. The temperature conditions were: 30 s at 94° C, 25 x (30 s at 94° C, 30 s at 60° C, 2 min. at 72° C) followed by 5 min. at 72°C. The resulting PCR products were then digested with XhoI and SpeI and ligated to pXT7

plasmid previously digested with XhoI and SpeI. These constructs were transfected into *E. coli*. Clones were sequenced to verify that no mutation had been introduced by PCR. A wild type clone was linearized with SalI and cRNA was synthesized using the T7 mMessage mMachine kit (Ambion). Cloning of full-length ORF of *Ciona*Kv4 and construction of an N-truncation mutant of *Ciona*Kv4 (nt*Ciona*Kv4) has been described previously (Salvador-Recatalà et al., submitted).

Alignment and phylogenetic tree

Amino acid sequences of a set of seventeen representative KChIP sequences from vertebrates and invertebrates were aligned with T-Coffee software (Notredame et al., 2000). The sequences of two invertebrate KChIPs were found in BLAST searches of their respective genomes using the sequence of mammalian KChIPs. MrBayes (Huelsenbeck and Ronquist, 2001) was used to determine the phylogenetic relationships of the KChIP sequences. The default parameters for protein sequences were used. A total of 200,000 cycles were run; the topology and branch length of every 100^{th} tree was saved. The Bayesian maximum likelihood tree was obtained by taking a consensus of the collected trees after a 101 tree burn-in. The nodes on the tree are labeled with the posterior probability for each node; nodes with a probability of one were left unlabelled. The tree was visualized using Treeview (Page, 1996).

Oocyte preparation

Oocytes from *Xenopus laevis* were surgically removed, dissociated and incubated as previously described (Salvador-Recatalà et al., submitted). 24 or 48 hours following oocyte isolation, 40 nL of *Ciona*Kv4 cRNA (~16 ng) or nt*Ciona*Kv4 (~8 ng) were injected into each *Xenopus* oocyte. For co-expression experiments, 20 nL (~8 ng) of *Ciona*Kv4 or 20 nL (~4 ng) of nt*Ciona*Kv4 cRNA solution was mixed with 20 nL (~7 ng) of *Ciona*KChIP cRNA solution, to give a final volume of 40 nL that was injected into each oocyte. The approximate molar ratio was [1 *Ciona*Kv4 : 3 *Ciona*KChIP] or [1 nt*Ciona*Kv4 : 6 *Ciona*KChIP]. Immediately prior to each experiment the vitelline membrane was manually removed after treatment in a hyperosmotic solution containing (mM): NaCl (96), KCl (2), $MgCl_2$ (20), HEPES (5) and mannitol (400), at pH 7.4.

Voltage-clamp recordings

All recordings were made from cell-attached macro-patches. The pipettes contained ND96 solution, with the following composition (mM): NaCl (96), KCl (2), $MgCl_2$ (1), $CaCl_2$ (1.8) and HEPES (5), at pH 7.4. During the recordings, oocytes were bathed in a grounded isopotential solution thereby ensuring that the potential applied by the recording pipette would be the actual membrane potential for the macro-patch. This bath solution contained (mM): NaCl (9.6), KCl (88), EGTA (11), HEPES (5), pH 7.4. Patch pipettes were pulled from aluminosilicate glass, and were coated with dental wax, and fire-polished before each experiment. Only pipettes that had resistances between

0.7 and 1.4 MΩ were used. Membrane seals were obtained by applying negative pressure. Voltage-clamp and data acquisition were carried out with an EPC-9 patch-clamp amplifier (HEKA, Lambrecht, Germany) controlled with PULSE software (HEKA) running on a Power MacIntosh G4 computer. Data were acquired at sampling intervals of 50 μs and low-pass filtered at 5 kHz during acquisition. Bath temperature was maintained at 12 ± 0.2° C with a Peltier device controlled by an HCC-100A temperature controller (Dagan, Minneapolis, MN, USA). The holding potential was set at –100 mV and leak subtraction was performed with a P/4 protocol. PulseFit (HEKA), Igor Pro (Wavemetrics, Lake Oswego, OR, USA) and Instat (GraphPad Software, San Diego, CA, USA) software were used for analyses and graphing. Conductances were calculated using the equation $g_K = I_{peak} / (V-E_K)$, where g_K is the potassium conductance, I_{peak} is the peak amplitude of the K^+ current to a test pulse, V is the voltage at which the current was measured, and E_K is the measured potassium equilibrium potential. Conductance-voltage relationships and steady-state inactivation curves were fitted in Igor Pro by a sigmoid (Boltzmann) distribution of the form: $f(V) = G_{max}/\{1 + \exp[(V_{0.5} - V) / k]\}^n$, where G_{max} is the maximal conductance, V is the voltage of the depolarizing pulse (for activation) or the prepulse voltage (for inactivation), and k is the slope factor. For a first order Boltzmann (n = 1), used to fit conductance-voltage relationships and steady-state inactivation curves, $V_{0.5}$ is the voltage at which activation or inactivation is half maximal. For a fourth order Boltzmann (n=4), used to fit conductance-voltage relationships only, $V_{0.5}$ is the voltage

at which each subunit is activated half of the time. Time constants of activation were obtained from fitting the rising phase of the currents to the Hodgkin-Huxley model of the form: $I(t) = I_{max} \{1- \exp[-t/\tau]\}^n$ where I_{max} is the maximum current obtained in the absence of inactivation, τ is the activation time constant and n = 4. The rate of decay (slope) of an exponential function that fitted the relationship between activation time constants and voltage was used to estimate the voltage necessary to increase the current amplitude by a factor of e. To study the decay of the current as a function of time, decaying phases of the outward currents evoked by test pulses between +30 mV and +80 mV were fitted to the equation: $I(t) = I_0 + I_1 \exp(-t/\tau_1) + I_2 \exp(-t/\tau_2)$, where τ_1 and τ_2 represent the fast and the slow time constants of inactivation, respectively, I_1 and I_2 represent the relative contribution of each component to inactivation, and I_0 is the offset. The voltage dependence of steady-state inactivation was determined by measuring the peak current evoked with a depolarizing pulse to +50 mV as a function of the voltage of a preceding 10 s prepulse test (between –130 and –30 mV). To investigate the kinetics of channel closing, tail currents were evoked at several membrane potentials, from –160 to –40 mV, from a brief (10-15 ms) depolarizing pulse to +50 mV. Tail currents obtained with pulses from –160 to –100 mV were used for analyses.

Statistical analyses

Statistical comparisons were carried out using the Student t test, or the alternative Welch t test when there were significant differences between the standard deviations of the two groups. Data are represented as the mean ± SEM, and n is the number of macro-patches or oocytes, because recordings from one macro-patch *per* oocyte were included in the analyses.

3.3 Results

Cloning of a transcript for a KChIP-like subunit from the heart of *C. intestinalis*

BLAST searches in the release version 1.0 of the *C. intestinalis* genomic database (http://genome.jgi-psf.org/ciona4/ciona4.home.html) for KChIP-like genes using the amino acid sequences of mammalian KChIP subunits and subsequent detailed evaluation of the results resulted in one robust hit. The alignment between a mammalian KChIP and scaffold 457 (Fig. 3-1A) was used to predict the exon/intron organization of the tunicate KChIP gene. Using this information, we designed an internal forward primer that was used in a 3'-RACE assay (Fig. 3-1B). The annotated sequence for KChIP in the genomic database was also used to design forward and reverse primers to amplify the 5'-end of the transcript, as explained in Materials and Methods. The DNA fragments corresponding to the 5' end and the 3'-end of the KChIP transcript were sequenced on both strands. The nucleotide sequence of the KChIP

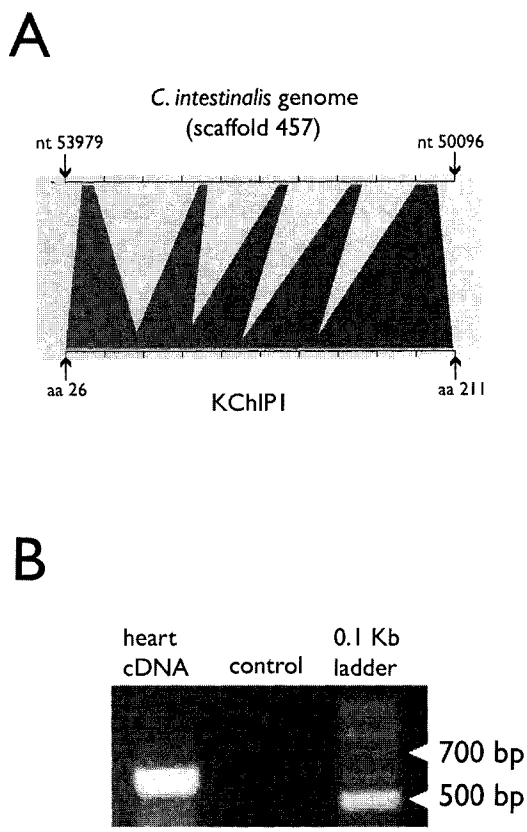

Figure 3-1. The myocardium of *Ciona intestinalis* expresses a KChIP-like subunit. *A,* Alignment of the deduced amino acid sequence of a mammalian KChIP subunit (accession number AAH50375) and scaffold 457 of the *C. intestinalis* genomic database (release version 1.0). *B,* Amplification of the 3'end of a KChIP transcript by 3'-RACE using cDNA from the heart of *C. intestinalis.* The size of these fragments was ~600 bp. No cDNA was added to the control reaction.

transcript (ORF and the 3'-UTR region) was deposited in GenBank (*Ciona*KChIP, accession number AY514487[4]). The open reading frame (ORF) for *Ciona*KChIP was inserted into and maintained in pXT7.

Genomic structure and deduced amino acid sequence of *Ciona*KChIP

The exon/intron organization of the gene encoding *Ciona*KChIP was deduced by comparing the cDNA sequence for *Ciona*KChIP with the genomic sequence of scaffold 457 (*Ciona intestinalis* genomic database, release version 1.0), which contained the *Ciona*KChIP gene. The exon sequences and the corresponding regions of the transcript were at least 94% identical. *Ciona*KChIP is encoded in ~7 Kb of genomic DNA, of which the ORF occupies ~ 0.7 Kb distributed in seven exons with sizes between 69 and 162 bp (Fig. 3-2). Figure 3-3 shows an alignment between the deduced amino acid sequences of *Ciona*KChIP and representatives of the four major isoforms of mammalian KChIPs (KChIP1 to 4). As with other KChIPs, the sequence of the N-terminus of *Ciona*KChIP was the most variable region of the protein (An et al., 2000) whereas the sequence corresponding to the C- terminus was conserved, containing four EF-hand Ca^{2+}-binding motifs (Kretsinger, 1987). The N-terminus of *Ciona*KChIP is encoded by exons 1 and 2. The coding region for the first EF-hand was partitioned between exons 2 and 3. Similarly, the codons for the second and the third EF-hands were partitioned between exons 4 and 5 (second EF-hand), and between exons 5 and 6

[4] The published GenBank script for *Ciona*KChIP is shown in Appendix B

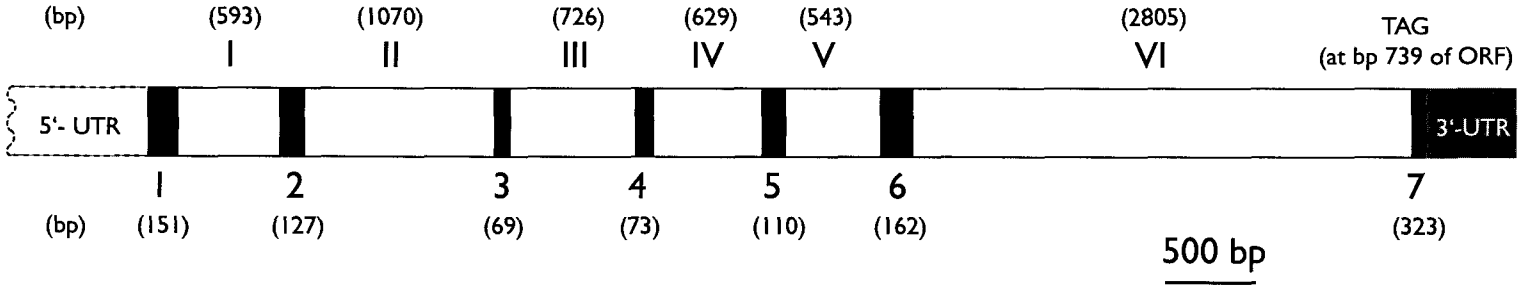

Figure 3-2. Exon/intron structure of the *Ciona*KChIP gene. Diagram showing the organization of the *Ciona*KChIP gene, elucidated from an alignment between the sequence of the *Ciona*KChIP transcript and scaffold 457 of the genomic database for *C. intestinalis* (release version 1.0). Exons are shown as black boxes and numbered in Arabic numerals (from 1 to 7). Introns are shown as white boxes and numbered in Roman numerals (from I to VI). Intron and exon sizes (in bp) are indicated, respectively, above or below the diagram. Sizes are drawn approximately to scale. The 3'-UTR region is represented by a grey box. The 5'-UTR region is delimited with a discontinuous line to indicate that its sequence was not determined in this study.

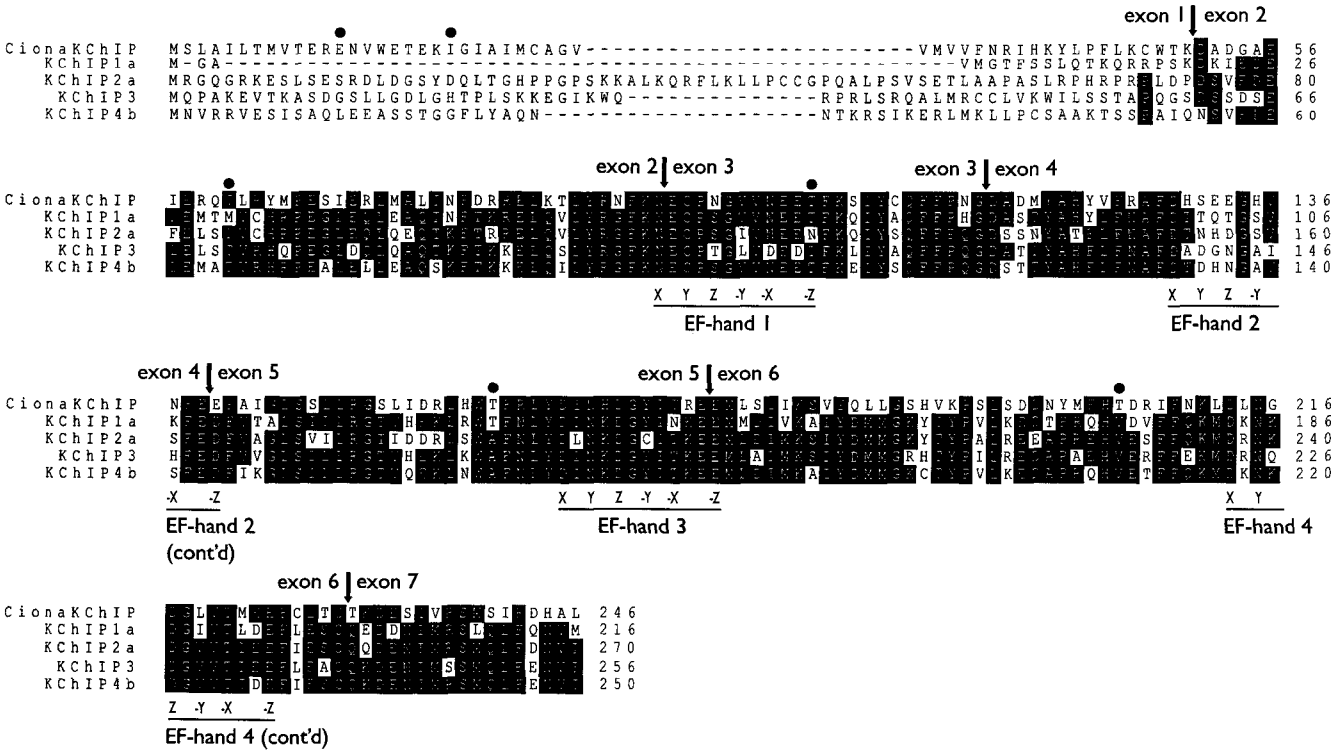

Figure 3-3. Alignment and sequence comparison between *Ciona*KChIP and representatives of the four vertebrate KChIP isoforms. T-Coffee software (Notredame et al., 2000) was used to align these sequences, with the following accession numbers: *Ciona*KChIP, AAS00647; KChIP1a, AAL12489; KChIP2a, AAF81755; KChIP3, Q9Y2W7; KChIP4b, NP_079497. Residues that are identical for at least three of the five KChIPs are shown in reverse lettering (white on black). The position of the four EF-hands is underlined and labeled below the alignment. X, Y, Z, -Y, -X and –Z are the residues that coordinate Ca^{2+} (Bairoch and Cox, 1990). Arrows indicate exon/intron boundaries for *Ciona*KChIP only. A Prosite scan predicted several phosphorylation sites for protein kinase C (PKC), which are indicated with filled circles.

(third EF-hand). The fourth EF-hand is encoded by exon 6. The last section of the C-terminus is coded by exon 7. A Prosite scan of *Ciona*KChIP suggested the location of six putative sites for PKC phosphorylation but no sites for PKA phosphorylation (Fig. 3-3).

In the phylogenetic tree shown in Figure 3-4, the single *Ciona*KChIP branches basal to the four mammalian KChIP isoforms. Furthermore, this tree indicates that there is 99% likelihood that the KChIP1 isoform is the sister group of the other three isoforms. However, the phylogenetic relationships between the KChIP isoforms 2, 3 and 4 are unclear, with posterior probabilities of approximately 50-60%. However, there is strong support for the presence of all four isoforms in the common ancestor of modern fish (represented by zebrafish) and the tetrapods (represented by human, mouse, rat and chicken). Although not all four paralogues are found in all of the vertebrates, all of the vertebrate KChIP sequences partition robustly into one of the four paralogue families, indicating that the paralogues all originated prior to the origins of the vertebrates.

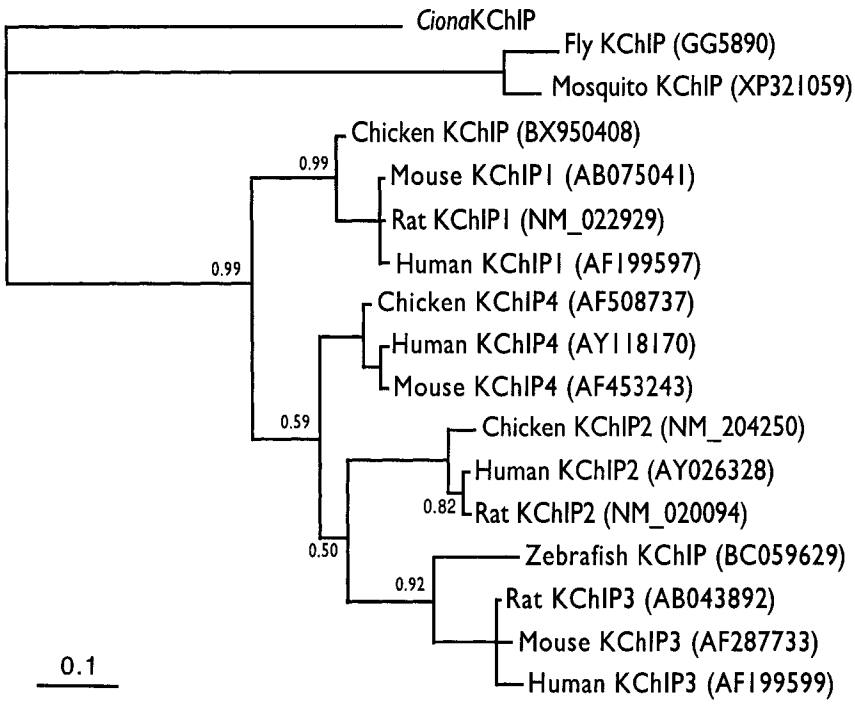

Figure 3-4. Phylogenetic relationships of KChIPs from different species. Two arthropod KChIPs that were found in BLAST searches of the genomes of *Drosophila* (fly) and *Anopheles gambiae* (mosquito) were used as an out-group to polarize the relationships of the other KChIPs. Numbers above or below the lines indicate Bayesian posterior probability, calculated with the MrBayes program. Unlabelled nodes have a posterior probability of 1. Accession numbers of the protein sequences are indicated in parentheses. The scale bar represents a divergence equivalent to an average of a 10% change in amino acids.

Activation properties of *Ciona*Kv4 and an N-deletion mutant of *Ciona*Kv4 (nt*Ciona*Kv4) in the presence/absence of *Ciona*KChIP

*Ciona*Kv4 channels conducted transient A-type currents (Fig. 3-5A, see also Fig. 2-6A). In contrast, currents mediated by *Ciona*Kv4 channels co-expressed in oocytes with *Ciona*KChIP subunits displayed minimal inactivation during depolarizing pulses lasting 0.5 s (Fig. 3-5B), indicating that *Ciona*Kv4 and *Ciona*KChIP formed functional complexes when co-expressed in *Xenopus* oocytes. The amplitudes of the currents produced by *Ciona*Kv4 channels co-expressed with *Ciona*KChIP subunits were larger than for *Ciona*Kv4 channels alone, even though half the amount of *Ciona*Kv4 cRNA was injected for co-expression experiments. For example, the average peak amplitude of the currents produced by *Ciona*Kv4 and *Ciona*Kv4/KChIP for a test pulse to +50 mV from a holding potential of –100 mV was 207 ± 27 pA (n = 15) and 867 ± 62 pA (n = 17), respectively ($p < 0.0001$, Fig. 3-6A). However, *Ciona*KChIP did not modulate activation kinetics of *Ciona*Kv4 channels, since the activation time constants obtained from a Hodgkin-Huxley fit to the rising phase of the currents during a pulse to +50 mV were not significantly different: 3.4 ± 0.2 ms (n = 11) for *Ciona*Kv4, and 3.3 ± 0.2 ms (n = 10) for *Ciona*Kv4/KChIP ($p > 0.05$, Student t test). The voltage-dependence of activation time constants was similar for channels expressed alone or with *Ciona*KChIP, increasing by e-fold every 29 or 33 mV, respectively (Fig. 3-6B). First order Boltzmann fits to the relationships between normalized peak conductance *versus* voltage had midpoints ($V_{0.5}$) of +20 ± 2 mV (n = 16) for *Ciona*Kv4 and –5.7 ± 1.4 mV

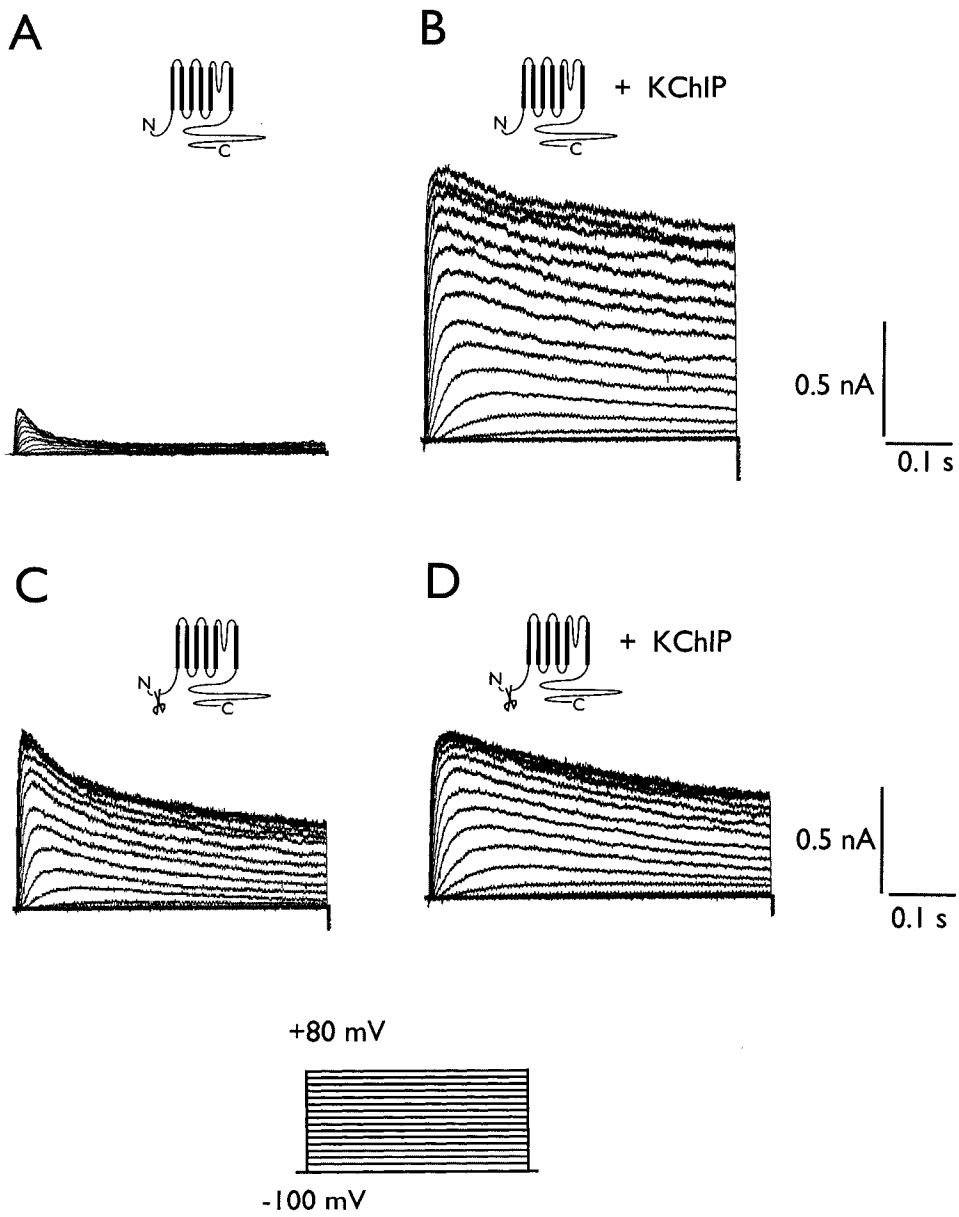

Figure 3-5 (Legend on next page)

Figure 3-5. Currents produced by *Ciona*Kv4 and an N-terminal deletion mutant of *Ciona*Kv4 (nt*Ciona*Kv4) in the presence/absence of *Ciona*KChIP. *A,* Representative currents from *Ciona*Kv4 channels expressed alone. *B,* Currents produced by *Ciona*Kv4 co-expressed with *Ciona*KChIP . *C,* Currents produced by nt*Ciona*Kv4 channels expressed alone. *D,* Currents produced by nt*Ciona*Kv4 co-expressed with *Ciona*KChIP. All recordings were obtained using the macro-patch technique. Currents were evoked by depolarizing the macro-patches for 0.5 s. from a holding potential of –100 mV from –100mV to +80mV in 10 mV steps. These currents are representative examples of 15-17 experiments.

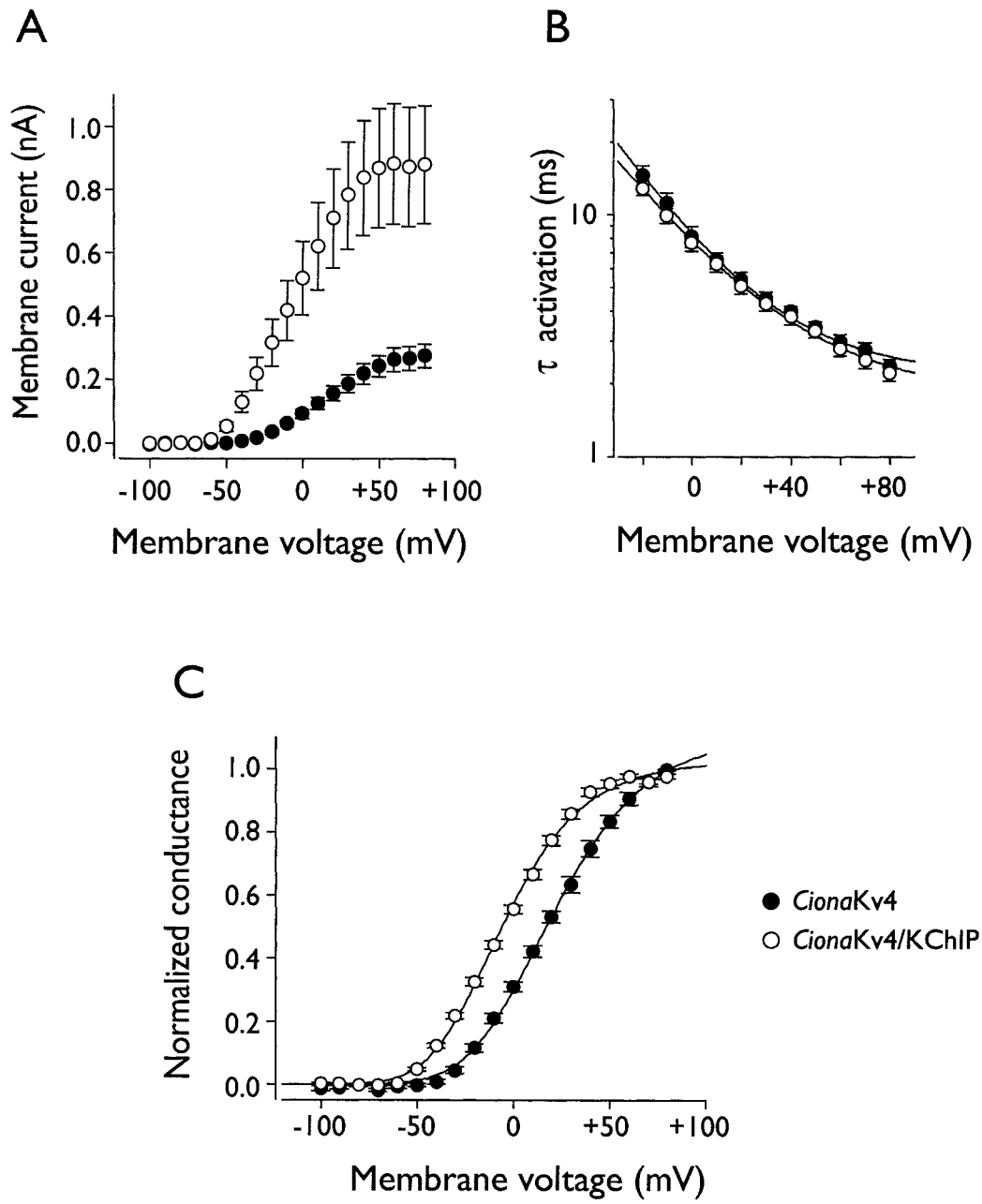

Figure 3-6 (Legend on next page)

Figure 3-6. Activation properties of *Ciona*Kv4 in the presence/absence of *Ciona*KChIP. *A,* Averaged current-voltage relationships for *Ciona*Kv4 (filled circles) and *Ciona*Kv4/KChIP (open circles). *B,* Relationship between time constants of activation (τ activation) and voltage for *Ciona*Kv4 and *Ciona*Kv4/KChIP. Time constants of activation were derived from Hodgkin-Huxley fits to the rising phase of macroscopic outward currents during test pulses between –20 mV and +80 mV from a holding potential of –100 mV. Solid curves represent single exponential fits to these relationships. *C,* Normalized peak conductance-voltage relationships for *Ciona*Kv4 and *Ciona*Kv4/KChIP. Solid curves represent fits of these relationships to first order Boltzmann functions. Data represent mean ± SEM.

(n = 17) for *Ciona*Kv4/KChIP ($p < 0.0001$, Student t test, Fig. 3-6C). Therefore, *Ciona*KChIP enhanced activation of *Ciona*Kv4 by shifting the midpoint of activation (the voltage necessary to activate half the channels) in the hyperpolarizing direction. The slope values of these curves were 22 ± 1 mV/e-fold (*Ciona*Kv4) and 20 ± 1 mV/e-fold (*Ciona*Kv4/KChIP) ($p = 0.06$, Student t test, Figure 3-6C). The midpoint voltage of activation ($V_{0.5}$) corresponding to fourth order Boltzmann fits to relationships between normalized peak conductance and test voltage were –27 ± 2 mV (n = 16) for *Ciona*Kv4 alone and –48 ± 1 mV (n = 17) for *Ciona*Kv4/KChIP ($p < 0.0001$, Student t test). The conductance at these voltages represented approximately 7% of the maximal conductance. The slope factors of the fourth order Boltzmann fits were 31 ± 2 mV/e-fold (n = 16) for *Ciona*Kv4, and 26 ± 1 mV/e-fold (n = 17) for *Ciona*Kv4/KChIP ($p < 0.05$), which confirms a role for *Ciona*KChIP in enhancing activation of *Ciona*Kv4, as these values indicate that *Ciona*Kv4/KChIP complexes require less depolarization than *Ciona*Kv4 channels to produce the same increase in conductance.

To investigate the involvement of the N-terminus of *Ciona*Kv4 in modulation by *Ciona*KChIP, a *Ciona*Kv4 mutant lacking amino acids 2-32 (nt*Ciona*Kv4) was expressed in *Xenopus* oocytes alone or with *Ciona*KChIP. Before reporting the effects of *Ciona*KChIP on nt*Ciona*Kv4, it is necessary to understand how the activation properties of these mutant channels that lack the N-terminal domain differ from the activation properties of wild type channels. A detailed comparison between activation properties of wild-type *Ciona*Kv4 and N-terminal deletion mutant *Ciona*Kv4 (nt*Ciona*Kv4) channels was provided in Chapter 2 (Figures 2-6 and 2-7). Prior to

describing the effect of *Ciona*KChIP on each activation parameter of nt*Ciona*Kv4, I will briefly summarize how these two *Ciona*Kv4 channels (wild-type and N-terminal deletion mutant) differ for each activation parameter, and refer the reader to the parts of Chapter 2 where a detailed quantitative comparison was provided.

Figures 3-5C and 3-5D show families of currents produced by nt*Ciona*Kv4 channels expressed alone or with *Ciona*KChIP, respectively. Note that the currents produced by nt*Ciona*Kv4 channels were larger than the currents produced by wild type *Ciona*Kv4 channels (Fig. 3-5A, see also Fig. 2-7A). The amplitudes of currents produced by nt*Ciona*Kv4 channels alone were not altered by co-expression with *Ciona*KChIP ($p > 0.05$, Figs. 3-7A). Activation kinetics of nt*Ciona*Kv4 channels, which did not differ from activation kinetics of wild-type channels (Figure 2-7B), were similarly unaffected by *Ciona*KChIP. For example, during a test pulse to +50 mV, nt*Ciona*Kv4 channels activated with a time constant of 3.2 ± 0.3 ms ($n = 12$), which was not significantly different ($p > 0.05$) from the activation time constant of nt*Ciona*Kv4 co-expressed with *Ciona*KChIP (3.5 ± 0.3 ms, $n = 12$, Fig. 3-7B). Interestingly, the voltage-dependence of activation kinetics was different for nt*Ciona*Kv4 channels alone (e-fold increase every 26 mV) than when co-expressed with *Ciona*KChIP (e-fold increase every ~37 mV), which suggests that *Ciona*KChIP decreased the voltage sensitivity of activation of nt*Ciona*Kv4 channels. The midpoint of activation of nt*Ciona*Kv4 channels, which was hyperpolarized with respect to wild-type *Ciona*Kv4 channels (Fig. 2-7C), was unaffected by *Ciona*KChIP (Fig. 3-7C), the $V_{0.5}$ of first order Boltzmann fits to the conductance-voltage relationships were

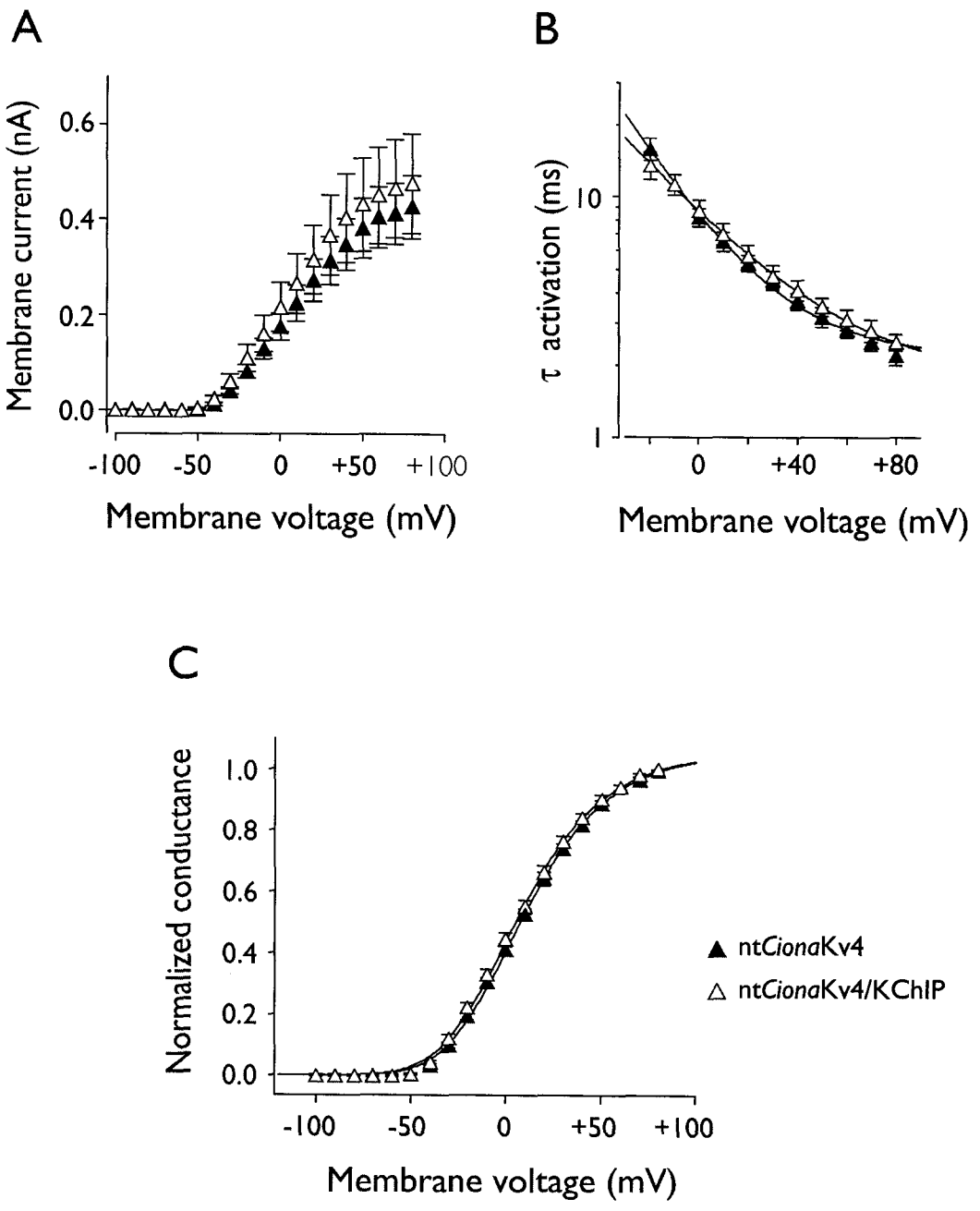

Figure 3-7 (Legend on next page)

Figure 3-7. Activation properties of an N-terminal deletion mutant of *Ciona*Kv4 (nt*Ciona*Kv4) in the presence/absence of *Ciona*KChIP. *A,* Averaged current-voltage relationships for *Ciona*Kv4 (filled triangles) and *Ciona*Kv4 co-expressed with *Ciona*KChIP (open triangles). *B,* Relationship between time constants of activation (τ activation) and voltage for nt*Ciona*Kv4 and nt*Ciona*Kv4 co-expressed with *Ciona*KChIP. Time constants of activation were derived from Hodgkin-Huxley fits to the rising phase of macroscopic outward currents during test pulses between –20 mV and +80 mV from a holding potential of –100 mV. Solid curves represent single exponential fits to these relationships. *C,* Normalized peak conductance-voltage relationships for nt*Ciona*Kv4 and nt*Ciona*Kv4 co-expressed with *Ciona*KChIP. Solid curves represent fits of these relationships to first order Boltzmann functions. Data represent mean ± SEM.

+8.3 ± 1.6 mV (n = 16) for nt*Ciona*Kv4 alone, and +7.4 ± 1.5 mV (n = 14) for nt*Ciona*Kv4 co-expressed with *Ciona*KChIP ($p > 0.05$, Student t test). The slope factors of these fits were: 20 ± 1 mV/e-fold (n = 16) for nt*Ciona*Kv4 channels expressed alone, and 21 ± 1 mV/e-fold (n = 14) for nt*Ciona*Kv4 channels co-expressed with *Ciona*KChIP subunits ($p > 0.05$, Student t test). The $V_{0.5}$ of fourth order Boltzmann fits were –36 ± 1 mV for nt*Ciona*Kv4 alone (n = 16) and –37 ± 1 mV (n = 14) for nt*Ciona*Kv4/KChIP ($p > 0.05$, Student t test). The conductance obtained with these potentials represented ~8% of the maximal conductance. The slope values of these fits were identical for nt*Ciona*Kv4 and nt*Ciona*Kv4 co-expressed with *Ciona*KChIP (28 ± 1 mV/e-fold).

These biophysical parameters are summarized in Table 3-1 (p. 122).

Inactivation parameters of *Ciona*Kv4 and an N-deletion mutant of *Ciona*Kv4 (nt*Ciona*Kv4) in the presence/absence of *Ciona*KChIP

Currents produced by *Ciona*Kv4/KChIP complexes inactivated clearly more slowly than currents produced by *Ciona*Kv4 channels (Fig. 3-8A). Whereas the inactivating phases of the currents produced by *Ciona*Kv4 channels were best fit with double exponential functions, the decaying phases of the currents produced by *Ciona*Kv4/KChIP complexes were well fit with single exponential functions (the two time constants of double exponential fits to currents produced by *Ciona*Kv4/KChIP complexes were close to identical in all cases). The single inactivation time constants of *Ciona*Kv4/KChIP currents were larger than the slow inactivation time constants of

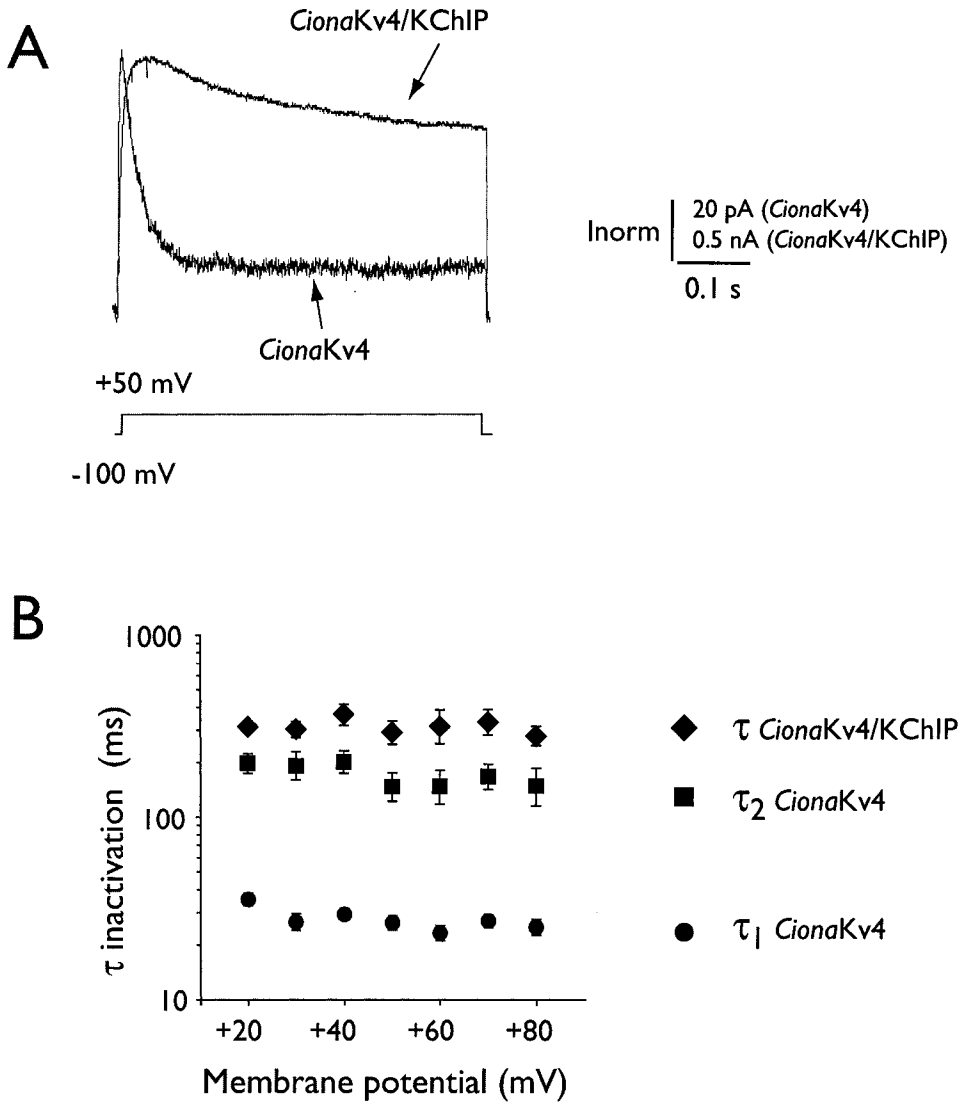

Figure 3-8. Inactivation kinetics of *Ciona*Kv4 in the presence/absence of *Ciona*KChIP. *A,* Comparison of inactivation of macroscopic currents produced by *Ciona*Kv4 channels or *Ciona*Kv4/KChIP complexes in response to a pulse to +50 mV from a holding potential of –100 mV. Currents were scaled to peak current for comparison. *B,* Relationships between time constants of inactivation (τ inactivation) and voltage. τ_1 and τ_2 are, respectively the time constants of the fast and slow components of inactivation of *Ciona*Kv4 currents. τ is the time constant of the one component of inactivation of *Ciona*Kv4/KChIP. The time constants were obtained from double exponential fits (*Ciona*Kv4) or single exponential fits (*Ciona*Kv4/KChIP) to the decay phase of currents evoked by test pulses between +20 mV and +80 mV from a holding potential of –100 mV. Circles and squares represent τ_1 and τ_2 respectively. Data represent mean ± SEM.

currents produced by *Ciona*Kv4 channels (Fig. 3-8B). For instance, the double exponential fit to the decay of currents produced by *Ciona*Kv4 in response to a pulse to +50 mV had a fast time constant of 26 ± 2 ms, which contributed to ~82 % of total current decay, and a slow time constant of 147 ± 26 ms, which contributed to ~18% of the current decay. A single exponential fit to the decay of currents conducted by *Ciona*Kv4/KChIP complexes at the same potential had a time constant of 291 ± 42 ms.

*Ciona*Kv4 channels lacking amino acids 2-32 from the N-terminus produced currents whose two inactivating phases had slower kinetics than those for the inactivating phases of wild-type *Ciona*Kv4 channels (Fig. 2-8B). Co-expression of nt*Ciona*Kv4 channels with *Ciona*KChIP subunits slowed inactivation kinetics relative to those for nt*Ciona*Kv4 channels alone (Fig. 3-9A). The decaying phases of currents produced by nt*Ciona*Kv4 channels were best fitted with a double exponential function (as explained in chapter 2), but the decaying phases for currents produced by nt*Ciona*Kv4 co-expressed with *Ciona*KChIP subunits were well fitted with single exponential functions. For instance, the decay phase of nt*Ciona*Kv4 currents during a test pulse to +50 mV is best described by a double exponential function with a fast time constant of 56 ± 6 ms (n = 15) and a slow time constant of 381 ± 50 ms (n = 15). These two inactivation components of nt*Ciona*Kv4 channels contributed equally to inactivation, as explained in Chapter 2. However, inactivation of nt*Ciona*Kv4/KChIP currents during a pulse to +50 mV was best described by a single exponential function with a time constant of 240 ± 29 ms (n = 8, Fig. 3-9B). These results suggest that *Ciona*KChIP still forms a complex with *Ciona*Kv4 channels that lack the N-terminus.

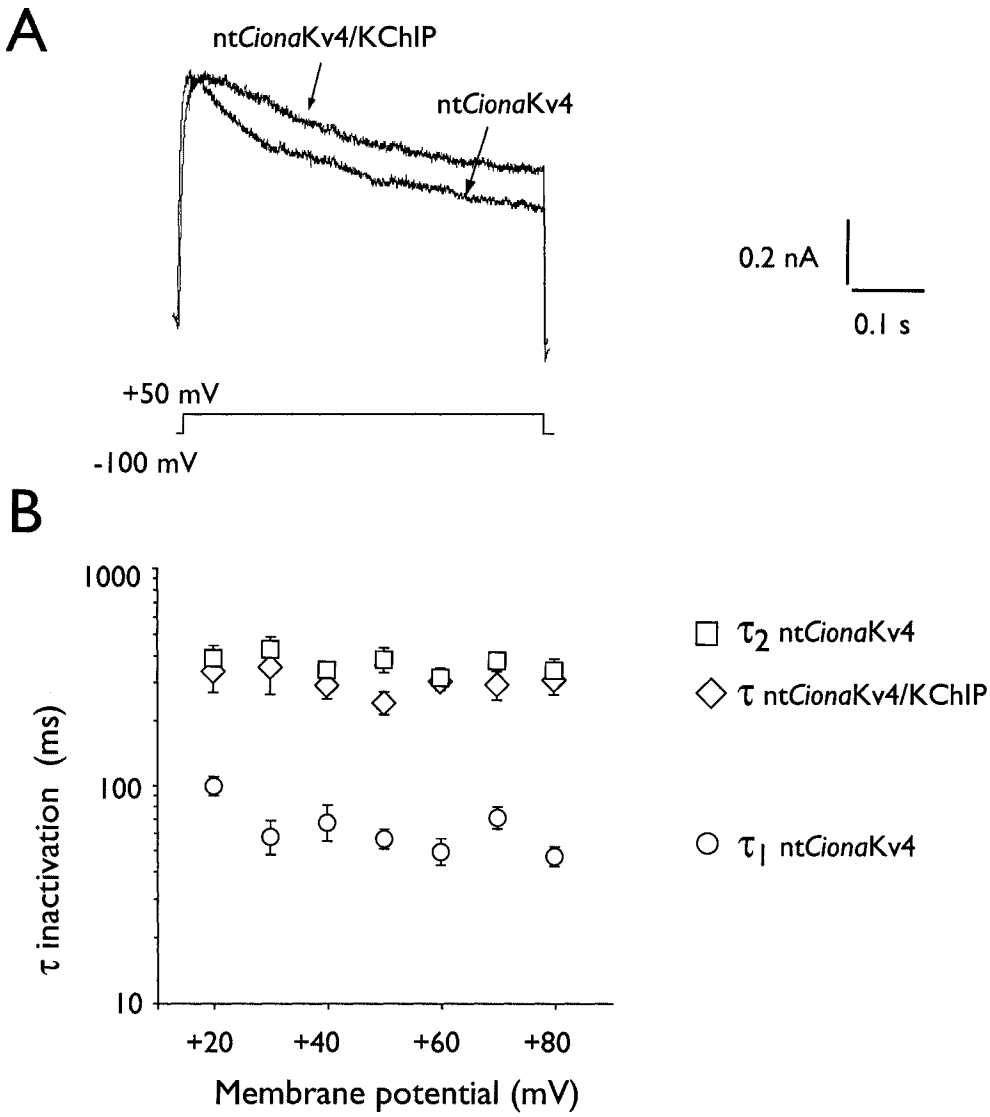

Figure 3-9. Inactivation kinetics of an N-terminal deletion mutant of *Ciona*Kv4 (nt*Ciona*Kv4), in the presence/absence of *Ciona*KChIP. *A*, Comparison of macroscopic currents produced by nt*Ciona*Kv4 channels or putative nt*Ciona*Kv4/KChIP complexes in response to a pulse to +50 mV from a holding potential of –100 mV. *B*, Relationships between time constants of inactivation (τ inactivation) and voltage. τ_1 and τ_2 are, respectively, the time constants of the fast and slow components of inactivation of nt*Ciona*Kv4 currents. τ is the inactivation time constant of the one component of inactivation of nt*Ciona*Kv4/KChIP complexes. The time constants were obtained from double exponential fits (nt*Ciona*Kv4) or single exponential fits (nt*Ciona*Kv4/KChIP) to the decay of currents evoked by test pulses between +20 mV and +80 mV from a holding potential of –100 mV. Circles and squares represent τ_1 and τ_2 respectively.
Data represent mean ± SEM.

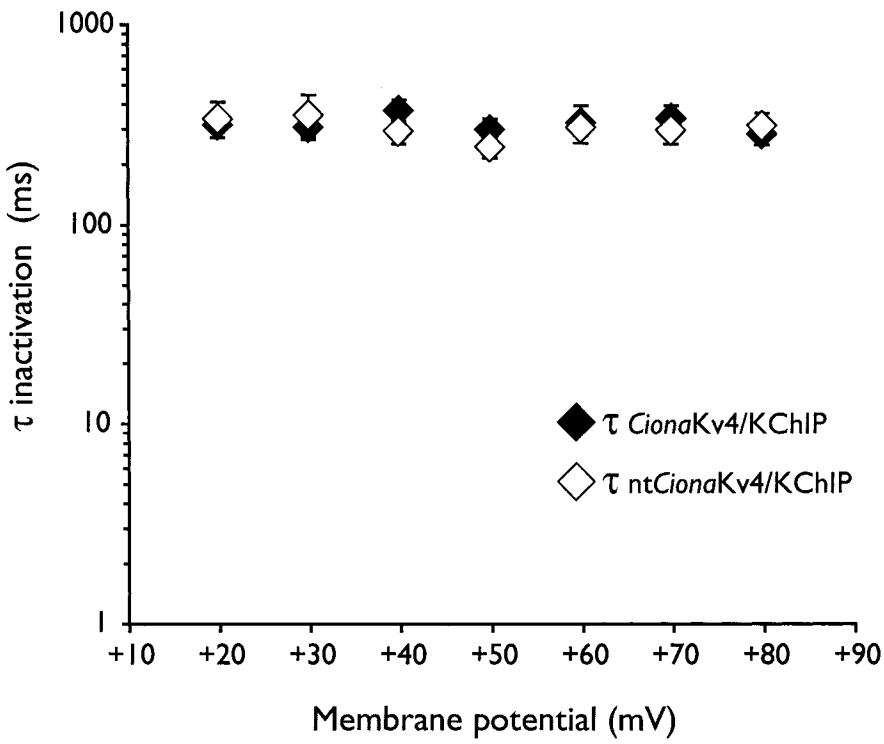

Figure 3-10. Comparison between inactivation time constants of *Ciona*Kv4/KChIP currents and nt*Ciona*Kv4/KChIP currents. The time constants (τ) were obtained from single exponential fits to the decay phase of currents evoked by test pulses between +20 mV and +80 mV from a holding potential of -100 mV.
Data represent mean ± SEM.

The inactivation time constants of *Ciona*Kv4/KChIP currents were not different than for nt*Ciona*Kv4/KChIP (Fig. 3-10).

The midpoints of single order Boltzmann fits to steady-state inactivation curves of *Ciona*Kv4 and *Ciona*Kv4/KChIP were significantly different (Fig. 3-11A): –72 ± 2 mV (n = 7) for *Ciona*Kv4 and –88 ± 2 mV (n = 7) for *Ciona*Kv4/KChIP ($p < 0.001$, Student t test). The slope factors of these Boltzmann fits to steady-state inactivation were also significantly different: 3.6 ± 0.2 mV/e-fold (n = 7) for *Ciona*Kv4 and 4.3 ± 0.2 mV/e-fold (n = 7) for *Ciona*Kv4/KChIP ($p < 0.001$, Student t test). Rates of recovery from inactivation for *Ciona*Kv4 channels in the presence/absence of *Ciona*KChIP subunits were assessed with a double pulse protocol, in which a first test pulse to +50 mV lasting for 1 s. was separated by a recovery pulse to -100 mV of increasing duration (50-1500 ms) from a second pulse to +50 mV. Inactivation recovery data were plotted as the amplitude of the current evoked by the second pulse relative to the current evoked by the first pulse as a function of the recovery interval duration. These relationships were well fitted by a single exponential function with time constants of recovery from inactivation (τ_{rec}) of 387 ± 47 ms (n = 7) for *Ciona*Kv4 and 927 ± 47 ms (n = 6) for *Ciona*Kv4/KChIP (Fig. 3-11B). These time constants were significantly different ($p < 0.01$, Student t test), suggesting that *Ciona*KChIP slowed recovery from inactivation in *Ciona*Kv4 channels.

The N-terminus of *Ciona*Kv4 is not essential to determine steady-state inactivation properties of this channel, because deletion of amino acids 2-32 did not result in modified parameters of steady-state inactivation (midpoint or slope) with

respect to wild type channels, as was shown in Chapter 2 (Fig. 2-9A). Midpoints and slopes of single order Boltzmann fits to steady-state inactivation curves of nt*Ciona*Kv4 channels and nt*Ciona*Kv4/KChIP complexes were not significantly different ($p > 0.05$ for both parameters, Student t test). Midpoints of inactivation were -73 ± 2 mV ($n = 7$) for nt*Ciona*Kv4 and -74 ± 2 mV ($n = 8$) for nt*Ciona*Kv4/KChIP. Slope factors were 3.7 ± 0.2 ($n = 7$) for nt*Ciona*Kv4 and 4.1 ± 0.3 ($n = 8$) for nt*Ciona*Kv4/KChIP (Fig. 3-12A). This demonstrates that the N-terminus of *Ciona*Kv4 is essential to modulation of steady-state inactivation by *Ciona*KChIP.

Inactivation recovery kinetics in *Ciona*Kv4 channels are not dependent on the N-terminus of this channel, because deletion of this domain did not increase or decrease the time constant of this parameter (Fig. 2-9B). The N-terminus of *Ciona*Kv4 appears to have a partial involvement in modulation by *Ciona*KChIP on inactivation recovery kinetics. Recovery time constants were 331 ± 51 ms ($n = 8$) for nt*Ciona*Kv4 and 587 ± 76 ms ($n = 8$) for nt*Ciona*Kv4/KChIP ($p < 0.05$, Student t test). This strongly suggests that *Ciona*KChIP can slow the kinetics of recovery of a *Ciona*Kv4 channel that lacks the N-terminus, but not as much as when the N-terminus is intact (Fig. 3-12B).

These biophysical parameters are summarized in Table 3-1 (p. 122).

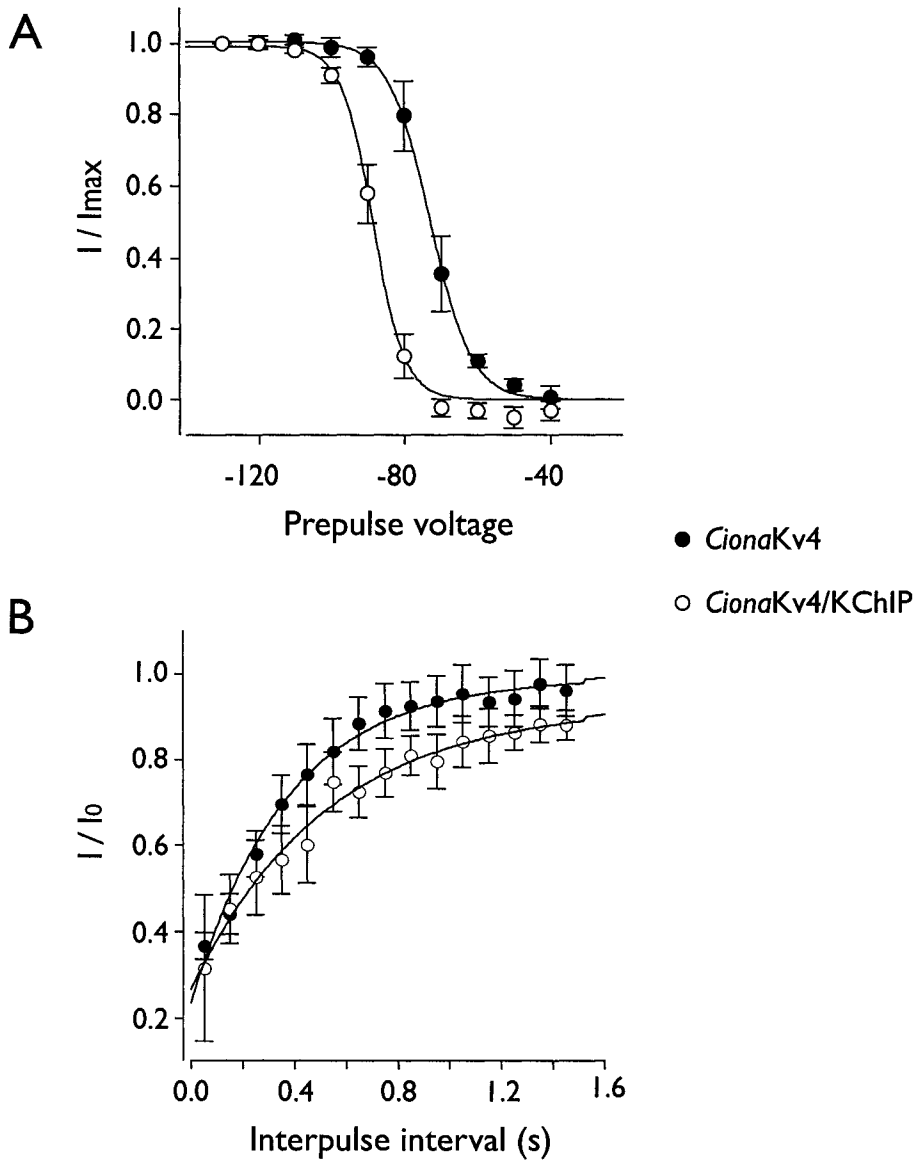

Figure 3-11. Steady-state inactivation and inactivation recovery kinetics of *Ciona*Kv4 in the presence/absence of *Ciona*KChIP. *A,* Voltage dependence of steady-state inactivation for *Ciona*Kv4 channels or *Ciona*Kv4/KChIP complexes, plotted as the relationship between normalized peak current values during a pulse to +50 mV and the voltages of the conditioning prepulses (from –130 mV to –30 mV). Solid curves represent first order Boltzmann fits of the averaged data. *B,* Inactivation recovery kinetics of *Ciona*Kv4 channels or *Ciona*Kv4/KChIP complexes, measured with a double-pulse protocol, in which two test pulses to +50 mV were separated by a recovery pulse to -100 mV of increasing duration (50-2000 ms). Peak currents during the second pulse (I) were normalized to peak currents during the first pulse (I_0)and plotted against the duration of the interpulse interval. Solid curves represent single exponential fits of the averaged data. Data represent mean ± SEM.

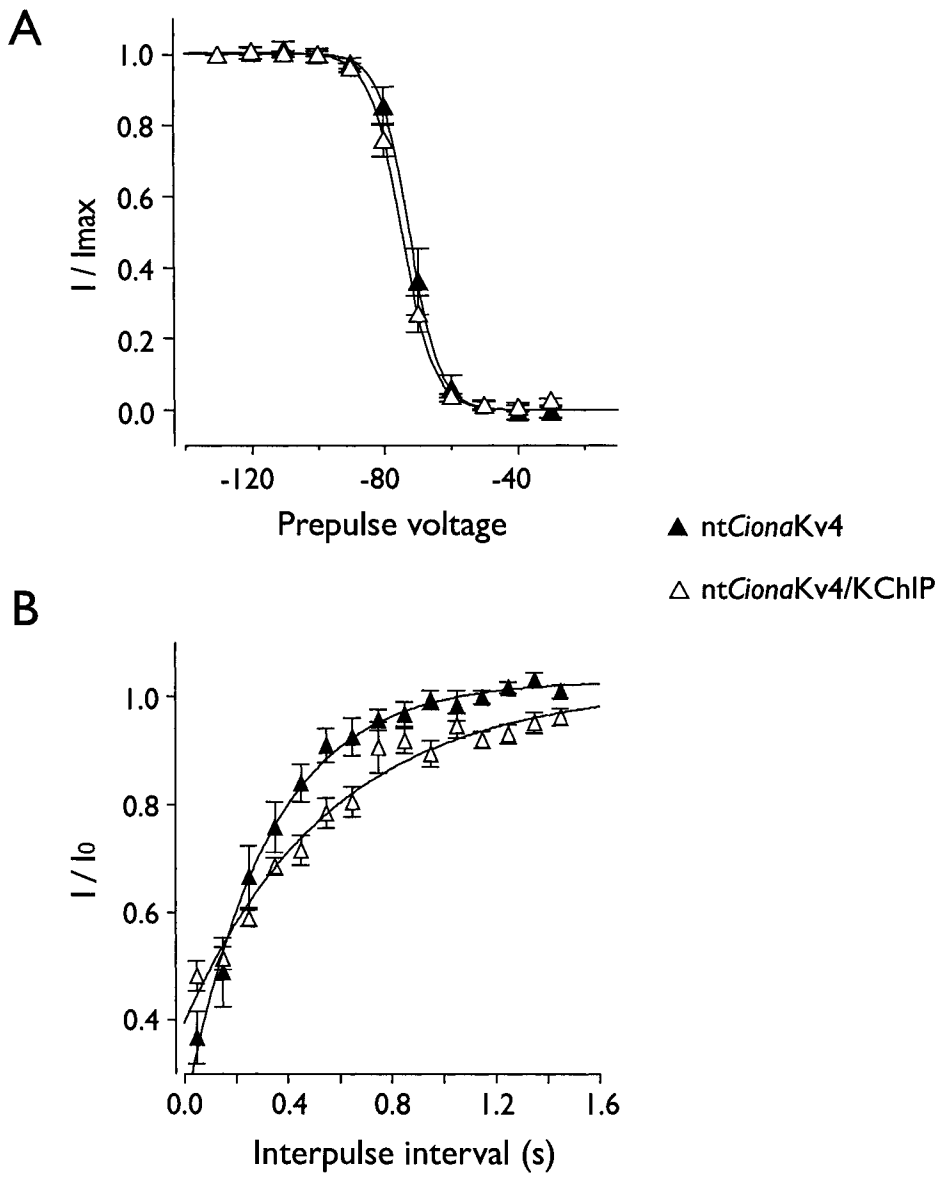

Figure 3-12. Steady-state inactivation and inactivation recovery kinetics of an N-terminal deletion mutant of *Ciona*Kv4 (nt*Ciona*Kv4) in the presence/absence of *Ciona*KChIP. *A,* Voltage dependence of steady-state inactivation for *Ciona*Kv4 channels or *Ciona*Kv4/KChIP complexes, plotted as the relationship between normalized peak current values during a pulse to +50 mV and the voltages of the conditioning prepulses (from –130 mV to –30 mV). Solid curves represent first order Boltzmann fits of the averaged data. *B,* Inactivation recovery kinetics of *Ciona*Kv4 channels or *Ciona*Kv4/KChIP complexes, measured with a double-pulse protocol, in which two test pulses to +50 mV were separated by a recovery pulse to -100 mV of increasing duration (50-2000 ms). Peak currents during the second pulse (I) were normalized to peak currents during the first pulse (I_0) and plotted against the duration of the interpulse interval. Solid curves represent single exponential fits of the averaged data. Data represent mean ± SEM.

Deactivation kinetics of *Ciona*Kv4 and an N-deletion mutant of *Ciona*Kv4 (nt*Ciona*Kv4) in the presence/absence of *Ciona*KChIP

We hypothesized that *Ciona*KChIP slowed inactivation kinetics of *Ciona*Kv4 channels (Figs. 3-8) to some degree by interfering with channel closure. To address this question, we measured the kinetics of tail currents produced by *Ciona*Kv4 channels and *Ciona*Kv4/KChIP complexes in response to re-polarizing pulses from –160 to –100 mV delivered after a brief (10-15 ms) depolarizing pulse to +50 mV, which would activate a maximum number of channels. Our results suggest that channel closing of *Ciona*Kv4 channels is indeed inhibited by *Ciona*KChIP subunits (Fig. 3-13). For example, during a re-polarizing pulse to –130 mV, *Ciona*Kv4 tail currents deactivated with a time constant of 4.1 ± 0.3 ms (n = 10), whereas *Ciona*Kv4/KChIP tail currents deactivated with a time constant of 8.3 ± 0.4 ms (n = 16). These values were significantly different ($p < 0.0001$, Welch t test). Before describing the effects of CionaKChIP on closing kinetics of CionaKv4 that lack the N-terminus, it is important to note that the N-terminus of *Ciona*Kv4 has a role in accelerating closure kinetics of this channel. *Ciona*Kv4 channels whose N-terminus had been deleted produced tail currents with slower kinetics than wild-type channels (Figure 2-10). The N-terminus of *Ciona*Kv4 seems to be required for modulation of closing kinetics by *Ciona*KChIP because the deactivation kinetics of tail currents produced by nt*Ciona*Kv4 channels and nt*Ciona*Kv4/KChIP complexes were not significantly different ($p > 0.05$, Student t test). For example, at the re-polarizing voltage of –130 mV, deactivation time constants for

nt*Ciona*Kv4 and nt*Ciona*Kv4/KChIP were 5.7 ± 0.5 ms (n = 12) and 6.5 ± 0.6 ms (n = 10) respectively (Fig. 3-14).

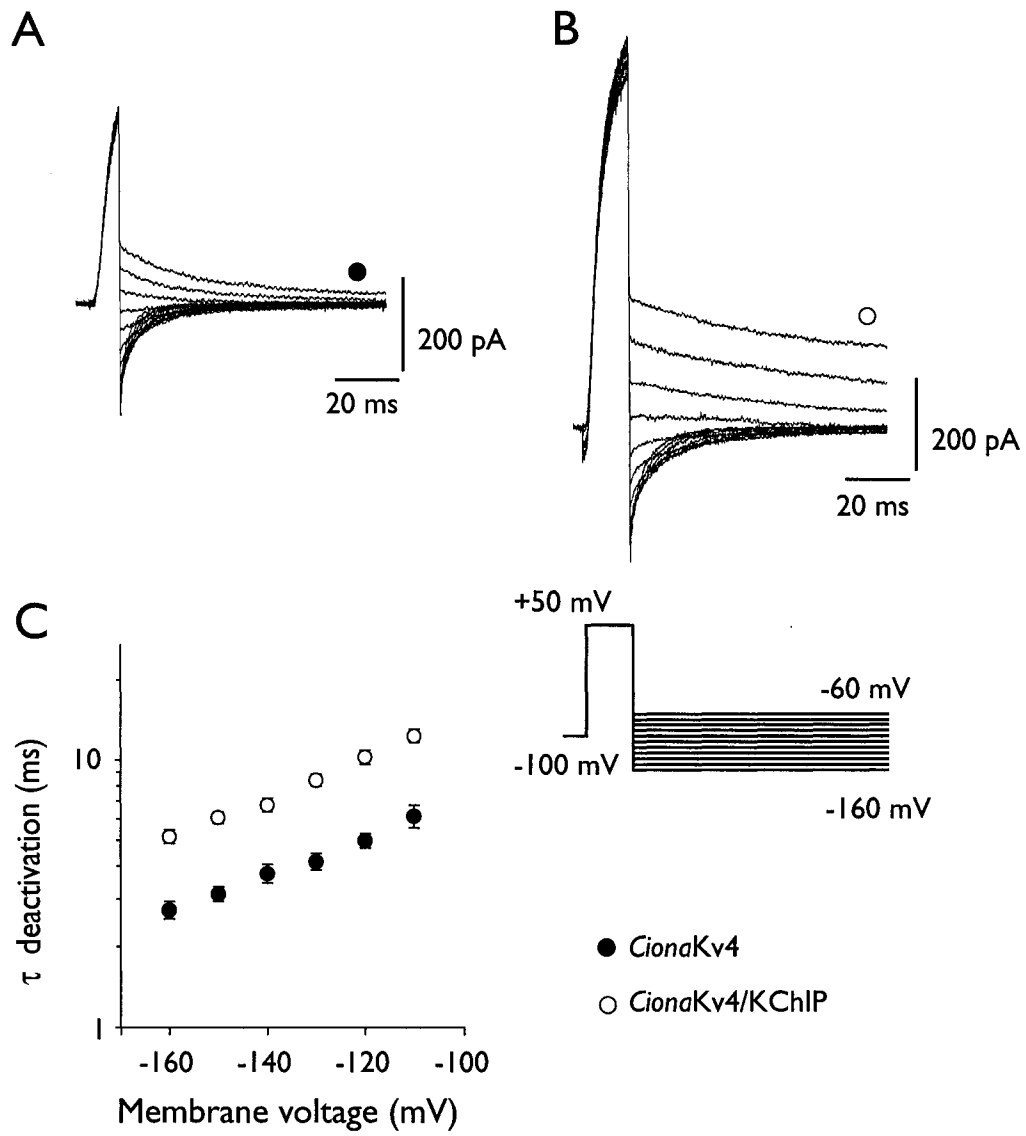

Figure 3-13. Deactivation kinetics of *Ciona*Kv4 in the presence/absence of *Ciona*KChIP. *A*, Representative set of tail currents from *Ciona*Kv4 channels. *B*, Representative set of tail currents from *Ciona*Kv4/KChIP complexes. *C*, Relationships between time constant of deactivation (τ deactivation) and voltage for *Ciona*Kv4 channels (filled circles) and *Ciona*Kv4/KChIP complexes (open circles). Time constants of deactivation were obtained from single exponential fits to the inward tail currents during test potentials between –160 and –100 mV. Tail currents shown in *A* and *B* were evoked by repolarizing pulses to potentials between –160 mV and –40 mV following a pulse to +50 mV. The length of the depolarizing pulse (between 10 and 15 ms) was adjusted each time to activate a maximum number of channels just prior to reaching peak amplitude. Data represent mean ± SEM.

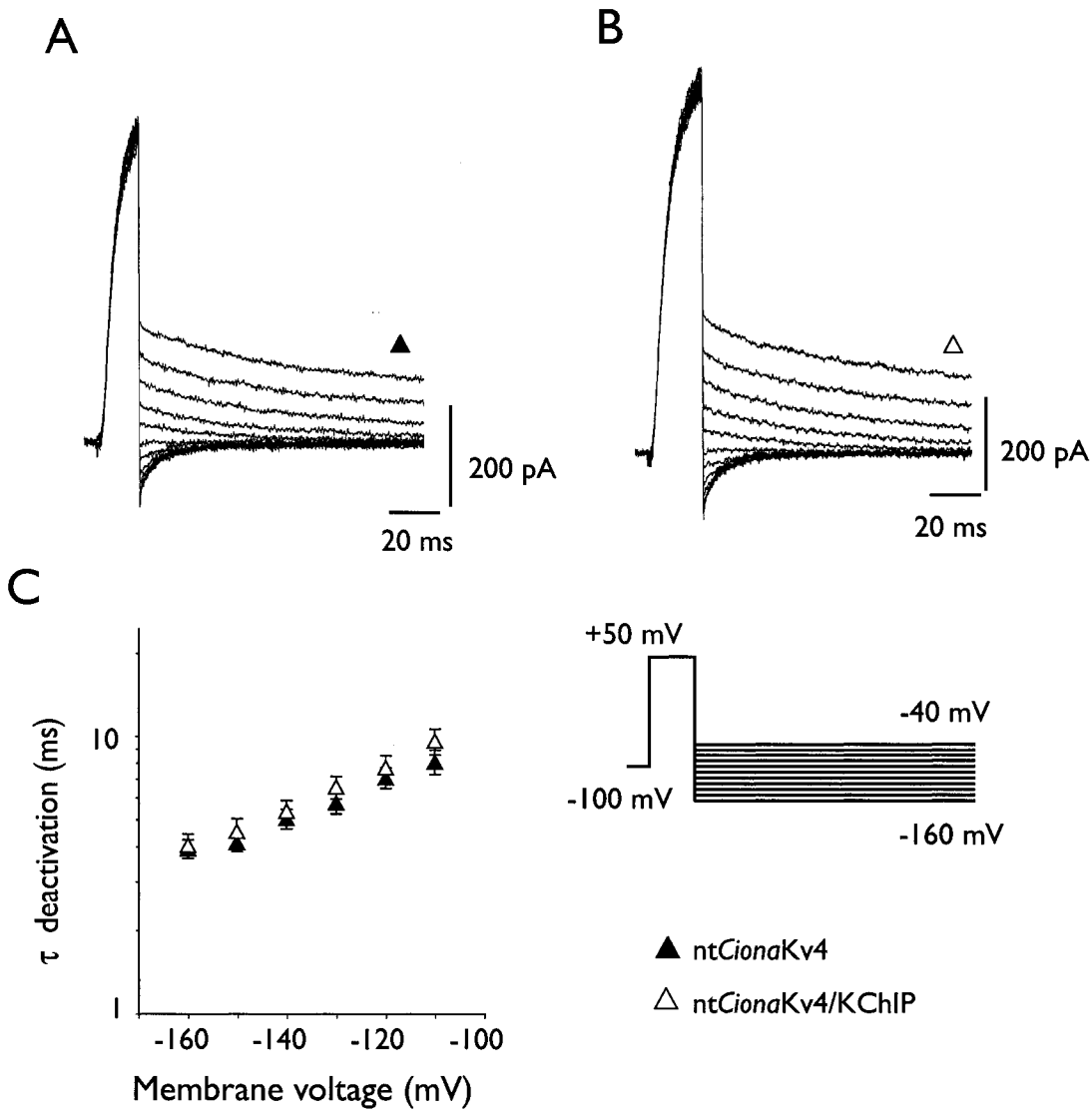

Figure 3-14. Deactivation kinetics of an N-terminal deletion mutant of *Ciona*Kv4 (nt*Ciona*Kv4) in the presence/absence of *Ciona*KChIP. *A*, Representative set of tail currents from nt*Ciona*Kv4 channels. *B*, Representative set of tail currents from nt*Ciona*Kv4/KChIP complexes. *C*, Relationships between time constant of deactivation (τ deactivation) and voltage for nt*Ciona*Kv4 channels (filled triangles) and *Ciona*Kv4/KChIP complexes (open triangles). Time constants of deactivation were obtained from single exponential fits to the inward tail currents during test potentials between –160 and –100 mV. Tail currents shown in *A* and *B* were evoked by repolarizing pulses to potentials between –160 mV and –40 mV following a pulse to +50 mV. The length of the depolarizing pulse (between 10 and 15 ms) was adjusted each time to activate a maximum number of channels just prior to reaching peak amplitude. Data represent mean ± SEM.

Table 3-1. Comparison between the gating parameters of *Ciona*Kv4 channels, *Ciona*Kv4/KChIP complexes, nt*Ciona*Kv4 channels and nt*Ciona*Kv4/KChIP complexes. Number of replicates is indicated in parentheses.

	*Ciona*Kv4		nt*Ciona*Kv4	
Biophysical parameter	- *Ciona*KChIP	+ *Ciona*KChIP	- *Ciona*KChIP	+ *Ciona*KChIP
I_{peak} in pA at +50 mV	207 ± 27 (15)	867 ± 62 (17) [a]	307 ± 33 (16)	432 ± 97 (15)
τ_{act} in ms at +50 mV	3.4 ± 0.2 (11)	3.3 ± 0.2 (10)	3.2 ± 0.3 (12)	3.5 ± 0.3 (12)
Inactivation in ms at +50 mV				
τ_1	26 ± 2 (15)	291 ± 42 (9)	56 ± 6 (15)	240 ± 29 (8)
A_1	82.%	100%	49%	100%
τ_2	147± 26 (15)	-	381 ± 50 (15)	-
A_2	18%	-	51%	-
τ_{rec} in ms at -100 mV	387 ± 47 (7)	927 ± 47 (6) [a]	331 ± 51 (8)	587 ± 76 (8) [b]
τ_{deact} in ms at -130 mV	4.1 ± 0.3 (10)	8.3 ± 0.4 (16) [a]	5.7 ± 0.6 (12)	6.5 ± 0.6 (10)
Steady-state activation in mV *				
$V_{0.5}$	+20 ± 2 (16)	-5.7 ± 1.4 (17) [a]	8.3 ± 1.6 (16)	7.4 ± 1.5 (14)
k	22 ± 1 (16)	20 ±1 (17)	20 ± 1 (16)	21 ± 1 (14)
Steady-state inactivation in mV				
$V_{0.5}$	-72 ± 2 (7)	-88 ± 2 (7) [a]	-73 ± 2 (7)	-74 ± 2 (8)
k	3.6 ± 0.2 (7)	4.3 ± 0.2 (7) [a]	3.7 ± 0.2 (7)	4.1 ± 0.3 (8)

[a] significantly different from *Ciona*Kv4 with $p < 0.01$

[b] significantly different from nt*Ciona*Kv4 with $0.01 < p < 0.05$

*calculated from first order Boltzmann fits

3.4 Discussion

We have described the sequence and the genomic organization of a tunicate K^+ channel interacting protein (*Ciona*KChIP). Although BLAST searches in the genomes of *Drosophila* and *Anopheles* revealed the presence of KChIP genes in these arthropod genomes (Fig. 3-3), *Ciona*KChIP is the first KChIP subunit from an invertebrate that has been cloned and characterized. We investigated whether *Ciona*KChIP modulated currents produced by a Kv4 channel that we had previously cloned from cDNA of the heart of *Ciona intestinalis*, and analyzed the role of the N-terminus on modulation by *Ciona*KChIP.

Comparing the genomic structure of *Ciona*KChIP and mammalian KChIPs

The only gene for KChIP subunits in the genome of *Ciona intestinalis* branches basal to all vertebrate KChIPs in a phylogenetic tree (Fig. 3-4). Thus, it is likely that the common ancestor of tunicates and vertebrates had a single gene encoding a KChIP subunit, and that early in the evolution of the vertebrates this gene duplicated, leading to two clades (the KChIP1 clade and the KChIP2/3/4 clade). However, our phylogenetic analyses did not resolve the relationships between KChIP2, KChIP3, and KChIP4.

Comparison between the genomic structures of *Ciona*KChIP (Fig. 3-2) and the KChIPs cloned from several mammalian species revealed that most exon/intron boundaries of KChIPs are highly conserved. For example, the last exon of *Ciona*KChIP, KChIP2 and KChIP3 are identical in length (Decher et al., 2004;

Spreafico et al., 2001; this thesis). Each of the EF-hands 1 to 3 of *Ciona*KChIP is encoded by two exons, as in KChIP3, and the partition of these three EF-hands into two exons occurs in the same positions in *Ciona*KChIP and KChIP3. The fourth EF-hand is similarly encoded in a single exon in *Ciona*KChIP, KChIP2 and KChIP3 (Decher et al., 2002; Spreafico et al., 2001; Figure 3-3). The number of exons that encode the different mammalian KChIPs is variable, since numerous splice variants from a single KChIP gene are possible; for example, the gene encoding KChIP2 subunits can be spliced differently to produce at least eight isoforms: KChIP2a (An et al., 2000), KChIP2b (Bähring et a., 2001), KChIP2c (Decher et al., 2001), KChIP2d (Patel et al., 2002), KChIPs 2e-g (Decher et al., 2004), and KChIP2t (Deschênes et al., 2002). The KChIP2a variant has the longest N-terminal domain, which is encoded by four exons. The N-terminus of the KChIP2b variant is the result of splicing out the third exon from KChIP2a (Decher et al., 2004); variants KChIP2c, KChIP2e, KChIP2f and KChIP2t do not contain the information encoded by exons 2 and 3, which is present in KChIP2a. The sequence of the N-terminal domain of KChIP2g does not contain information from exons 2 and 3 either, and is encoded by an alternative exon 1 (Decher et al., 2004).

The fact that *Ciona*KChIP is, similarly to the mammalian KChIP isoforms, encoded by several exons (Fig. 3-2) suggests that in theory several splice variants of *Ciona*KChIP are possible, although only one variant was detected in our experiments. Although most splice variants of KChIPs differ in their N-termini, variants that differ in their C-termini have been also cloned (Decher et al., 2004). Our results suggest that splice variants of *Ciona*KChIP that differ in their C-termini are not expressed, or are

expressed at very low levels in the heart of *Ciona intestinalis*, because theoretically these would have been detected with the 3'-RACE assay. Regarding expression of splice variants of *Ciona*KChIP with different N-termini in the heart of *C. intestinalis*, only partial conclusions can be derived from this study. Since we did not perform a 5'-RACE assay, we do not know the information that would have been provided, theoretically, by this assay. Therefore, it is still not known whether alternatively spliced variants of *Ciona*KChIP with one or more alternative N-terminal exon, variants containing the information encoded by possible additional exons, or splice variants without an N-terminus, similarly to the minimal isoform KChIP2d (Patel et al., 2002), are expressed in the heart of *C. intestinalis*. However, we can suggest that splice variants that do not contain the information of one or more of exons 2 to 5 are not expressed, or expressed at relatively low levels, otherwise it is likely that these would have been detected when amplifying the ORF of *Ciona*KChIP.

Comparing modulation by *Ciona*KChIP and mammalian KChIPs

Modulation of current amplitude and activation parameters

*Ciona*KChIP clearly increased the amplitude of *Ciona*Kv4 currents, as can be seen in Figures 3-5 and 3-6A, similarly as do mammalian KChIP isoforms 1 to 3 (An et al., 2000). It has been shown that the mammalian KChIP isoforms do not increase the Kv4 current amplitude by a direct effect on single channel conductance (Beck et al., 2002), but by facilitating the insertion of Kv4 channels into the plasma membrane (Shibata et al., 2003). Whether *Ciona*KChIP increases the amplitude of the currents

produced by *Ciona*Kv4 by facilitating insertion of these channels in the plasma membrane, like the mammalian KChIP 1 to 3 isoforms or, differently from these mammalian isoforms, by increasing the conductance of *Ciona*Kv4 channels, was not determined in this study.

The effect of mammalian KChIPs on the activation rate of Kv4 currents is highly variable. For instance, KChIP1 accelerates the rate of activation of Kv4.1 and Kv4.2 channels (Nakamura et al., 2001), but not of Kv4.3 channels (Beck et al., 2002). KChIP2 does not have an effect on the rate of activation of any of the three mammalian Kv4 channel isoforms (Bähring et al., 2001; Wang et al., 2002). KChIP4, on the other hand, slows the rate of activation of Kv4 channels (Holmqvist et al., 2002). *Ciona*KChIP did not appear to modulate the rate of activation of *Ciona*Kv4 currents (Fig. 3-6B). However, *Ciona*KChIP shifted the midpoint of activation of *Ciona*Kv4 in the hyperpolarizing direction (Fig. 3-6C), consistently with the effect of most mammalian KChIPs (An et al., 2000; Van Hoorick et al., 2003), with some exceptions such as KChIP2b and 2d, which do not shift the midpoint of activation (Patel et al., 2004), or KChIP4, which appears to shift the midpoint of activation of Kv4 channels in the depolarizing direction (Holmqvist et al., 2002).

Modulation of macroscopic inactivation

KChIP2 and KChIP3 moderately slow the rate of inactivation of Kv4 currents (Decher et al., 2004). In contrast, KChIP1 accelerates the rate of decay of Kv4.1 currents (Beck et al., 2002; Nakamura et al., 2002), but moderately slows the decay of

Kv4.2 currents (Nakamura et al., 2001). The slowing effect of these three KChIP isoforms on inactivation kinetics of Kv4 currents is not dramatic, as it does not eliminate the transient nature of these Kv4 currents. In contrast, *Ciona*KChIP converted the transient currents produced by *Ciona*Kv4 into currents that barely inactivated over a period of 0.5s, which was reminiscent of the effects of the mammalian isoform KChIP4a on mammalian Kv4 channels (Holmqvist et al., 2002). A K inactivation suppressor (KIS) domain within the first ~34 amino acids of the N-terminus of KChIP4a is a requirement for the dramatic action of this mammalian subunit on inactivation kinetics, because deletion of these amino acids suppressed these effects (Holmqvist et al., 2002). In order to find out whether the N-terminus of *Ciona*KChIP bears resemblances with the N-terminus (the KIS domain) of KChIP4a, we aligned the first 40 amino acids of *Ciona*KChIP with the first 40 amino acids of KChIP4a using T-Coffee software (Notredame et al., 2000). The results of this alignment are shown in Figure 3-15A. For comparison, we also aligned the first 40 amino acids of *Ciona*KChIP with the first 40 amino acids of representatives of the other vertebrate KChIP subfamilies (KChIP1 to 3), as shown in Figure 3-15B-D. The N-terminus of *Ciona*KChIP was more similar to the N-terminus of the KChIP4a isoform than of the other KChIP isoforms. The alignment between *Ciona*KChIP and KChIP4a revealed that two leucines, at positions 3 and 6 in both subunits, and a methionine, at position 8 also in both subunits, are conserved between KChIP4a and *Ciona*KChIP (Fig. 3-15A). Other residues that could be conserved between the N-terminus of KChIP4a and *Ciona*KChIP are a glutamic acid residue and a glycine residue at positions 19 and 22,

respectively, in *Ciona*KChIP (and positions 23 and 26 in KChIP4a), an alanine-glycine motif located at position 28 in *Ciona*KChIP (position 30 in KChIP4a), and a valine residue at position 34 in *Ciona*KChIP, corresponding to position 32 of KChIP4a (Fig. 3-15A). It seems likely that at least some of these conserved amino acids are crucial to the dramatic effect of these two KChIP subunits on inactivation kinetics of Kv4 channels, although it is also possible that KChIP4a and *Ciona*KChIP exert their effects on inactivation kinetics by independent mechanisms. The alignments between *Ciona*KChIP and KChIP2a or KChIP3a had extensive gaps (Figure 3-15C,D). The alignment between *Ciona*KChIP and KChIP1a has fewer and smaller gaps than in the previous cases, and therefore it might reveal some genuine similarities between the N-termini of these two subunits (Fig. 3-15B).

Modulation of voltage-dependence of steady-state inactivation and inactivation recovery kinetics

Most KChIP isoforms either do not affect the midpoint of inactivation (*e.g.* KChIP1a: Nakamura et al., 2001; Van Hoorick et al., 2003) or shift the midpoint of inactivation in the depolarizing direction (*e.g.* KChIP2b: Bähring et al., 2001). However, the splice variant KChIP2g, which has an alternative exon 1 (Decher et al., 2004) and KChIP 1b, which contains the information of an additional exon in its N-terminus (Van Hoorick et al., 2003) shift the midpoint of inactivation in the hyperpolarizing direction, similarly as *Ciona*KChIP (Fig. 2-11A).

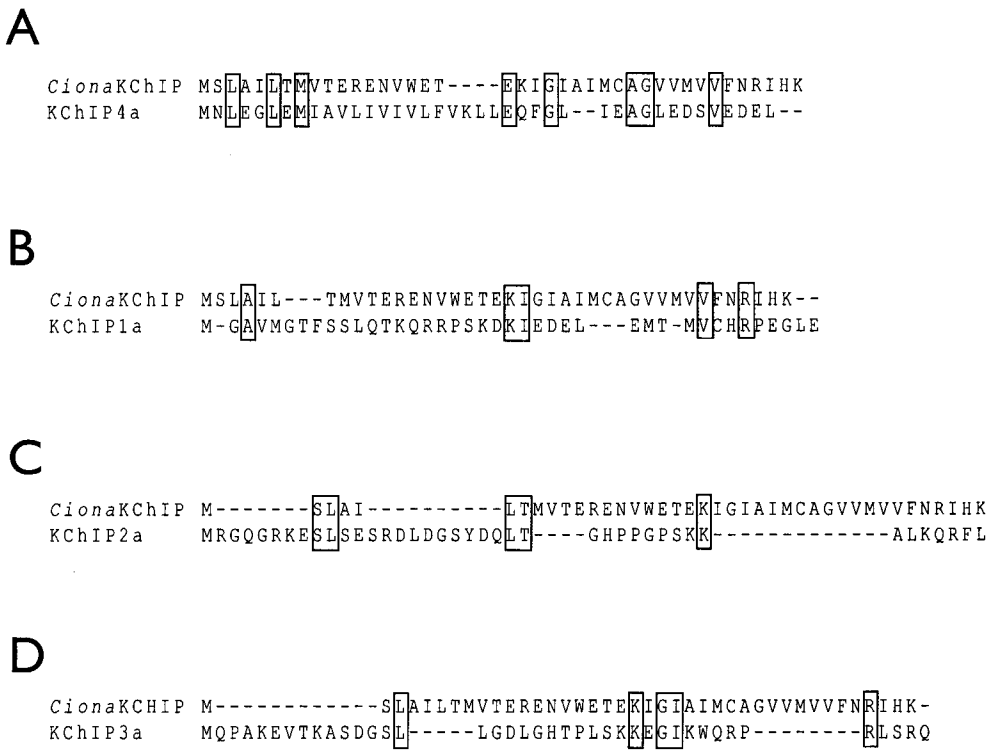

Figure 3-15. Comparisons between the N-terminus of *Ciona*KChIP and the N-terminus of representatives of each vertebrate KChIP subfamily. *A,* Aligment between *Ciona*KChIP and KChIP4a (accession number AAL86766). *B,* Alignment between *Ciona*KChIP and KChIP1a (accession number AAL12489). *C,* Alignment between *Ciona*KChIP and KChIP2a (accession number AAF81755). *D,* Alignment between *Ciona*KChIP and KChIP3a (accession number Q9Y2W7), which contains the K inactivation suppressor domain (KIS). T-Coffee software (Notredame et al., 2000) was used to align these sequences. Residues that identical for each pair of sequences are boxed.

However, the N-terminus of these mammalian KChIP splice variants and *Ciona*KChIP did not bear any similarity (not shown). Perhaps a similar effect on the voltage-dependence of inactivation can be achieved by different mechanisms, but it appears clearly that the effects of KChIPs on steady-steady inactivation depends upon their N-terminal sequences.

Most KChIP isoforms accelerate the rate of recovery of Kv4 channels (An et al., 2000), in spite of having largely divergent N-termini. Even a minimal KChIP2 isoform, which has only the highly conserved last 70 amino acids of longer KChIP isoforms, can accelerate the rate of recovery from inactivation of Kv4 channels (Patel et al., 2002). These data strongly suggest that the C-terminus of KChIPs is sufficient to accelerate the rate of recovery kinetics of Kv4 channels, and that this effect is independent of the sequence of the N-terminus of KChIPs. Surprisingly, our data suggests that *Ciona*KChIP slowed the rate of recovery from inactivation of *Ciona*Kv4 channels. Because, as stated before, all evidence so far indicates that the C-terminus of KChIPs is the domain involved in its effects on inactivation recovery kinetics, we inspected the last 17 amino acids of the C-terminus of *Ciona*KChIP, after EF-hand 4, and compared these with the last 17 amino acids of the mammalian KChIPs. This corroborated that the C-terminus of KChIPs is well conserved amongst mammalian KChIPs. For example, the C-terminus of KChIP3 and KChIP4 are identical, and the percentage conservation of amino acids between the C-termini of KChIP 2, 3 and 4 is ~88%. The C-terminus of KChIP1 is ~70% identical to the C-termini of the other mammalian isoforms (Table 3-2). However, these comparisons also revealed that the C-terminus of

*Ciona*KChIP is clearly different from that of mammalian KChIPs. The C-terminus of *Ciona*KChIP is more similar to the C-terminus of KChIP4 (percentage conservation of amino acids is ~47%) than to the C-termini of the other KChIP isoforms. Thus, the percentage conservation of amino acids between the C-termini of *Ciona*KChIP and KChIP1 and KChIP2 is of only ~30%; the C-termini of *Ciona*KChIP and KChIP3 are ~40% similar. Perhaps it is worth noting that the last amino acids of *Ciona*KChIP (-DHAL) are clearly different from the other KChIPs (Table 3-2).

Modulation of deactivation

We found that *Ciona*KChIP increased the values of deactivation time constants of tail currents produced by *Ciona*Kv4 channels (Fig. 3-13). Since Kv4 channels mostly inactivate from the closed state (Bahring et al., 2001; Gebauer et al., 2004), and *Ciona*KChIP prevented inactivation of *Ciona*Kv4, our results are consistent with what is known about inactivation of Kv4 channels. Therefore, it is plausible that the dramatic slowing effects *Ciona*KChIP on inactivation of *Ciona*Kv4 were partly mediated by an slowing effect on closure kinetics. This is consistent with the effects of KChIP1 on Kv4.1 channels, since this accessory subunit accelerates inactivation of Kv4.1 channels, and furthermore it accelerates closing kinetics of this channel (Beck et al., 2002).

Table 3-2. Percentage conservation of amino acids between the C-termini (last seventeen amino acids) of KChIP subunits

	*Ciona*KC hIP	KChIP1a[1]	KChIP2a[2]	KChIP3[3]	KChIP4b[4]
*Ciona*KC hIP	1	–	–	–	–
KChIP1a[1]	29%	1	–	–	–
KChIP2a[2]	29%	71%	1	–	–
KChIP3[3]	41%	65%	88%	1	–
KChIP4b[4]	47%	71%	88%	100%	1

[1] accession number AAL12489
[2] accession number AAF81755
[3] accession number Q9Y2W7
[4] accession number NP_079497

The N-terminus of *Ciona*Kv4 is essential to modulation by *Ciona*KChIP

Like the N-terminus of mammalian Kv4 channels (Bähring et al., 2001), the N-terminus of *Ciona*Kv4 is essential to modulation by KChIP subunits, since in the absence of this domain, *Ciona*KChIP did not increase current amplitude, shift midpoint values of activation or inactivation or affect the kinetics of deactivation of *Ciona*Kv4 channels which lack the N-terminal amino acids 2-32. However, the macroscopic decay of nt*Ciona*Kv4/KChIP currents was slower than the decay of nt*Ciona*Kv4 channels alone. It is likely that *Ciona*KChIPs, in addition to interacting with the proximal amino acids of the N-terminus of *Ciona*Kv4, also binds to a second domain of the N-terminus, that was not affected by the deletion performed on *Ciona*Kv4 channels, since mammalian KChIPs interact with at least two domains of the N-terminus of Kv4 channels, one within residues 7 to 11 and another comprising residues 71 to 90 (Scannevin et al., 2004), and this second binding site is sufficient for binding to KChIPs. Our findings are therefore not inconsistent with what is known about the Kv4 channel/ KChIP subunit association.

Summary and Conclusions

We have cloned a KChIP homologue expressed in the heart of the tunicate *Ciona intestinalis*, *Ciona*KChIP, the first KChIP subunit cloned from an invertebrate. *Ciona*KChIP branches basal to the four vertebrate KChIP isoforms in a phylogenetic tree. When heterologously co-expressed in *Xenopus* oocytes with *Ciona*Kv4, *Ciona*KChIP dramatically slowed inactivation of *Ciona*Kv4 currents, which was

reminiscent of the effects of the mammalian isoform KChIP4a. By comparing the first 34 amino acids of KChIP4a (containing the KIS domain) with the first amino acids of *Ciona*KChIP, we have identified possible residues that may underlie the modulating effects of this subunit on macroscopic inactivation.

It is likely that the *Ciona*Kv4/KChIP complex is an element of the full *Ciona*Kv4 supra-macromolecular complex. It is known that Kv4 channels are modulated by a variety of accessory subunits, as recently reviewed by Birnbaum et al. (2004). Because *Ciona intestinalis* has a less diverse gene complement than vertebrates (Leveugle et al., 2004), the *Ciona*Kv4 supra-molecular complex likely represents a simplified version of the mammalian Kv4 supra-molecular complex, and thus may serve as a relatively simple model for the vertebrate case.

3.5 Literature cited

An WF, Bowlby MR, Betty M, Cao J, Ling HP, Mendoza G, Hinson JW, Mattsson KI, Strassle BW, Trimmer JS, Rhodes KJ (2000) Modulation of A-type potassium channels by a family of calcium sensors. Nature 403: 553-556

Bähring R, Dannenberg J, Peters HC, Leicher T, Pongs O, Isbrandt D (2001) Conserved Kv4 N-terminal domain critical for effects of Kv channel-interacting protein 2.2 on channel expression and gating. J Biol Chem 276:23888-23894

Bairoch A, Cox JA (1990) EF-hand motifs in inositol phospholipid-specific phospholipase C. FEBS Lett 269:454-456

Beck EJ, Bowlby M, An WF, Rhodes KJ, Covarrubias M (2002) Remodelling inactivation gating of Kv4 channels by KChIP1, a small-molecular-weight calcium-binding protein. J Physiol 538:691-706

Birnbaum SG, Varga AW, Yuan L-L, Anderson AE, Sweatt JD, Schrader LA (2004) Structure and function of Kv4-family transient potassium channels. Physiol Rev 84:803-833

Burgoyne RD, Weiss JL (2001) The neuronal calcium sensor family of Ca^{2+}-binding proteins. Biochem J 353:1-12

Decher N, Barth AS, Gonzalez T, Steinmeyer K, Sanguinetti MC (2004) Novel KChIP2 isoforms increase functional diversity of transient outward potassium currents. J Physiol 557.3:761-772

Decher N, Uyguner O, Scherer CR, Karaman B, Yüksel-Apak M, Busch AE, Steinmeyer K, Wollnik B (2001) hKChIP2 is a functional modifier of hKv4.3 potassium channels: Cloning and expression of a short hKChIP2 splice variant. Cardiovasc Res 52:255-264

Deschênes I, Tomaselli GF (2002) Modulation of Kv4.3 current by accessory subunits. FEBS Lett 528: 183-188

Dominguez I, Itoh K, Sokol SY (1995) Role of glycogen synthase kinase 3β as a negative regulator of dorsoventral axis formation in *Xenopus* embryos. Proc Natl Acad Sci USA 92:8498-8502

Guo W, Malin SA, Johns DC, Jeromin A, Nerbonne JM (2002) Modulation of Kv4-encoded K^+ currents in the mammalian myocardium by neuronal calcium sensor-1. J Biol Chem 277:26436-26443

Holmqvist MH, Cao J, Hernandez-Pineda R, Jacobson MD, Carroll KI, Sung MA, Betty M, Ge P, Gilbride KJ, Brown ME, Jurman ME, Lawson D, Silos-Santiago I, Xie Y, Covarrubias M, Rhodes KJ, Distefano PS, An WF (2002) Elimination of fast inactivation in Kv4 A-type potassium channels by an auxiliary subunit domain. Proc Natl Acad Sci USA 99: 1035-1040.

Huelsenbeck JP, Ronquist F (2001) MRBAYES: Bayesian inference of phylogenetic trees. J Bioinf 17:754-5

Kretsinger RH (1987) Calcium coordination and the calmodulin fold: divergent versus convergent evolution. Cold Spring Harbor Symp Quant Biol 52:499-510

Kriebel ME (1968) Conduction velocity and intracellular action potentials of the tunicate heart. J Gen Physiol 50: 2097-2107

Leveugle M, Prat K, Popovici C, Birnbaum D, Coulier F (2004) Phylogenetic analysis of *Ciona intestinalis* gene superfamilies supports the hypothesis of successive gene expansions. J Mol Evol 58:168-181

Litovsky SH, Antzelevitch C (1988) Transient outward current prominent in canine ventricular epicardium but not endocardium. Circ Res 62:116-126

Nadal MS, Ozaita A, Amarillo Y, Vega-Saenz de Miera E, Ma Y, Mo W, Goldberg EF, Misumi Y, Ikehara Y, Neurbert T, Rudy B (2003) The CD26-related dipeptidyl aminopeptidase-like protein DPPX is a critical component of neuronal A-type K^+ channels. Neuron 37:449-461

Nakahira K, Shi G, Rhodes KJ, Trimmer JS (1996) Selective interaction of voltage-gated K^+ channel β-subunits with α-subunits. J Biol Chem 271:7084-7089

Nakamura TY, Nandi S, Pountney DJ, Artman M, Rudy B, Coetzee WA (2001) Different effects of the Ca^{2+} -binding protein, KChIP1, on two Kv4 subfamily members, Kv4.1 and Kv4.2. FEBS Lett 499:205-209

Notredame C, Higgins D, Heringa J (2000) T-Coffee: a novel method for multiple sequence alignments. J Mol Biol 302:205-217

Page RD (1996) TreeView: an application to display phylogenetic trees on personal computers. J Compt Appl Biosci 12:357-358

Patel SP, Campbell DL, Strauss HC (2002) Elucidating KChIP effects on Kv4.3 inactivation and recovery kinetics with a minimal KChIP2 isoform. J Physiol 545:5-11

Patel SP, Parai R, Parai R, Campbell DL (2004) Regulation of Kv4.3 voltage-dependent gating kinetics by KChIP2 isoforms. J Physiol 557:19-41

Petrecca K, Miller DM, Shrier A (2000) Localization and enhanced current density of the Kv4.2 potassium channel by interaction with the actin-binding protein filamin. J Neurosci 20:8736-8744

Rosati B, Pan Z, Lypen S, Wang H-S, Cohen I, Dixon JE, McKinnon D (2001) Regulation of *KChIP2* potassium channel *β* subunit gene expression underlies the gradient of transient outward current in canine and human ventricle. J Physiol 533:119-125

Scannevin RH, Wang K, Jow F, Megules J, Kopsco DC, Edris W, Carroll KC, Lü Q, Xu W, Xu Z, Katz AH, Olland S, Lin L, Taylor M, Stahl M, Malakian K, Somers W, Mosyak L, Bowlby MR, Chanda P, Rhodes KJ (2004) Two N-terminal domains of Kv4 K^+ channels regulate binding to and modulation by KChIP1. Neuron 41:587-598

Shibata R, Misonou H, Campomanes CR, Anderson AE, Schrader LA, Doliveira LC, Carroll KI, Sweatt JD, Rhodes KJ, Trimmer JS (2003) A fundamental role for KChIPs in determining the molecular properties and trafficking of Kv4.2 potassium channels. J Biol Chem 278: 36445-36454

Spreafico F, Barski JJ, Farina C, Meyer M (2001) Mouse DREAM/Calsenilin/KChIP3: Gene structure, coding potential, and expression. Mol Cell Neurosci 17:1-16

Van Hoorick D, Raes A, Keysers W, Mayeur E, Snyders DJ (2003) Differential modulation of Kv4 kinetics by KCHIP1 splice variants. Mol Cell Neurosci 24: 357-366

Wang S, Patel SP, Qu Y, Hua P, Strauss HC, Morales MJ (2002) Kinetic properties of Kv4.3 and their modulation by KChIP2b. Biochem Biophys Res Comm 295:223-229

Yang E-K, Alvira MR, Levitan ES, Takimoto K (2001) Kvβ subunits increase expression of Kv4.3 channels by interacting with their C termini. J Biol Chem 276:4839-4844

Zhang Y, MacLean JN, An WF, Lanning CC, Harris-Warrick RM (2003) KChIP1 and frequenin modify *shal*-evoked potassium currents in pyloric neurons in the lobster stomatogastric ganglion. J Neurophysiol 89:1902-1909

Chapter 4 General Discussion

4.1 Thesis summary

In this thesis I describe the cloning of a voltage-gated potassium (Kv) channel of the Kv4 subfamily that is expressed in the myocardium of a basal chordate, the tunicate *Ciona intestinalis* (*Ciona*Kv4). This work was greatly facilitated by the genomic database for this species **http://genome.jgi-psf.org/ciona4/ciona4.home.html**, since a scan of this genomic database using vertebrate Kv4 channel sequences identified a single gene for Kv4 channels (*Ciona*Kv4), providing an initial prediction of the position of the initiation codon (ATG), as well as the codons for the trans-membrane segments of this channel. However, since the C-termini of Kv4 channels are highly divergent (see Fig. 2-4), it was not possible to predict the sequence of the C-terminus of *Ciona*Kv4 by similarity with the C-terminus of any other Kv4 channel in BLAST searches. Therefore, to determine the position of the stop codon for *Ciona*Kv4, I used an experimental assay, 3'-RACE. This made it possible to amplify and clone the full ORF for *Ciona*Kv4 from heart cDNA of *Ciona intestinalis*.

The exon/intron organization of the gene that encodes *Ciona*Kv4, determined by aligning the sequences of the transcript and the gene for *Ciona*Kv4, was similar to the genomic structure of vertebrate Kv4 channels (Isbrandt et al., 2000), except for the fact

that the codons for exon 1 of vertebrate Kv4 channels are partitioned into two exons in *Ciona*Kv4 (Fig. 2-3).

An alignment between *Ciona*Kv4 with vertebrate and invertebrate Kv4 channels revealed strong sequence similarity between *Ciona*Kv4 and other Kv4 channels, especially with a Kv4 channel cloned from the tunicate *Halocynthia roretzi* (TuKv4, Nakajo et al., 2003). When heterologously expressed in *Xenopus* oocytes, *Ciona*Kv4 produced outward transient currents (Fig. 2-6A) that were almost indistinguishable from currents produced by this tunicate Kv4 channel (Nakajo et al., 2003).

The N-terminus of Kv4 channels is highly conserved, perhaps because its two major roles as a structural element of inactivation and as a binding site for KChIP accessory subunits are essential to the function of these channels. The N-terminus of *Ciona*Kv4 does not differ from the N-terminus of the other Kv4 channels, except for amino acids at positions 3 and 4, which are conserved amongst the three mammalian Kv4 isoforms (corresponding to an alanine and an arginine, respectively), but are highly variable in invertebrate Kv4 channels (Fig. 2-4). To elucidate whether the N-terminus of *Ciona*Kv4 has the same functions as the N-terminus of the mammalian Kv4 channels, I created a mutant that lacked amino acids 2-32 and compared the biophysical parameters of this channel with those of wild-type *Ciona*Kv4 channels (Chapter 2). Deletion of the N-terminus significantly increased the amplitude of the *Ciona*Kv4 currents, shifted the midpoint voltage of activation leftwards (Fig. 2-7), slowed closing kinetics (Fig. 2-10), and dramatically slowed the decay of these currents (Fig. 2-6B) by increasing the time constants of the fast and the slow inactivating components (Fig. 2-

8B) and by increasing the relative contribution of the slower component of inactivation to total current decay. However, the N-terminus of *Ciona*Kv4 is not a structural determinant of activation kinetics, voltage-dependence of inactivation or inactivation recovery kinetics because deletion of this domain did not significantly change these parameters (Figs. 2-7B and 2-9).

The phenotype of the potassium current conducted by Kv4 channels depends on the tuning of the intrinsic biophysical properties of these Kv4 channels by accessory KChIP subunits (An et al., 2000). Therefore, for a comprehensive understanding of the role of Kv4 channels in the physiology of vertebrate and invertebrate tissues where they are expressed, it is important to characterize the modulation of their biophysical properties by KChIPs [and other] accessory subunits. For this purpose, I cloned a tunicate KChIP homologue (*Ciona*KChIP) from heart cDNA of this species using a similar approach as for *Ciona*Kv4 (chapter 3). As with mammalian KChIPs, the N-terminus of *Ciona*KChIP was the most variable part of this protein (Fig. 3-3). Interestingly, the portion of the C-terminus after the fourth EF-hand of *Ciona*KChIP showed a percentage similarity of ~47% with the same region of KChIP4 and of only 30-40% with the same region of the other mammalian KChIP isoforms, whereas this region is highly conserved between mammalian KChIPs (90-100% homology between KChIP isoforms 2 to 4, and ~70% between KChIP1 and KChIPs 2 to 4, see Table 3-2).

Co-expression experiments revealed that, like the mammalian KChIP isoforms, *Ciona*KChIP increased the current amplitude (Fig. 3-5A,B and Fig. 3-8) and shifted the midpoint of activation in the hyperpolarizing direction (Fig. 3-6). Like KChIP4a,

*Ciona*KChIP slowed the decay of *Ciona*Kv4 currents (Fig. 3-5B). However, *Ciona*KChIP shifted the midpoint of inactivation in the hyperpolarizing direction (Fig. 3-11A), whereas most KChIP isoforms shift the midpoint of inactivation in the depolarizing direction. Furthermore, whereas mammalian KChIPs consistently accelerate inactivation recovery kinetics, *Ciona*KChIP had an opposite effect on this parameter.

Since the N-terminus of *Ciona*Kv4 does not differ from that of mammalian Kv4 channels, I hypothesized that the N-terminus of *Ciona*Kv4 played a major role in interaction with *Ciona*KChIP. Co-expression of an N-terminal deletion mutant of *Ciona*Kv4 (nt*Ciona*Kv4, characterized in chapter 2) with *Ciona*KChIP confirmed that this is the case, since *Ciona*KChIP did not shift activation or inactivation midpoints (Figs. 3-7C and 3-11C) and did not affect deactivation kinetics of *Ciona*Kv4 (Fig. 3-13). However, *Ciona*KChIP further slowed inactivation of the currents produced by the N-terminal deletion mutant of *Ciona*Kv4, indicating an interaction between *Ciona*KChIP and nt*Ciona*Kv4. This is not surprising, since it is known that Kv4 channels have two binding sites for KChIP in their N-terminus. The deletion of amino acids 2-32 performed on *Ciona*Kv4 eliminated the first, but not the second binding site for KChIP, as this second site is within amino acids ~71-90. These results were described in Chapter 3.

In conclusion, this thesis has provided the sequence and a detailed characterization of the biophysical activity of a tunicate Kv4 channel (*Ciona*Kv4), a characterization of the functional role of the N-terminus of *Ciona*Kv4, and the sequence

and the modulatory action of a KChIP subunit (*Ciona*KChIP) on *Ciona*Kv4 channels. This is the first invertebrate KChIP subunit to be isolated. During the course of these investigations, Zhang et al. (2001) cloned a lobster frequenin subunit and characterized its effects on the activity of lobster Kv4 channels. Their results and the results presented in this thesis are the first indications that the activity of invertebrate Kv4 channels is tuned by endogenous accessory subunits. The elucidation of the structure and function of the mammalian Kv4 supra-molecular complex could benefit from the characterization of invertebrate orthologues.

4.2 Discussion

Conserved and adaptive features of Kv4 channels

A comparison between the biophysical properties of *Ciona*Kv4, provided in this thesis, and the published biophysical properties of each mammalian Kv4 isoform, has provided clues to identify the adaptive features of the mammalian Kv4 channel isoforms. Thus, the particular mechanism of inactivation of Kv4.1 channels, the relatively depolarized midpoint of inactivation of Kv4.2 and Kv4.3 channels, the fast inactivation recovery kinetics of Kv4.3 and Kv4.1 channels are exclusive features of these mammalian isoforms, and are therefore likely to be adaptive features.

The functional parameters of a cnidarian (jellyfish) Kv4 channel (Jegla and Salkoff, 1997) are clearly different from those of triploblast Kv4 channels. The alignment shown in Figure 2-4 indicates some interesting differences between the

jellyfish Kv4 channel (j*Shal*), and Kv4 channels from invertebrate triploblasts and vertebrates. For example, the S4 domain (a voltage-sensing domain) is strictly identical in all the triploblast Kv4 channels, however the S4 domain of j*Shal* differs by two amino acids (T293S and Q311K; positions refer to *Ciona*Kv4 in Fig. 2-4). Although the first substitution (a serine in j*Shal* for a threonine) is unlikely to induce functional changes, as both are neutral amino acids, the second substitution (a positively charged lysine in j*Shal* for a non-charged glutamine) is likely relevant to the voltage-sensing function of this domain, which is largely dependent on the charge of its amino acids. Also, there are channel motifs with important physiological functions that are present in all triploblast Kv4 channels but are not found in j*Shal*, such as a di-leucine motif that plays a role in targeting these channels to specific cellular regions (Rivera et al., 2003), or a two-arginine motif with an important role in determining midpoint of steady-state inactivation (Hatano et al., 2004) (Fig. 2-4). The structural differences between triploblast Kv4 channels and j*Shal* are likely correlated with discrepancies in their biophysical properties, though this should be confirmed by mutational analyses. For example, the midpoint of inactivation of j*Shal* is significantly more negative (around –106 mV), than the midpoint of inactivation of other *Shal* channels (between –50 and –70 mV), a parameter that is determined by the two-arginine motif in triploblast Kv4 channels (Hatano et al., 2004). Another peculiarity of j*Shal* is its slow kinetics of inactivation (τ_{fast} ~ 137 ms at room temperature, Jegla and Salkoff, 1997) when compared with inactivation of *Shal* channels of arthropods and chordates (τ_{fast} ~ 20-30

ms; *e.g.* Baro et al., 1996; Pak et al, 1991; this thesis). Since the N-terminus is essential for modulation by KChIPs (An et al., 2000; Bähring et al., 2001; Scannevin, 2004; this thesis), it is tempting to suggest that j*Shal* is not susceptible to modulation by KChIPs, since its N-terminus clearly diverges from that of triploblast channels (Fig. 2-4).

The jellyfish *Polyorchis* expresses heteromultimers of j*Shal*α and j*Shal*γ subunits that have distinct biophysical properties; however, homotetramers formed exclusively by Kvγ subunits are not functional (Jegla and Salkoff, 1997). Although several Kv2γ subunits are known to exist in mammals (Salinas et al., 1997), mammalian Kv4γ subunits have not been reported so far, which suggests that modulation by these Kvγ subunits may not be representative of a primitive modulatory mechanism of Kv4 channels, but is a derived feature in cnidarians. An alternative explanation is that the γ subunit that is specific for Kv4 channels represents a primitive modulator that was lost in the vertebrate lineage.

The less conserved region of Kv4 channels, the C-terminus, is rich in phosphorylation sites, especially in sites for protein kinase C (PKC). The C-termini of Kv4 channels share a PKA site, at position 549 in *Ciona*Kv4 (Fig. 2-4), but the other phosphorylation sites of the C-terminus of Kv4 channels are highly variable. This suggests that the number and location of PKC sites in the C-terminus of Kv4 channels have been selected because they have a specialized function, thus representing an adaptive feature of Kv4 channels. The N-termini of Kv4 channels also have several phophorylation sites but these are shared amongst diverse Kv4 channels (Fig. 2-4),

which suggests that these sites must be necessary for the basic functions common to all Kv4 channels.

Diversification of the Kv4 channel and the KChIP subunit in the vertebrate lineage

The finding that the genome of *Ciona intestinalis* contains only one gene for Kv4 channels (Chapter 2) and a single gene for KChIP subunits (Chapter 3) implies that both genes diversified during the evolution of vertebrates, since the mammalian genome contains three Kv4 paralogues and four KChIP paralogues. However, it is not clear whether the diversification of the Kv4 and the KChIP genes is the consequence of large-scale genomic duplications or resulted from duplications at a smaller scale. The prevailing theory, formulated by Ohno (1970), postulates two major genome duplications early in the evolution of the vertebrates, but the timing of these duplications has been debated. For example, Atkin and Ohno (1967) proposed that the first duplication occurred during the divergence of amphioxus from tunicates. However, Schmidtke et al. (1977) found the same number of enzyme genes in a tunicate (*Ciona*) and in the amphioxus, which suggests that the genome of the amphioxus is not duplicated relative to the genome of tunicates. Most (81%) vertebrate gene families are composed of two or three paralogues that derive from a single ancestral gene (Escriva et al., 2002), as is the case of the Kv4 channel gene family; however, the fact that there are three, and not four paralogues of the ancient gene would imply that one of the four tetralogues was lost after the second major genomic duplication (Spring, 1997). On the other hand, it appears that gene loss did not affect the diversification of the KChIP gene,

since vertebrates contain four KChIP paralogues. Using a system where A, B, C and D are the symbols that denote each of the vertebrate tetralogue genes, the pattern exhibited by the KChIP gene family is (A)(BCD), where "A" represents KChIP1 and "BCD" represents the KChIP isoforms 2, 3 and 4 (Fig. 3-4). Since this pattern is common amongst vertebrate gene families composed of four paralogues, Hugues (1999) has used this in his argument against the occurrence of two rounds of genomic duplication during vertebrate evolution, as this duplication pattern would have rendered a topology of the form: (AB)(CD). However, Sidow (1996) has suggested that duplications of single genes or fragments of the genome that were independent of large-scale genomic duplications have played a role in the evolution of the vertebrates and might explain these discrepancies.

In order to provide clues on the timing of diversification of the Kv channel genes during vertebrate evolution, Rashid and Dunn (1998) performed a degenerate PCR on genomic DNA from a teleost, the weakly electric fish (*Apteronotus leptorhynchus*) to amplify the highly conserved pore region of as many Kv channels as possible. Using this method, these authors identified ten Kv1 channel genes, two different Kv2 channel genes, five genes for Kv3 channels and two very similar sequences corresponding to Kv4 channel genes, although these authors noted that the differences in these two sequences for Kv4 channels could have arisen from a PCR or sequencing artifact. Nevertheless these results suggest that teleost fish contain at least two Kv4 channel genes, but these results do not imply that they lack any of the three isoforms identified in mammals, because there is no guarantee that even a degenerate

PCR would detect all possible Kv genes. In fact, it seems likely that this teleost, which belongs to the very derived Gymnotiformes would have most, if not all, of the Kv channel isoforms, since there is strong evidence for a relatively rapid rate of diversification of a variety of genes prior to the advent of the teleosts but relatively slow thereafter, as has been shown for genes for ionic transporters (Iwabe et al., 1996). Therefore, it is critical that the diversity of Kv4 channels and KChIPs be determined for the cephalochordates, such as the amphioxus, and early craniates such as the lamprey (Petromyzontiformes) and hagfish (Myxini).

Implications for the excitability properties of the tunicate heart

Since orthologous transcription factors control the early stages of cardiac morphogenesis in invertebrates (Bodmer, 1993), early chordates (Komuro and Izumo, 1993: Holland et al., 2003) and vertebrates (Davidson and Levine, 2003) it is reasonable to suppose that hearts are homologous across chordate phylogeny (Romer and Parsons, 1986) and perhaps with certain invertebrate lineages. Not surprisingly, the messages for a Kv4 channel and a KChIP accessory subunit, two proteins that are essential to the function of the vertebrate heart, were present in RNA extracted from the heart of the tunicate *Ciona intestinalis*.

The first re-polarization phase of the mammalian cardiac action potential is mediated by the A-type transient outward current, termed I_{TO} (Mitchell et al., 1984). Although I_{TO} currents are carried by Kv4 channels (Dixon et al., 1996), the amplitude of this current is correlated with the amount of KChIP mRNA and not with the amount of

Kv4 mRNA in the canine and human heart. For example, the I_{TO} current is larger in the epicardium, which expresses larger amounts of KChIP mRNA, than in the endocardium, which expresses lower amounts of KChIP mRNA (Rosati et al., 2001). The first re-polarization phase of the action potential is essential to heart physiology because variations in its biophysical parameters have important repercussions for the amplitude and duration of the cardiac action potential (*e.g.* Xu et al., 1999). It is not known whether different areas of the heart of *Ciona intestinalis* produce action potentials with different waveforms; about 70 % of all action potentials showed three phases of re-polarization and the remaining 30% had one or two phases of re-polarization (Kriebel, 1967). This author did not specify whether a single myocyte produced action potentials with a different number of re-polarization phases. However, this appears to be the case, as implied by his statement: "...Various shapes of action potentials were found, showing from one to three phases of repolarization..." (Kriebel, 1967). However, it is also possible that action potential shape is influenced by the nature of the propagation of action potentials in this sheet of electrically coupled cells. For example, if the rate of firing increases, there could be a slower rise time that may inactivate channels carrying inward current. However, Kriebel's observation that "...action potentials from a single cell before and after a reversal were usually identical..." (Kriebel, 1967) suggests that the recent firing history of a cell and its neighbors does not affect the action potential waveform of tunicate myocytes. Perhaps different regions of the tunicate heart express different amounts of *Ciona*KChIP

subunits, if modulation of Kv4 channels by KChIP subunits is an evolutionarily ancient strategy for increasing the diversity of the cardiac AP waveform.

By slowing inactivation kinetics and the rate of recovery from inactivation of *Ciona*Kv4 channels, *Ciona*KChIP might perform a regulatory function for controlling excitability of the tunicate heart. A slowly inactivating *Ciona*Kv4/KChIP complex will produce persistent outward currents that would (i) dampen the influence of the inward, depolarizing Na^+ current, and (ii) cumulative inactivation of I_{Na}, resulting in action potentials of relatively small amplitude. Consistent with this, the action potentials recorded by Kriebel (1967) had relatively low amplitude, as they barely overshoot 0 mV from a resting potential of –69 mV. However, one would expect that the small size of these cells (1-10 μm in height) would present technical difficulties to record intracellular action potentials and that the small APs may result from cell damage and loss of the resting potential, as a relatively depolarized membrane potential would result in a decrease in the number of available spike-producing Na^+ channels.

Currents produced by *Ciona*Kv4/KChIP complexes recover from inactivation with a time constant of ~1s (Table 3-1). A particular region of the tunicate heart contracts with an average rate of ~15 contractions min^{-1} (Kriebel, 1968). Assuming a ratio of 1 action potential *per* contraction, most Kv4 channels expressed in a particular myocyte would be available for activation and hence re-polarization of the action potential every time a wave of depolarization reaches it. Therefore, in theory the long re-polarization

phase of tunicate myocytes cannot be a consequence of minimal re-polarizing Kv4 current.

In summary, inactivation kinetics and inactivation recovery kinetics of the *Ciona*Kv4/KChIP complex are compatible with the physiology of the tunicate heart. However, the strong shift of the inactivation midpoint in the hyperpolarizing direction caused by *Ciona*KChIP (Fig. 3-11A) is difficult to reconcile with the physiology of the tunicate heart, since it renders *Ciona*Kv4 unavailable for activation at the measured resting potential of ~ -69 mV for *Ciona intestinalis* myocytes (Kriebel, 1967). However, one could reasonably argue that given the small size of tunicate myocytes, they would be easily damaged by the electrodes used to obtain these intracellular recordings (Kriebel). Although these electrodes were not static, but were suspended so that they would follow the impaled cells that were contracting, they could still easily damage and rupture cell membranes. The depolarization ensued by this damage to the cell membranes would account for the relatively depolarized membrane potential (-69 mV, Kriebel, 1967), and for the relatively short amplitude of these action potentials, since the depolarization would cause cumulative inactivation of I_{Na}. On the other hand, future characterization of the Kv4 macro-molecular complex and the effects of Ca^{2+} on the modulation of Kv4 channels by KChIP subunits may help solve this puzzle.

An intriguing feature of the tunicate heart is the alternating activity of the pacemakers located at each end of the heart (Anderson, 1968). It is currently believed that spontaneous electrical activity originates from calcium-dependent oscillations of the membrane potential (Grace, 1991). Because A-type currents operate in the sub-

threshold range they may be important determinants of the pacemaker frequency, as suggested by the early work on invertebrate neurons (Connor and Stevens, 1971a,b). Unfortunately, only speculations can be made at this point regarding the involvement of *Ciona*Kv4 and *Ciona*KChIP in the pacemaker of the tunicate heart, but analyses on expression of both proteins in the pacemaker and non-pacemaker regions of this tissue will help to reveal more about its physiology.

4.3 Final conclusions

This PhD thesis has provided the following contributions:

(i) Determined the exon-intron organization of a Kv4 channel gene orthologue, its nucleotide sequence and its deduced amino acid sequence, from the basal chordate *Ciona intestinalis*.

(ii) Provided a complete characterization of the biophysical properties a wild type Kv4 channel (*Ciona*Kv4) from a basal chordate.

(iii) Established the importance of the N-terminal 2-32 amino acids for proper expression of the biophysical properties of a Kv4 channel from a basal chordate.

(iv) Determined the genomic structure, nucleotide and amino acid sequence of the first non-vertebrate KChIP subunit, termed *Ciona*KChIP.

(v) Characterized the modulatory effects of *Ciona*KChIP on the biophysical activity of *Ciona*Kv4.

(vi) Established the importance of the N-terminus of *Ciona*Kv4 for modulation by *Ciona*KChIP.

4.4 Literature cited

An WF, Bowlby MR, Betty M, Cao J, Ling HP, Mendoza G, Hinson JW, Mattsson KI, Strassle BW, Trimmer JS, Rhodes KJ (2000) Modulation of A-type potassium channels by a family of calcium sensors. Nature 403:553-556

Anderson M (1968) Electrophysiological studies on initiation and reversal of the heart beat in *Ciona intestinalis*. J Exp Biol 49:363-385

Atkin NB, Ohno S (1967) DNA values of four primitive chordates. Chromosoma 23:10-13

Bähring R, Dannenberg J, Peters HC, Leicher T, Pongs O, Isbrandt D (2001) Conserved Kv4 N-terminal domain critical for effects of Kv channel-interacting protein 2.2 on channel expression and gating. J Biol Chem 276:23888-23894

Baro DJ, Coniglio LM, Cole CL, Rodriguez HE, Lubell JK, Kim MT, Harris-Warrick RM (1996) Lobster *shal*: comparison with *Drosophila shal* and native potassium currents in identified neurons. J Neurosci 16:1689-1701

Bodmer R (1993) The gene *tinman* is required for specification of the heart and visceral muscles in *Drosophila*. Development 118:719-729

Connor JA, Stevens CF (1971a) Voltage clamp studies of a transient outward membrane current ingastropod neural somata. J Physiol 213:21-30

Connor JA, Stevens CF (1971b) Prediction of repetitive firing behaviour from voltage clamp data on an isolated neurone soma. J Physiol 213:31-53

Davidson B, Levine M (2003) Evolutionary origins of the vertebrate heart: specification of the cardiac lineage in *Ciona intestinalis*. Proc Natl Acad Sci USA 100:11469-11473

Dixon JE, Shi W, Wang H-S, McDonald C, Yu H, Wymore RS, Cohen IS, McKinnon D (1996) The role of the Kv4.3 K^+ channel in ventricular muscle: a molecular correlate for the transient outward current. Circ Res 79:659-668

Escriva H, Manzon L, Youson J, Laudet V (2002) Analysis of lamprey and hagfish genes reveals a complex history of gene duplications during early vertebrate evolution. Mol Biol Evol 19:1440-1450

Grace AA (1991) Regulation of spontaneous activity and oscillatory spike firing in rat midbrain dopamine neurons recorded *in vitro*. Synapse 7:221-234

Hatano N, Ohya S, Muraki K, Clark RB, Giles WR, Imaizumi Y (2004) Two arginines in the cytoplasmic C-terminal domain are essential for voltage-dependent regulation of A-type K^+ current in the Kv4 channel subfamily. J Biol Chem 279:5450-5459

Holland ND, Venkatesh TV, Holland LZ, Jacobs DK, Bodmer R (2003) *AmphiNk2-tin*, an amphioxus homeobox gene expressed in myocardial progenitors: insights into evolution of the vertebrate heart. Develop Biol 255:128-137

Hugues AL (1999) Phylogenies of developmentally important proteins do not support the hypothesis of two rounds of genome duplication early in vertebrate history. J Mol Evol 48:565-576

Isbrandt D, Leicher T, Waldschütz R, Zhu X, Luhmann U, Michel U, Sauter K, Pongs O (2000) Gene structures and expression profiles of three human KCND (Kv4) potassium channels mediating A-type currents I_{TO} and I_{SA}. Genomics 64:144-154

Iwabe N, Kuma K-I, Miyata T (1996) Evolution of gene families and relationship with organismal evolution: Rapid divergence of tissue-specific genes in the early evolution of chordates. Mol Biol Evol 13:483-493

Jegla T, Salkoff L (1997) A novel subunit for Shal potassium channels radically alters activation and inactivation. J Neurosci 17:32-44

Komuro I, Izumo S (1993) Csx: A murine homeobox-containing gene specifically expressed in the developing heart. Proc Natl Acad Sci USA 90:8145-8149

Kriebel ME (1967) Conduction velocity and intracellular action potentials of the tunicate heart. J Gen Physiol 50:2097-2107

Kriebel ME (1968) Studies on cardiovascular physiology of tunicates. Biol Bull 134: 434-455

Mitchell MR, Powell T, Terrar DA, Twist VW (1984) Strontium, nifedipine and 4-aminopyridine modify the time course of the action potential in cells from rat ventricular muscle. Br J Pharmacol 81:551-556

Nakajo K, Katsuyama Y, Ono F, Ohtsuka Y, Okamura Y (2003) Primary structure, functional characterization and developmental expression of the ascidian Kv4-class potassium channel. Neurosci Res 45:59-70

Ohno S (1970) Evolution by gene duplication. Springer-Verlag, Heidelberg

Pak MD, Baker K, Covarrubias M, Butler A, Ratcliffe A, Salkoff L (1991) mShal, a subfamily of A-type K^+ channel cloned from mammalian brain. Proc Natl Acad Sci USA 88:4386-4390

Rashid AJ, Dunn RJ (1998) Sequence diversity of voltage-gated potassium channels in an electric fish. Mol Brain Res 54:101-107

Rivera JF, Ahmad S, Quick MW, Liman ER, Arnold DB (2003) An evolutionarily conserved di-leucine motif in Shal K^+ channels mediates dendritic targeting. Nat Neurosci 6:243-250

Romer AS, Parsons TS (1986) The Vertebrate Body (6^{th} ed.). Philadelphia, PA: Saunders, p. 1 679

Rosati B, Pan Z, Lypen S, Wang H-S, Cohen I, Dixon JE, McKinnon D (2001) Regulation of *KChIP2* potassium channel β subunit gene expression underlies the gradient of transient outward current in canine and human ventricle. J Physiol 533:119-125

Salinas M, de Weille J, Guillemare E, Lazdunski M, Hugnot J-P (1997) Modes of regulation of *Shab* K^+ channel activity by the Kv8.1 subunit. J Biol Chem 272:8774-8780

Scannevin RH, Wang K, Jow F, Megules J, Kopsco DC, Edris W, Carroll KC, Lü Q, Xu W, Xu Z, Katz AH, Olland S, Lin L, Taylor M, Stahl M, Malakian K, Somers W, Mosyak L, Bowlby MR, Chanda P, Rhodes KJ (2004) Two N-terminal domains of Kv4 K^+ channels regulate binding to and modulation by KChIP1. Neuron 41:587-598

Schmidtke J, Weiler C, Kunz B, Engel W (1977) Isozymes of a tunicte and a cephalochordate as a test of polyploidisation in chordate evolution. Nature 266:532-533

Sidow A (1996) Gen(om)e duplications in the evolution of early vertebrates. Curr Op Gen Dev 6:715-722

Spring J (1997) Vertebrate evolution by interspecific hybridization-are we polyploid? FEBS Letters 400:2-8

Xu H, Li H, Nerbonne JM (1999) Elimination of the transient outward current and action potential prolongation in mouse atrial myocytes expressing a dominant negative Kv4α subunit. J Physiol 519:11-21

Zhang Y, MacLean JN, An WF, Lanning CC, Harris-Warrick RM (2003) KChIP1 and frequenin modify *shal*-evoked potassium currents in pyloric neurons in the lobster stomatogastric ganglion. J Neurophysiol 89:1902-1909

APPENDIX A: cDNA sequence of *Ciona*Kv4

```
LOCUS       AY514487                2900 bp    mRNA    linear   INV 02-FEB-2004
DEFINITION  Ciona intestinalis potassium channel Kv4 mRNA, complete cds.
ACCESSION   AY514487
VERSION     AY514487.1  GI:41351866
KEYWORDS    .
SOURCE      Ciona intestinalis
  ORGANISM  Ciona intestinalis
            Eukaryota; Metazoa; Chordata; Urochordata; Ascidiacea; Enterogona;
            Phlebobranchia; Cionidae; Ciona.
REFERENCE   1  (bases 1 to 2900)
  AUTHORS   Salvador-Recatala,V., Gallin,W.J. and Spencer,A.N.
  TITLE     Ciona intestinalis CionaKv4 mRNA for Kv4-type voltage-gated
            potassium channel
  JOURNAL   Unpublished
REFERENCE   2  (bases 1 to 2900)
  AUTHORS   Salvador-Recatala,V., Gallin,W.J. and Spencer,A.N.
  TITLE     Direct Submission
  JOURNAL   Submitted (29-DEC-2003) Biological Sciences, University of Alberta,
            Edmonton, AB T6G 2E9, Canada
FEATURES             Location/Qualifiers
     source          1..2900
                     /organism="Ciona intestinalis"
                     /mol_type="mRNA"
                     /db_xref="taxon:7719"
     CDS             1..2403
                     /note="voltage-gated potassium channel; CionaKv4"
                     /codon_start=1
                     /product="potassium channel Kv4"
                     /protein_id="AAS00646.1"
                     /db_xref="GI:41351867"
                     /translation="MATAVAAWLPFARAAAIGWVPVATNNLPPIPFNRRKTKDTLITL
                     NISGRRFQTWKNTLEKFPDTMLGSQEKEFFYDDDRKEYFFDRDPEIFRHILSFYRTGK
                     MHFPRTECISSIDDELAFFGILPEMIADCCYEDYRDRKRENDERLVDDASDAPGGPAL
                     GKAPPPALSLRKRMWRAFENPHTSTPALVFYYVTGFFIAVSVFANIVETVPCGAMPGT
                     LEVKQCGERYQLTFFCLDTACVMIFTVEYFMRLFASPNRCKFLRSVMSIIDVVAILPY
                     YIGLIITDNEDVSGAFVTLRVFRVFRIFKFSRHSQGLRILGYTLKSCASELGFLLFSL
                     TMAIIIFATVMFYAEKGMEGTTFTSIPAAFWYTIVTMTTLGYGDMVPKTIAGKIFGSV
                     CSLSGVLVIALPVPVIVSNFGRIYSQNQRQDKRRAQKRARLARIRAGKPTSAMTYCQN
                     KGDHDFEQDPPPDVSEAETSSSNNINATFEKNHFHLLHCLERTTDHEITENQMCNSSS
                     VIAIRGGDNESESLISTHSANQNQSNIYHQQMSLQRGRRETTSTCSLQRHNDVSSRSS
                     SVSHTSQHDNACELDDDSFLSNEKTNFGFSGTKDVTSPPPFSLNQSPCATSFAVADNL
                     RSMDDVESDVIIPSIALPDVTDQFCNIPSRFTNYVTTPSSTRNLQADNLSVPMTSLSS
                     SDASSSTSGVSGSSDYYRYGGSDDDERIPNLIPTHESRSQHRRSEPGIDAFRRSSRTR
                     ENYDGPRKSSPKSPPSTVTCVAPPHADAADQRHRVSAEKSGILPANVDGSNSSVIRIS
                     SL"
     3'UTR           2404..2900
ORIGIN
        1 atggcaacag cagtagcagc ttggctacct tttgcaaggg cagcagccat aggttgggtt
       61 ccagttgcta ccaataacct acccccccatc ccgtttaacc gacgtaaaac aaaagacaca
```

```
 121 ctcatcactc tcaatataag cggtcgacgg tttcaaacgt ggaagaacac acttgaaaag
 181 ttcccagata caatgttggg aagccaggag aaagagtttt tctacgacga cgataggaaa
 241 gaatatttct tcgaccgaga ccccgagatc tttcgacata tcctgagttt ttatagaacg
 301 ggcaagatgc actttccgcg gacagaatgc atcagttcta tcgacgacga gctggcgttc
 361 ttcggtatat tgcctgagat gatagctgat tgttgctatg aagactacag agatcgtaaa
 421 agggaaaacg atgaacgatt agttgacgat gctagcgatg ctcctggagg acctgctctt
 481 ggaaaggccc cgcctcccgc tttatctctt agaaagcgaa tgtggcgagc gtttgagaat
 541 ccccacacta gcaccccagc tcttgtgttt tattatgtga ccgggttttt cattgccgtt
 601 tccgtgtttg ctaacatagt cgaaaccgtg ccgtgcggag cgatgccggg aacgcttgaa
 661 gtcaaacagt gtggcgaaag ataccagctg acgtttttt gcttggacac ggcatgcgtg
 721 atgatattta cagtcgaata cttcatgaga ctttttgctt caccaaaccg atgtaaattc
 781 ctacgatccg tcatgagcat tatagacgtt gtagcaatcc taccttacta catcggtctc
 841 atcatcactg acaacgaaga tgtaagcggg gcgttcgtta ccctgcgtgt gttccgggtc
 901 ttccgtatat tcaagttctc gcgacattca caagggcttc gtatcctggg ctatacattg
 961 aaaagttgtg ccagtgaact tggcttcctt ttgttttctc taaccatggc aatcattata
1021 ttcgcaactg ttatgttcta tgccgagaaa ggaatggaag gcactacatt cacgagcata
1081 ccggcagcgt tctggtacac catagtaacg atgaccaccc tcggatacgg tgacatggtg
1141 ccaaagacaa tcgccggcaa gatattcggc agtgtgtgtt cattaagcgg ggtgctcgtg
1201 attgcgttgc cagttcctgt catcgtaagt aactttgggc ggatctacag ccaaaatcaa
1261 agacaagaca aacgaagagc ccaaaagaga gctcgcttag ctcggatacg agcagggaaa
1321 cctacgagtg cgatgacgta ttgtcagaat aaaggagatc acgactttga gcaagacccc
1381 ccacccgatg tgagtgaagc cgagacctcc agctccaaca atataaacgc aacattcgag
1441 aaaaatcatt tccatctttt gcactgcctc gaacgaacaa cggaccatga gataaccgaa
1501 aaccagatgt gtaactcctc atccgtgata gccatacgng gtggcgacaa tgaatccgaa
1561 tctctcattt ccactcactc ggctaatcag aaccagtcaa atatttacca ccagcagatg
1621 tcgctacaga gagggcggcg tgaaacaaca agcacgtgtt cattgcaacg tcataatgac
1681 gtcagctcta gatcatctag cgtttcccac actagtcaac atgataacgc atgcgaactc
1741 gatgacgatt cattttaag caatgaaaaa acaaattttg gattttctgg aacaaaagac
1801 gtcacatcac ccccgccctt ctcgctcaac caatcacctt gcgccacgtc attcgctgtg
1861 gctgacaatc tgagatcaat ggatgacgta gagtctgacg tcatcattcc gtcaatcgcg
1921 ctgcctgatg tcacggatca gttttgcaac atcccgtctc ggtttactaa ttacgtaacg
1981 acgccatctt cgacgagaaa cctccaagcc gataatcttt ctgttcctat gacatctttg
2041 tcctcgtcgg acgcgtcttc ttccacgtcc ggagttagcg ggtcatcgga ttattataga
2101 tacggaggca gcgatgatga tgagagaatc cccaacctca tcccgacaca tgagagcaga
2161 tcacaacayc gaaggtcgga gccagggatt gatgctttta gacgaagttc gaggacaagg
2221 gaaaattatg acggcccccg gaaatcgagc cctaaatccc cgccgtctac ggttacatgc
2281 gtcgccccac cacacgccga cgccgccgac cagcgacata gagtttctgc tgaaaagagc
2341 gggatattgc cagcgaatgt tgatggttca aactccagcg tgattcgtat ttcctcactg
2401 tagcggcggg actttgaaga gaacttttac gttttgcaca aagtcggcaa actttcgccg
2461 caatttaact gtcaaactag ccaggataga aacttataaa tcgtggcgat atatctwaga
2521 cattgtagca ttactaagat aaccgtcttc atttaagcgt gtgttgttta cgcagttttg
2581 tggcataacg tgcaatcata tactttagct gatgtgtttt taaagcgagt tggtctattt
2641 tcatctgacg aaaccgggag gttacttttt cttaatgttt ttgtttcgta gttttagaag
2701 cgtgaagttt caacggctat tctgtgttac gaaaggtaat aataaccact gtgttagaga
2761 cctatataga cccgctggta accttgatgt cattggttct gtgctcgctg tagagtgaat
2821 cggtttacaa tgatgkasta ttgcgttata attaactttc cgaaagaaaa tttattccgg
2881 aaaaaaaaaa aaaaaaacaa
//
```

APPENDIX B: cDNA sequence of *Ciona*KChIP

```
LOCUS       AY514488                1254 bp    mRNA    linear   INV 02-FEB-2004
DEFINITION  Ciona intestinalis potassium channel-interacting protein KChIP
            mRNA, complete cds.
ACCESSION   AY514488
VERSION     AY514488.1  GI:41351868
KEYWORDS    .
SOURCE      Ciona intestinalis
  ORGANISM  Ciona intestinalis
            Eukaryota; Metazoa; Chordata; Urochordata; Ascidiacea; Enterogona;
            Phlebobranchia; Cionidae; Ciona.
REFERENCE   1  (bases 1 to 1254)
  AUTHORS   Salvador-Recatala,V., Gallin,W.J. and Spencer,A.N.
  TITLE     Kv channel-interacting protein (KChIP) expressed in Ciona
            intestinalis heart tissue
  JOURNAL   Unpublished
REFERENCE   2  (bases 1 to 1254)
  AUTHORS   Salvador-Recatala,V., Gallin,W.J. and Spencer,A.N.
  TITLE     Direct Submission
  JOURNAL   Submitted (29-DEC-2003) Biological Sciences, University of Alberta,
            Edmonton, AB T6G 2E9, Canada
FEATURES             Location/Qualifiers
     source          1..1254
                     /organism="Ciona intestinalis"
                     /mol_type="mRNA"
                     /db_xref="taxon:7719"
     CDS             1..741
                     /note="calcium-binding protein; Kv channel-interacting
                     protein"
                     /codon_start=1
                     /product="potassium channel-interacting protein KChIP"
                     /protein_id="AAS00647.1"
                     /db_xref="GI:41351869"
                     /translation="MSLAILTMVTERENVWETEKIGIAIMCAGVVMVVFNRIHKYLPF
                     LKCWTKDADGAEIERQTLRYMPESIERLMALTNFDRRELKTLYRNFKNECPNGVVNEE
                     TFKSIYCQFFPNGDADMYAHYVFRAFDHSEEGHVNFEEFAIGLSSLLRGSLIDRLHWT
                     FRLYDINHDGYITREEMLSIIKSVYQLLGSHVKPSLSDDNYMEHTDRIFNKLDLNGDG
                     LVTMEEFCETCTKDESIVRSMSIFDHAL"
ORIGIN
        1 atgtctctcg ctatcttaac catggtgaca gagagagaga atgtttggga gacagagaag
       61 attggaatag cgattatgtg cgctggtgtg gtcatggttg tgtttaatag aattcacaag
      121 tatctgccct ttctcaaatg ctggacgaaa gatgcggacg gagcagaaat cgagcggcaa
      181 acactgcgat atatgccgga aagcattgaa agattaatgg ccctcactaa cttcgataga
      241 cgggagctta agacgttgta cagaaacttc aaaaacgagt gcccgaacgg cgttgtgaac
      301 gaagagacct tcaaatcaat ctactgtcaa ttctttccca acggagatgc ggacatgtac
      361 gctcattatg tgttccgtgc atttgaccac tcggaagaag gccatgtcaa tttcgaggag
      421 tttgcaatcg gtttatcttc cctactgcgc ggaagtttga tcgataggtt acattggacg
```

```
       481 ttcagattat atgacatcaa ccacgacgga tatataaccc gggaggagat gctaagcata
       541 ataaagtcag tataccagtt gttgggatcg catgttaagc cgtcgctatc ggacgataac
       601 tacatggaac acacggacag gatatttaac aaacttgatc ttaatggaga tggtttagtt
       661 acgatggaag agttctgtga gacgtgtact aaggacgaat ctattgtacg atcaatgagt
       721 atattcgacc atgcgttata gctccatcaa ggcggttttc ctcacattct tccattgaca
       781 atgcgcagaa gagcgaatac acaaaaactc agagaaactc gtagagaata tttctccatg
       841 caaatcgcgg gataaacaca cagagatttc ccctctgcag tattttggtc ccagtatata
       901 cctggccacc gtgattttct ctcacgcttt atcagaattg gtgattttta caatgtgcaa
       961 tatctttacc gcgtcgtatt tactcgtgat tgttttggaa tggtgcgata gaagcagcaa
      1021 actcttataa aacgcgctgg aaaaagtcca attttccata cttttgtaca caatgcttct
      1081 gacataaatc agtttacaaa acaccgcgtt aggccgccgt tgtttctatt tttaatatag
      1141 ctacggattt gtatttgcac tttatgttht gcngctccnt tgsnaatttg kncnncnktc
      1201 ngnnaarant ncgyngtnga wtaaccaaaw nargaaamca aaaaaaaaaa aaaa
//
```